UCLouvain

AGRO LOUVAIN

Faculté des bioingénieurs

Heteropolyacid ($H_3PW_4O_{24}$) hybridized with terpyridine ($C_{15}H_{11}N_3$) as heterogeneous catalyst for epoxydation of olefins

Auteur : Van Roey Pierrick
Promoteur(s) : Pr. E. Gaigneaux
Encadrant : Gabriel Hidalgo
Lecteur(s) : Pr. M. Devillers et Pr. B. Elias
Année académique 2018-2019
Intitulé du master et de la finalité : Bioingénieur en chimie et bio-industries

Acknowledgments

First, I would like to thank my thesis supervisor, Professor Gaigneaux, who guided me and dedicated his time to steer me in the right direction whenever I needed it. I am grateful to him for allowing this study to happen in his laboratory and welcoming me in his team.

I would also like to acknowledge Gabriel, who was my mentor during whole this project. We spent 9 months in the same office, sharing our thoughts about Polyoxometalates, Keggin structure, PW4, and ordinary curiosity about science. I will always remember these friendly moments and talks we have had together.

I also want to thank everyone in Pr. Gaigneaux research of the C3 part of the Lavoisier building. A very nice atmosphere surrounds this place, with people from all over the world, glad to share their experience in chemistry and catalysis. In particular a special mention goes to Francois who was always volunteer to answer every one of my questions.

Also, I would like to thank the football team “Cata” and its members William, Alès, Isaac, Gabriel, Samuel, Thibault, Francois, Damien and Antoine.

For all the jokes, lunchtimes, coca breaks and services rendered, I thank Antoine with whom we have had so many nice moments talking about football, politics, Game of thrones or even chemistry.

Eventually, I want to thank my parents who encouraged me during my 5 years of studies. In addition, a special mention goes to all my roommates who have been supporting me for 1 year and without whom this last year would have been way different.

Acronyms, Abbreviations & Symbols

AES	Atomic Emission spectroscopy
BET	Brunauer, Emmett and Teller's theory
Cl-TPY	Chlorophenyl-terpyridine
EDG	Electron donating group
EDW	Electron withdrawing group
F-TPY	Fluorophenyl-terpyridine
GC	Gas chromatography
-I	Inductive captor group
ICP	Inductive coupled plasma
IR	Infrared
MS	Mass spectroscopy
Naked-TPY	Naked-terpyridine (= TPY)
Ph-TPY	Phenyl-terpyridine
POMs	Polyoxometalates
PW12	$H_3PW_{12}O_{40}$
PW4	$PW_4O_{24}^{-3}$
PWx	PW4, PW3 and PW2
Py-TPY	Pyridil-terpyridine
SPS	Subsequent peroxo species
TGA	Thermogravimetric analysis
Theta	scattering angle
TPD	Temperature Progamme desorption
TPY	2,2':6',2''-Terpyridine
Tri-TPY	Trimethoxyphenyl-terpyridine
XRD	X-rays diffraction

Abstract:

In the field of catalysis, epoxides production has seen many diverse types of catalysts being developed over the years. The uses of oxiranes compounds are broad, they are either employed to produce paints, resins, adhesives or even as intermediates in organic synthesis. Several processes have been exploited yet nowadays, the direct oxidation by air of alkenes on silver-based catalyst is the most widespread one. However, the latter is a major carbon emitter of the industry. Consequently, industries are looking for new eco-friendly catalytic processes to obtain a sustainable production of epoxides. Among the potential candidates to accomplish this reaction, polyoxometalates (POMs) have demonstrated their property of being a good oxidation catalyst for a wide variety of reactions. These large anionic molecules have many properties such as a strong acidity when protonated, thermal stability and eventually their ability to accept and release electrons without decomposing or changing their structures. One of them, $\{PO_4[W(O)(O_2)_2]_4\}^{3-}$ (=PW4) was reported to be very active and selective towards epoxidation of olefins in homogeneous conditions. Nevertheless, industries prefer having heterogeneous catalytic processes, especially when large quantities are produced. Changing the nature of this homogeneous catalyst to a heterogeneous one remains though a challenge. The hybridization of this POM species with organic ligands have already been reported being successful using bipyridine.

PW4 was chosen to be hybridized with organic terpyridines ligands containing different functionalization. The main objective is to assess the influence of the catalyst polarity, by hybridizing a hydrophilic peroxo-tungstate acid ($H_3PW_4O_{24}$) with hydrophobic terpyridine ligands, for the heterogeneous catalytic epoxidation of cyclooctene by hydrogen peroxide. To do so, trials to synthesize PW4 and then hybridize it with the organic ligands were performed. The idea is to use 6 distinct ligands, giving 6 hybrids to obtain the catalyst with the highest affinity with the reactants. The situation is that PW4 itself is very hydrophilic compared to an alkene, but the hydrophobicity brought by the terpyridine ligand is supposed to increase the affinity between reactants and catalyst.

These hybrids were synthesized even if, there is no certainty about the exact content in their inorganic part. Then, the catalytic activity of these hybrids was tested in the epoxidation of cyclooctene using hydrogen peroxide as oxidant and acetonitrile as solvent. Large differences

between the hybrids were observed. Nonetheless for the best one of them, results similar to the Venturello anion in homogeneous phase were obtained.

Eventually, leaching tests to judge the catalyst heterogeneity were operated. These have exposed that the hybrids catalysts are prone to leaching. These tests were followed by other ones demonstrating that the active species of the hybrids are the leached compounds.
To conclude, this study has revealed that the hybridization of peroxotungstates with functionalized terpyridines yields an active catalyst that leaches. The nature of the leached species was not established, further works still has to be carried out. Additional investigation is needed concerning the exact identification of the inorganic part of the hybrids which seems to be composed of a mix of PW4, PW3 and PW2 species.

Table of content:

1. Introduction of the Master Thesis:

1.1 Catalysis:

Catalysis is an area of particular significance in chemistry. In fact, it is the field where the largest contribution to industrial chemical processes is found [1]. In this field, a catalyst is a chemical substance that increases the rate of a chemical reaction, by decreasing the energy barrier necessary for the reaction to occur, this without being consumed. It only affects the kinetics of the reaction and not its thermodynamics. Moreover, it has the capability to selectively direct the reaction towards targeted products [2]. In a chemical reactor, the catalyst is added in a much smaller quantity compared to the reactants and is, by definition, retrievable. The spectrum of catalyst sorts in terms of composition, texture, and physicochemical properties is very broad. Indeed, one catalyst might only work for one specific reaction, and in most cases, its catalytic activity is restricted to very specific conditions. Therefore, the challenge remains in designing efficiently the right catalyst for a reaction of interest.

The field of catalysis is divided in two groups called, homogeneous and heterogeneous catalysis. Both offer advantages and drawbacks. In homogeneous catalysis, the catalyst and reactants coexist in a single fluid phase, usually the liquid phase [3]. The main advantages of this type of catalysis are the high diffusivity and heat transfer rate that the catalyst active species present in solution. In addition, high selectivities and well-defined catalyst active sites are precious advantages against the heterogenous route. However, catalyst separation and recyclability are undoubtedly big issues regarding homogeneous catalysis. Indeed, the catalyst separation from the reaction mixture is hard and expensive, which makes the catalyst recycling a difficult challenge. [4] Eventually, homogeneous catalysis is used for simple batch reactions. On the other hand, heterogeneous catalysis offers opposite benefits compared to the homogeneous route. At an industrial level, heterogeneous catalysis is preferred for continuous processes, with large amounts of converted products. [5] Heterogeneous catalysis happens when the phase of the catalyst is different from the phase of the reactants, it can be solid-liquid, and solid-gas phase conditions. The catalyst is therefore a solid. The basic phenomenon of catalysis is the ability of the catalyst surface to adsorb the reactants and

trough this, lowering the activation energy of the reaction of interest which eventually enables the reaction. [6] Once the reaction is completed, the separation process between the heterogeneous catalyst and the products can be simply performed by centrifugation, filtration or decantation.

Catalytic epoxidation plays an important role for the industrial production of many compounds and the diversity of catalysts used is large and encompasses all the known categories of catalyst: homogeneous, heterogeneous and biological. [7] Epoxidation reaction is one of the most powerful tools in synthetic chemistry, from the lab scale to the industrial one. It is used to produce bulk chemicals but also high added-value chemicals. [8]

1.2 Catalysis for epoxidation reactions:

1.2.1 Epoxidation

Epoxidation is a chemical reaction which converts a carbon-carbon double bond into oxiranes (epoxides). [9] These molecules are key intermediates in the oxy-functionalization of other molecules of interest in fine chemicals. Currently, the direct oxidation of ethylene to ethylene oxide (EO) is the largest commercial epoxidation process in the world [10] with an annual production of 19 million metric tons (in both 2008 and 2009) [11], and a worldwide demand expected to reach 32 thousand tons per year in 2023 [12]. Historically, the original process to epoxidize ethylene was based on chlorohydrin. The major drawback of this process was the use of chlorine and lime, which were converted to useless non eco-friendly waste by-products. Since then, many efforts have been done to overcome these issues and develop more performant catalysts as illustrated in the next section.

1.2.2 Epoxides uses, current common and new production system:

Currently, the process to produce EO, as illustrated on figure 1, is based on oxygen over silver-based catalyst at temperatures that range between 220-300°C. It is important to mention that during this process, the ethylene conversion is around 10%, with 85% of selectivity towards ethylene oxide. Still, this process is considered as one of the major carbon dioxide emitters in the industrial chemical technologies. [13]

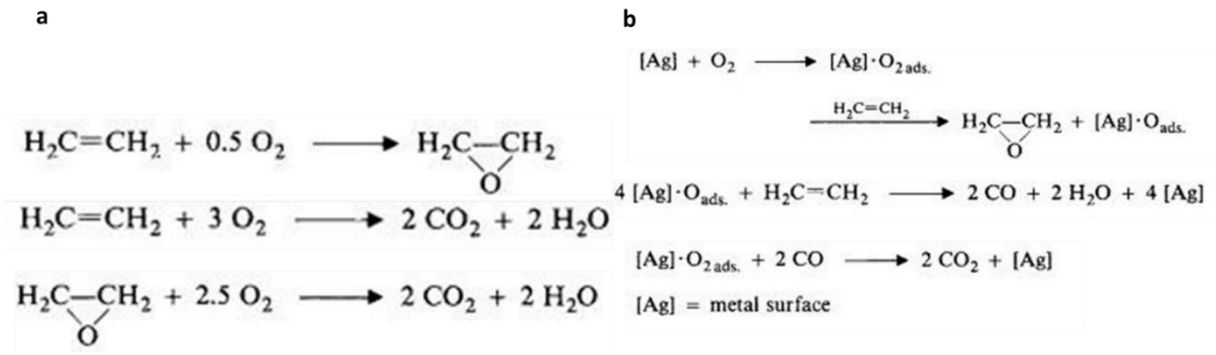

Figure 1 : Current industrial EO production via the oxygen-based process: (a) general reaction steps; (b) role of the silver-based catalyst in the epoxidation process [14].

The uses of epoxide compounds are numerous. For instance, EO is used as a precursor for detergents, surfactants, fumigant and antifreeze among other products. [15] Epoxides have the ability to react with amines and form the so-called epoxy glue adhesive, which is a product that is formed via a polymer assembly molecular process [16].

Currently, new epoxide production processes are developed like in Belgium at Antwerp by BASF and Dow Chemical, using hydrogen peroxide as an oxydant. The latter offers the advantages of being less pollutant. Indeed, hydrogen peroxide can be considered as a green oxidant in catalytic reactions, since it only produces water and oxygen as by-product. [17] However, its production is not eco-friendly since it uses noble metal (Palladium), difficult to extract. Therefore, in a close future one can hope that hydrogen peroxide will really be a green oxidant, including its production process [17], [18]. This is important because hydrogen peroxide could be used in many redox processes and lowering their ecologic footprint [19].

1.2.3 A candidate for epoxidation reaction

To epoxidize carbon-carbon double bonds, or more commonly what is called olefins, many catalysts are being scrutinized at the lab scale. Several oxidants can be used for epoxidation (air, O_2, hydrogen peroxide, organic hydroperoxides, peroxyacids) and the choice is linked to the substrate type, the characteristics of the catalyst plus the sustainability of the whole process. [13] There are many metals that catalyses the oxidation of organic molecules (olefins) with hydrogen peroxide. Among them, Cr, Mo, V, Ti and W usually in their d° electronic configurations [20]. Concerning the epoxidation of alkenes (such as cyclooctene) with hydrogen peroxide and transition metal, polyoxometalates complexes containing one or more peroxo groups have shown great results.

1.3 Polyoxometalates:

Polyoxometalates (POMs) are large polyatomic metal-oxo anions. They can be divided in two main broad families, the isopolyanions $[M_m O_y]^{q-}$ composed of one kind of metal (e.g. Mo,W,V), and heteropolyanions $[X_r M_m O_y]^{q-}$, composed of a metal with an additional element from the p block (e.g. P, Si, As). POMs can be accompanied by different types of cations in their structures, which makes them ionic salts type compounds. When such cations are protons and the anion is a heteropolyanion, then the compound is classified as a heteropolyacid (HPA). Depending on the type of heteropolyanion, HPAs can become very strong acids [21]. POMs are connected by oxygen atoms that are differentiated by how they connect the different units of the anionic structure [22].

The formation of POM can happen as illustrated in the following Equation 1 [23]:

$$nMO_4^{2-} + 2mH^+ \leftrightarrow M_nO_{(n-m)}^{(2n-m)-} + mH_2O \qquad \text{Eq. 1}$$

oxoanion (tetrahedral) isopolyanion (octahedral assemblies)

POMs are attractive in terms of applications, such as in catalysis, biotechnology, nanotechnology, medicine, materials science and others. Among the various properties that POMs have shown in the field of catalysis, some of them rely on their redox properties. In fact, they are considered as electron reservoirs thanks to their high capability to bear and release electrons without decomposing or change their structural arrangement. They can also be present in different structural configurations rendering large variety in shape, size and composition. Furthermore, their attractive biochemical and biological characteristics have increasing interest for their uses in the field of medicine, as for example anti-tumoral, anti-bacterial and anti-viral properties [24].

The first synthesized POM was reported by Berzelius in early 19th century [25]. POM structures are frequently formed in aqueous medium, but they can also assemble in non-aqueous media or even in the solid state such as in mineral compounds. [26]

Among the different types of heteropolyanions of POM series, the Keggin structure is the best-known polyatomic configuration adopted by POMs. Its structure was first described by Keggin via X-ray diffraction in 1933. It contains a general formula of $(XM_{12}O_{40})^{-n}$ in which the alpha form is its most stable isomer. [27]

One of the main characteristics of Keggin heteropolyacids is their strong Brönsted acidity in aqueous media because of the easy protons dissociation. These species are therefore soluble

in several polar solvents. Despite the lack of studies on their acidity constants in water, phosphotungstic acid $H_3PW_{12}O_{40}$ (PW12) is considered as the heteropolyacid with the highest Bronsted acidity among the Keggin series. It presents even higher acid properties than concentrated $HClO_4$ or H_2SO_4 mineral acids. [28] [29] This fact explains their use in acidic homogeneous catalytic reactions for esterification or dehydration processes. [30] The anion size of the Keggin POM allows the protons to be delocalized over the whole polyoxoanion negative charge structure, which makes these counter cations very acidic species. [27] In some cases, POMs are deposited on substrates for their use in heterogeneous electrocatalysis, in order to take advantage of their redox properties in the manufacturing of electrochemical sensors. [27] As a matter of fact, redox catalysis of Keggin POMs constitutes one of their principal fields of application.

POMs have also demonstrated to serve as catalysts for desulfurization processes, for removal of thiophene sulphides for instance. [31]
POMs can also be used for other types of applications than homogeneous or heterogeneous catalysis, even if 80% of their uses are catalysis related. To cite some of them, they have been used as sensors for analytical devices [32], film-forming corrosion inhibitors, [33] and even as protein precipitation agents [34],[35], [36].

The interesting redox property of POMs was presented. In this field, some POMs offer even more interesting properties towards epoxidation reaction. Indeed, when POMs react with hydrogen peroxide, peroxo groups are created and these structures are key chemical constructions for oxidation reactions.

1.4 POMs as catalysts for epoxidation reactions

Many polynuclear complexes of polyoxometalates containing one or more peroxo groups have been studied for the oxidation of organic substrates with hydrogen peroxide as oxidant. Nevertheless, the only polyperoxotungstate complex that has been isolated and fully characterized is from the Italian group of Venturello. This complex has shown to have very competent oxidation capabilities in redox reactions, which will be described in the next section. [37]

1.4.1 Ishii-Venturello catalysts:

In 1983, the Italian research group of Venturello reported the direct oxidation of alkenes with hydrogen peroxide and polyoxophosphotungstate-based catalyst.[37] Five years later, the Japanese research group of Ishii, stated the epoxidation of allylic alcohol under two phase conditions using hydrogen peroxide and a (cetylpyridinium)$_3$ ($PW_{12}O_{40}$) catalyst. [38] Therefore, they are the pioneers of the use of polyoxometalates species for the epoxidation of alkenes. Thanks to extra investigation, the group of Venturello published a new paper about the isolation of the presumed active POM species $\{PO_4[W(O)(O_2)_2]_4\}^{3-}$ (=PW4), also called Venturello anion, responsible for the selective epoxidation of olefins.

Further studies conducted by other research groups [29] [40], have claimed that PW4 species could be formed either by reaction of their tungstate and phosphate precursors (as shown in Equation 2) or by degradation of $H_3PW_{12}O_{40}$ with H_2O_2 and H_3PO_4. [41] These two stoichiometric reactions are illustrated by Eq. 2 and Eq. 3. An excess of hydrogen peroxide is used, it is called the Venturello conditions (molar ratio H_2O_2/W = 8.5), which is not shown in the following equations. [42]

$$4\,H_2WO_4 + H_3PO_4 + 8H_2O_2 \underset{\leftarrow}{\rightarrow} [PW_4O_{24}]^{3-} + 12H_2O + 3H^+ \qquad \text{Equation 2}$$

$$H_3PW_{12}O_{40} + 2H_3PO_4 + 24H_2O_2 \underset{\leftarrow}{\rightarrow} 3[PW_4O_{24}]^{3-} + 24H_2O + 9H^+ \qquad \text{Equation 3}$$

Both reactions lead to the formation of stoichiometric amounts of PW4. Besides, both reactions form many other peroxo species products than PW4. As Gao et al [43] demonstrated, there exists a large number of peroxo species formed by the decomposition of the Keggin clusters with hydrogen peroxide in Eq. 3. Species with low W/P ratio are present and are written $[P_mW_nO_o(O_2)_p]^{x-}$. The most reported ones are mono-, bi-, tri- and tetranuclear anions $[PW_nO_q]^{x-}$ (where n = 1-4). [41] This phenomenon has not been demonstrated yet for Eq. 2.

As these peroxo species possess similar vibration bands and fingerprints in IR and in Raman spectroscopies, their identification is difficult to certify.

Subsequent studies of the Ishii-Venturello catalysts explain the presence of these different peroxo species in the catalytic reaction process. These include spectral characterizations of several peroxotungstates species, including PW4, a dinuclear metal peroxo species

$\{[WO(O_2)_2(H_2O)]_2O\}^{2-}$ and $[PW_nO_q]^{x-}$ (where n = 1-4). All these species derive from PW12 and excess aqueous hydrogen peroxide. As Hill's group experimented, the catalytic reaction does not produce one clean inorganic product. It generates three resonances in the liquid ^{31}P-NMR spectrum, none of which being characteristic of known Keggin derived polyoxotungstophosphates. The PW4 species is believed to be, the active species responsible for the active oxygen transfer toward the olefin to form the epoxide [40]. However, it is known that the problem of isolation of intermediate species that appear during the catalytic reaction is difficult. In fact, these active species have a short live-time, and present in low concentrations in order to be isolated. By opposition, species that are isolable are usually not the true catalyst(s) but, they represent kinetic repositories of species in equilibrium with the true catalysts or by-products, that are irrelevant to the catalysis. [39]

Consequently, even if a fully detailed mechanism has not been elaborated yet for the Ishii-Venturello epoxidation; however, some key points have been already clarified. One is that the rate law for the stoichiometric epoxidation of the alkene by PW4 is = k [PW4] [alkene]. Also, liquid ^{31}P-NMR experiments indicate clearly that, the catalysts (PW4) form subsequent peroxospecies (SPS) after transferring the oxygen from the PW4 structure to the cyclooctene. It also shows that these SPS readily convert back to PW4 under turnover conditions (here being biphasic with aqueous peroxide) and that PW4 is by far the dominant polyoxotungstophosphate species present under such conditions. This implies that the regeneration of PW4 after the oxygen transferring is faster than the epoxide formation itself [39].

The general reaction scheme is illustrated as follows:

$$[PW_{12}O_{40}]^{3-} \xrightarrow{H_2O_2 \rightarrow H_2O} [P_mW_nO_o(O_2)_p]^{x-} \xrightarrow{H_2O_2 \rightarrow H_2O} [PW_4O_{24}]^{3-}$$

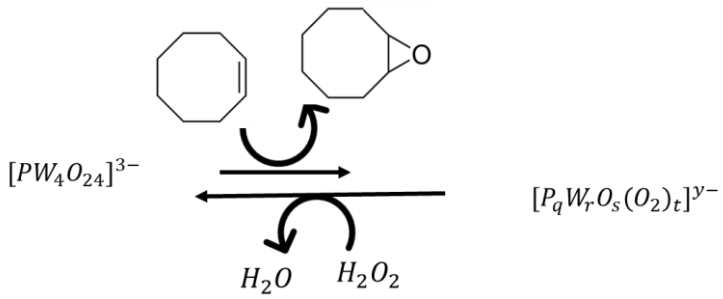

Equation 4: The main process of the Ischii-Venturello epoxidation. The upper part concerns the PW12 precursor that is activated by the hydrogen peroxide to give different peroxo species, including PW4 that is the active species., On the bottom-part, PW4 catalyses the reaction and acts as an oxygen carrier in between the hydrogen peroxide and the cyclooctene. This latter is then regenerated thanks to hydrogen peroxide as well.

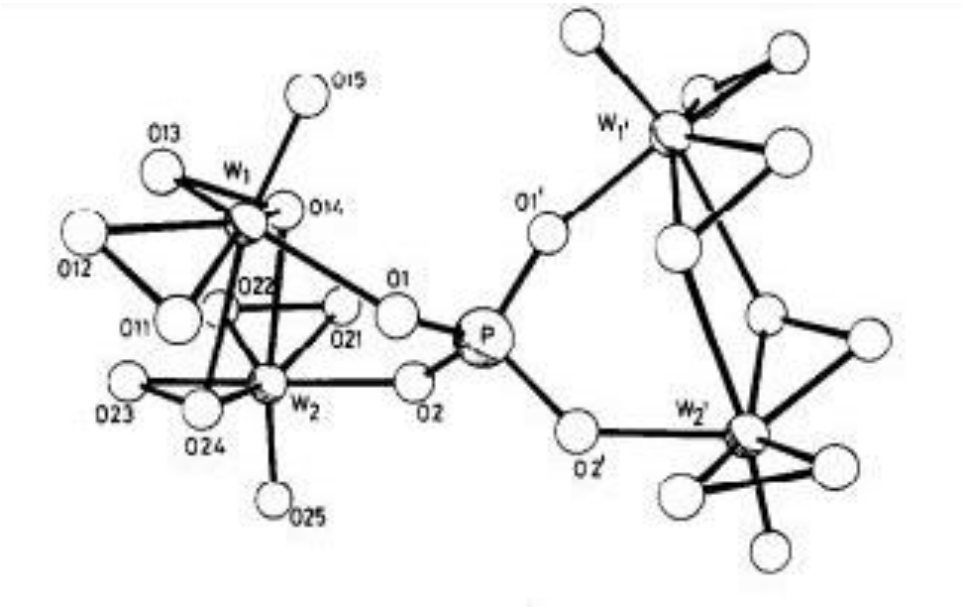

Figure 2: Ischii-Venturello anion $PW_4O_{24}^{-3}$ illustrating the atomic structure and composition of the anion. [42]

The PW4 structure represented on figure 2, is not the only active species responsible for the epoxidation reaction, but it is the most kinetically significant one. Therefore, the dominant process of the epoxidation reaction by the Ischii-Venturello PW4 catalyst, is the one represented by the last part of the reaction in Equation 4 illustrated by Hill et al.

Even if the mechanism is not completely understood, results given by theoretical calculations are very similar to the mechanism of Sharpless as illustrated on Figure 3 below. [44, 45]

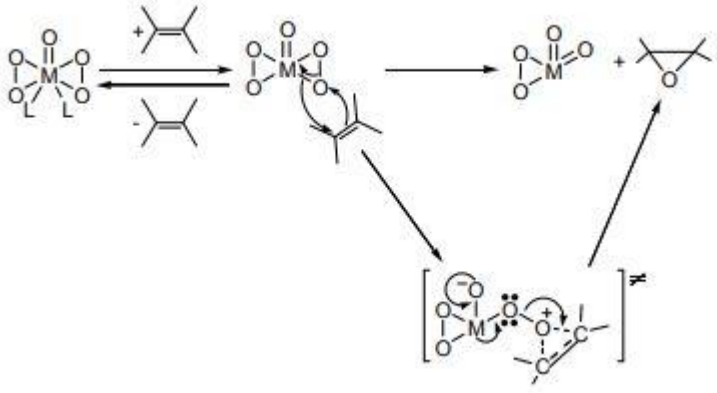

Figure 3: Mechanism of Sharpless epoxidation for Ischii-Venturello anion. [45]

However, this process shares several limiting factors that defeat the potential value of the catalytic epoxidation reaction. Toxic and carcinogenic chlorocarbon solvents are required in order to successfully achieve such high catalytic epoxidation performance. Also, turnover

experiments have shown modest values since the catalyst can rapidly deactivate during the catalytic reaction.[39] Finally, the catalyst can decompose irreversibly in the presence of high concentrations of epoxide at the end of the catalytic reaction. [39]

1.4.2 Heterogenization of the PW4 catalyst:

Considering the ecological disadvantages of the massive worldwide production of epoxides, and active catalysts like those of Ischii-Venturello, greener heterogeneous catalyst processes could be one of the most favourable options from an economic and ecological point of view. The heterogenization of the soluble PW4 catalyst of Venturello, could be an interesting approach in order to render those soluble species, insoluble particles in the catalytic mixture. Several strategies have already been developed to form heterogeneous catalysts from soluble POMs in liquid-phase oxidation reactions. These strategies follow two ways, one is to immobilize the POMs on a solid support, and the other is to form insoluble POM materials by selecting an appropriate counter-cation. [46]

Nevertheless, heterogenization of POM species still remains a difficult challenge. On one hand, the immobilization of POMs is commonly performed through adsorption, encapsulation, covalent linkage or ion exchange processes onto insoluble particles. On the other hand, the heterogenization of POMs by the selection of an appropriate counter-cations, suitable for a targeted reaction can sometimes trigger undesirable side effects. [41]

One important aspect to bear in mind, is that during a catalytic reaction, the substrate adsorption and product desorption on the catalyst surface are crucial steps in the catalytic reaction mechanism. As stated by the Sabatier principle, the reaction rate of a catalytic reaction is maximized for an optimal interaction between the substrate molecules and the catalyst surface. [47]

Next to that, the nature of the catalyst surface polarity, can increase the overall activity and selectivity of an alkene epoxidation reaction. [48] Therefore, it is assumed that the hydrophobic / hydrophilic properties of the catalyst surface, can impact among others, the catalytic performance of an epoxidation reaction, and it can be considered as much important as the number of catalyst active sites [41]. In this case, PW4 being hydrophilic and since the epoxide present a higher polarity than the alkene substrate (cyclooctene for instance), an over-adsorption of the epoxide product on the catalyst surface can lead to ring-opening and hydrolysis side reactions. Then, the epoxide can be transformed to diols side products which

by over adsorption, can poison the catalyst surface. As a result, the catalyst activity and selectivity are affected because undesired products are formed, as shown on the path (d) of figure 4. [41]

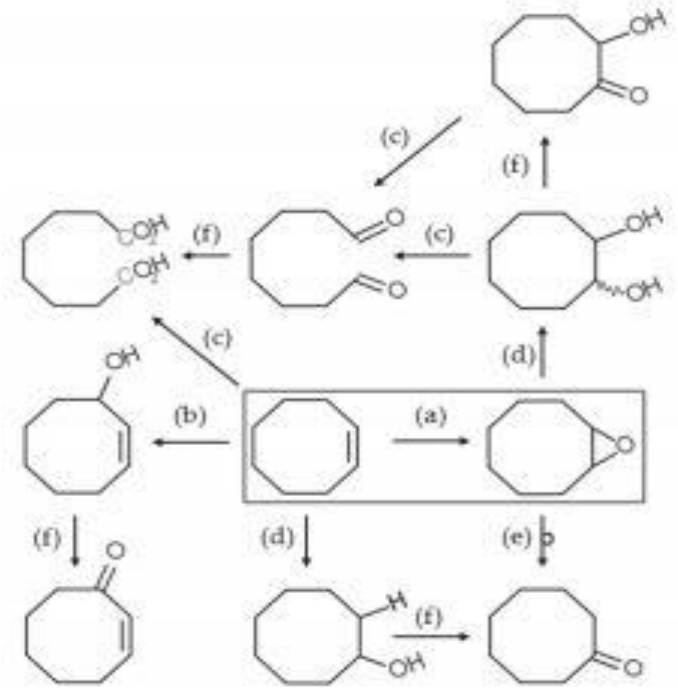

Figure 4: Schematic representation of the cyclooctene reactivity in the presence of H_2O_2 and a catalyst in acidic conditions. (a) epoxidation (= main reaction), (b) allylic oxidation, (c) oxidative cleavage, (d) electrophilic addition of water, (e) acid catalysed rearrangement, (f) over-oxidation reactions. [41]

In the example shown on figure 4, the targeted product is cyclooctane oxide which must be obtained by the catalytic epoxidation of cyclooctene with PW4 as catalyst. But if there is over adsorption of the epoxide product on the catalyst, many side reactions can occur. These side reactions can give alcohol products or ketones as shown by the paths (a)→(d) or (a)→ (e).

As Ischii & Venturello have exposed, PW4 is a very selective and active catalyst to perform this reaction. POM constitutes a strong negatively charged ion, therefore hydrophilic, whereas an olefin is very hydrophobic compared to the POM. While, hydrogen peroxide is more hydrophilic. Consequently, some adsorptions and affinity problems might arise, the overall hydrophobicity of the catalyst must be carefully chosen.

The POM hydrophobic properties need to be shifted in order to maximize the interactions between PW4 (the catalyst) and the alkenes. The catalyst needs to be hybridized to form a solid, so it becomes a heterogeneous catalyst. But it must also be complexed with the appropriate cation or ligands to form meso structures and therefore, have the right affinity with cyclooctene, hydrogen peroxide and the epoxide to have satisfying selectivity. Therefore,

the choice of the ligand is a crucial step. Recently, C. Swalus, a former PhD student who worked in the laboratory of Professor Gaigneaux, opted for the hybridization of the PW4 anion with a polycationic matrix containing alkyl sidechains with varying lengths [41]. With this strategy, 97% conversion with 85-90% of selectivity in epoxides were achieved.

Furthermore, organic-inorganic hybrids of PW12 have already been reported by some groups using bipyridine to hybridize Keggin structures. [39] Indeed, the creation of electrostatic interactions between nitrogens[1] of bipyridine and the terminal oxygens of PW12 create the connections between the organic and inorganic moieties. [40] In addition, other studies have described the ability of PW12 to form stable complexes with organic molecules, showing interesting results for organic ligands presenting electron donating nitrogen groups. [41] Knowing the relationship between the anions of PW12 and PW4, it is very likely that PW4 could also form stable complexes with organic molecules. Combining the hypothesis of PW4 heterogenization based on the chemistry of PW12, and C. Swalus research, a new strategy of heterogenization has emerged.

Unlike playing with a matrix of different alkyl sidechains lengths, giving different hydrophobic properties to the different matrixes; the homogeneous PW4 catalyst can be hybridized with organic ligands that can offer hydrophobic properties to the overall solid material. In addition, the polarity of the organic ligands can be finely modulated by functionalization with different functional groups attached to their structures. Indeed, the hydrophilic / hydrophobic organic environment that is brought by the ligand is thought to induce specificity. The influence that the different organic ligands have on the catalyst behaviour is essential to obtain high conversion and selectivity.

Therefore, terpyridines ligands (that must be able to bind the PW4 species) can be suitable candidates to form solid hybrid materials with PW4 species. Since bipyridine have proven to bind successfully PW12 anions via hydrogen bonding interactions, it is very likely that terpyridine will be able to bind PW4.

1.4 Objectives

In the framework of the present Master thesis, the main objective is to evaluate the influence of the catalyst polarity on the catalytic epoxidation reaction of cyclooctene. This main

[1] The cationic nature of the ligand comes from the protonation of the nitrogen in the pyridine. [49]

objective will be conducted by hybridizing a hydrophilic peroxo-tungstate acid $H_3PW_4O_{24}$ with hydrophobic functionalized terpyridine ligands.

Therefore, the catalytic reaction that will be chosen for the present work is the epoxidation of cyclooctene to cyclooctane oxide, using hydrogen peroxide as oxidizing agent. These two reactants were chosen for several reasons. Hydrogen peroxide contains a relatively high number of active oxygen species and only forms H_2O and O_2 as by-products. The alkene cyclooctene, is highly used in literature to probe catalytic epoxidation reactions, since it can achieve relatively high conversion and epoxide selectivity rates. [52]

In the frame of heteropolyanions containing P and W atoms, the groups of Ischii and Venturello have claimed that PW4 species is the best polynuclear peroxotungstate anion catalyst to perform efficiently such kind of epoxidation. Therefore, the choice of this catalyst precursor reveals itself to be relevant. However, several limitations of the PW4 catalyst process have already been demonstrated like the use of carcinogenic solvents.

Finally, since the hypothesis is that the limiting steps of the epoxidation reaction are the accessibility of the olefins to the catalyst active site and the product desorption steps, the challenge remains to find a compromise between both. Indeed, the resulting hybrid must contain a hydrophobic part that will favour the cyclooctene adsorption and epoxide desorption, and a hydrophilic part where the hydrogen peroxide is able to oxidize the anion. Thus, an equilibrium has to be found to satisfy both the reactant and product adsorption-desorption steps. This reason supports the idea to use different terpyridine ligands to optimize the hydrophobic properties of the catalyst. This challenge is illustrated on figure 5.

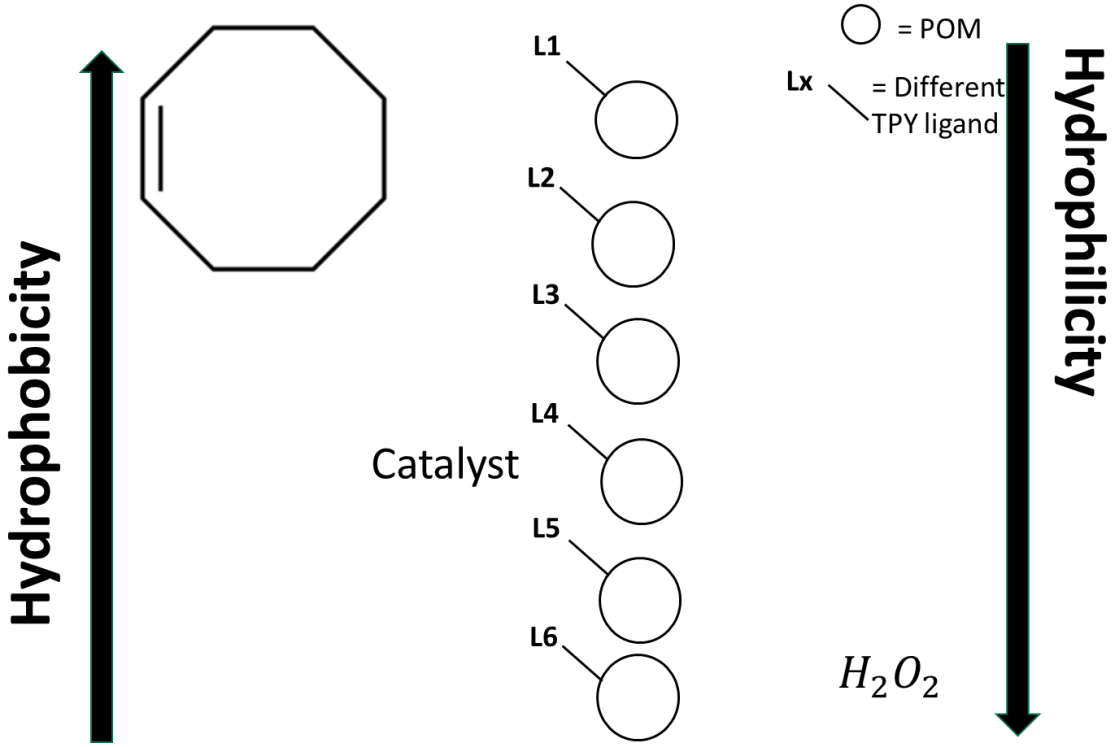

Figure 5: Challenge of the hybridization to reach an equilibrium between the hydrophobicity of the olefins and the hydrophilicity of the hydrogen peroxide.

Thus, 6 different terpyridine ligands are used to modulate the hydrophobic character of the hybrid catalysts. The ligands structures are then presented on figure 6. They all contain the same terpyridine core, five of them containing different functionalizations that were specifically chosen. Indeed, ligands with similar properties were chosen like with Cl-Tpy and F-Tpy. Comparable catalytic activities are to be expected from their corresponding hybrid. On the contrary, functionalization with opposite properties were chosen like, for instance electron withdrawing group (Py-TPY) and electron donating group (Ph-TPY & Tri-TPY). One can expect that these oppositions will be reflected in the catalytic performances of their related hybrids as well.

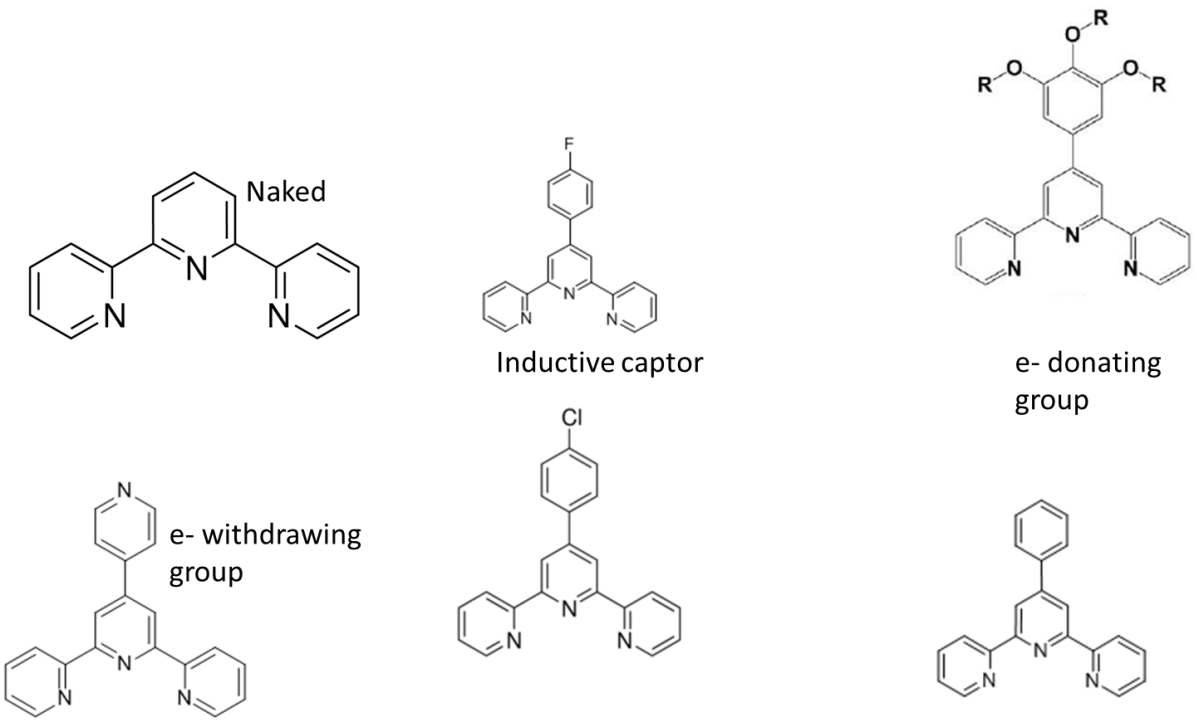

Figure 6: the first upper row from left to right: Naked-TPY (=naked-TPY), Fluorophenil-TPY (=F-TPY), TrimethoxyPhenyl-TPY (=Tri-TPY).
The second row, from left to right: Pyridil-TPY (Py-TPY), Chlorophenyl-TPY (Cl-TPY) and Phenyl-TPY (Ph-TPY).

1.5 Experimental strategy:

Here, the experimental strategy implemented to reach the objectives of this Master thesis is described.

1.5.1 Hybrids synthesis

First, it starts with the synthesis of the PW4 catalyst[2] with a bottom-up approach, using its precursors. Next, the organic ligands are synthesized with exception to the readily available unsubstituted terpyridine ligand. The purity of the different ligands is characterized by H-NMR and IR spectroscopy. Then the ligands and the solution containing the PW4 anion are mixed and the hybrid collected.

1.5.2 Hybrids characterization

Second, the resulting hybrids are characterized by various techniques such as IR & solid Raman spectroscopies, XRD, NH_3-TPD, nitrogen physisorption and ICP in order to ascertain the

[2] No protocol indicates the possibility of synthesizing pure crystals of {PO4[W(O)(O2)2]4}3-. This latter is always conjugated with a cation different than H^+

presence of both organic and inorganic parts but also, assess the thermal stability of the hybrids, their acidity and surface properties.

1.5.3 Catalytic tests and post-test characterizations

Third, the catalytic tests were performed to determine the activity of the hybrid catalysts for the epoxidation reaction of cyclooctene. This was done in heterogeneous conditions and to follow the catalytic reaction, GC measurements were taken. The goal is to check if different catalytic activities are observed among the hybrids. These would reflect the influence of the functionalization of the ligands and therefore, of the overall polarity of the hybrids and their affinity with the reagents.

Finally, the heterogeneity of the catalysts was studied as well as their recyclability to verify if they underwent any modifications during the catalytic reactions. Leaching test and post-catalytic test were thus carried out.

2. Materials & Methods

In this section, the materials that were used as well as the methods on how to use them are presented.

2.1 ATR-FTIR technique:

Fourier transform infrared spectroscopy is a characterization technique where an IR beam is passed through a sample, one part of the radiation is absorbed by the sample, the rest is transmitted to the detector. The resulting signal is translated into a spectrum containing the absorption and transmission of the beam representing the molecular fingerprint of the sample. Molecules in general vibrate according to different modes that are independent. A molecular vibration can be excited by an electromagnetic wave of a certain frequency, by absorbing a quantum of energy. The particularity is that a molecular vibration can have different levels of vibrational energy. The energy gap between these diverse states corresponds to the infrared region of the spectrum. Therefore, by shining IR light on molecules, these latter absorb these energy quanta and change their vibrational states.

The outcoming beam possess less intensity at the energy which is absorbed, which results in a peak on the spectrum. Two different molecules having the same IR fingerprint do not exist. This makes FTIR a technique of choice for sample analysis [53]. The intensity of a peak is a direct indication of the amount of absorbing species present according to Beer's law. FTIR offers the advantage to measure all of the infrared frequencies simultaneously and is therefore a fast-acquisition technique. The measured interferogram signal cannot be interpreted directly. Applying the Fourier transformation allows to plot the intensity at each individual frequency. [53]

Several modes of acquisition exist, mainly there are three types of accessories namely Transmission, ATR and diffuse reflectance. For this work, the Attenuated total reflection (ATR) mode is used. This operates by measuring the changes that occur in an internally reflected IR beam when the beam comes into contact with the sample. This is done by directing an IR beam onto an optically dense crystal with a high refractive index at a certain angle, giving total reflection. The internal reflectance creates an evanescent wave that extends until the sample

where it is attenuated. This attenuated beam returns to the crystal and is detected by the detector as illustrated by Figure 7. [54]

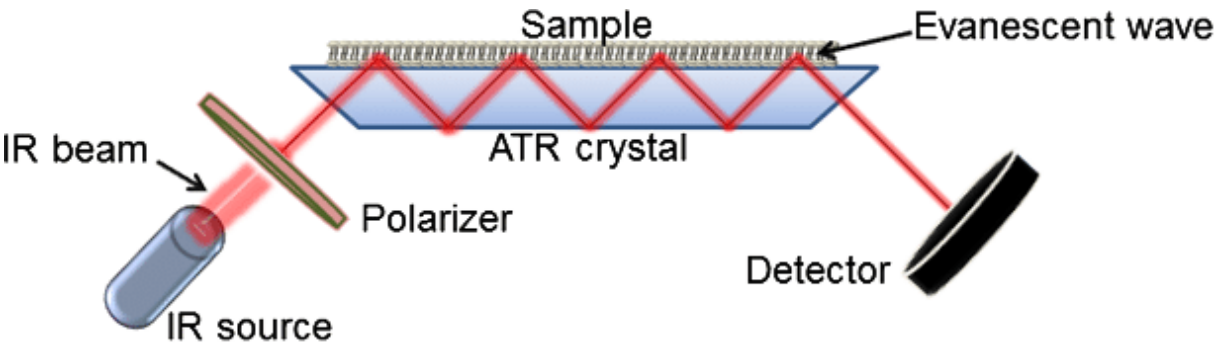

Figure 7: Schematic representation of an IR spectrometer working in ATR mode. [55]

Many samples were analysed through ATR-FTIR, mainly the ligands and the hybrid catalysts, in order to determine the nature of these species. The samples are slightly crushed before analysis. The spectrometer was a Bruker Equinox 55 FTIR, with a Bruker ATR Platinum cell containing a diamond crystal. The detector of the outgoing infrared beam is a dielectric DTGS with an iris aperture of 5000 µm.

The spectra were collected within the wavelength range from 400 to 4000 cm^{-1} at room temperature. An accumulation of 100 scans with a spectral resolution of 4 cm^{-1} yields the obtained spectra.

2.2 TGA-MS

Thermogravimetric analysis is a powerful technique that can characterize solid and liquid samples. The mass of the sample material is monitored while it is heated following a chosen heating program. Heat induces reactions and physical changes in the material. Mass changes are sometimes induced by these phenomena. Such measurements can be applied at different chosen heat rate either under air (or pure oxygen), nitrogen or argon. Therefore, a mass loss is plotted as function of temperature and time. Eventually, researchers can determine the temperature at which a mass loss occurs and thanks to a MS connected to the TGA apparatus, the gaseous compounds loss are identified. [56]

All the hybrid catalysts, precursors and ligands were analysed through TGA coupled with MS. Concerning the hybrids, the goal is to assess the number of ligands per POM unit that were present in those hybrids. The degree of polarity of a hybrid can already by evaluated by TGA by measuring the water loss. This water can either be physisorbed or chemisorbed.

5 to 20 mg of samples were introduced into a 70 µl alumina crucible cleaned at the red flame to avoid the presence of any remaining contamination. The crucible was introduced into a Mettler Toledo TGA/SDTA851e Thermogravimetric Analyzer, equipped with a Mettler Toledo TS081RO sample Robot and a Mettler Toledo GC10 Gas controller. The analysis was performed under a 50 ml/min air (class 2, UN 1002) flow, with a temperature rise of 10°C per minute starting at room temperature and going until 800°C. The TGA apparatus was connected to a Mass spectrometer (MS) Pfeiffer Vacuum (Thermostar) used to identify the gas molecules that were released during the heating process.

2.3 XRD

Crystalline materials are characterized by their orderly periodic arrangements of atoms. A crystal is defined by its unit cell, the basic repeating unit. Therefore, parallel planes of atoms intersecting the unit cell are used to define directions and distances in the crystal. Diffraction occurs when each object in a periodic array scatters radiation coherently, producing concerted constructive interference at specific theta angles. This is due to the wavelength of X-rays that are similar to the distance between atoms. Bragg's law is a model to understand this phenomenon.

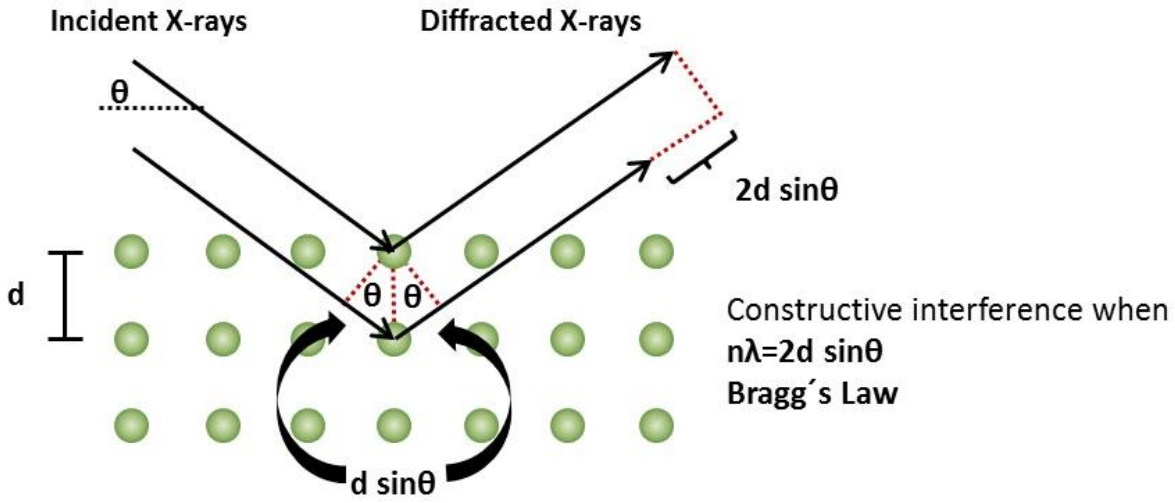

Figure 8: Schematic representation of XRD diffraction [57]

For parallel planes of atoms, with a space d_{hkl} between the planes, constructive interference only occurs when Bragg's law is satisfied. The space d illustrated on Figure 8, determines the peak positions. Peak areas are much more reliable than peak heights as a measure of intensity. [58].

The machine used is a Bruker diffractometer D8 Advance. The X-ray source works with a power of 1200 W (30 mA, 40 kV). Analyses are run are at room temperature, via the ray $K\alpha_{1,2}$ of the Copper (λ = 0.15418 nm), with a range of 2θ angle going from 5° to 80°, with a step of 0.02 ° and 0.15 second per step. The detector is a Lynxeye XE-T from Brucker as well.

2.4 Raman Spectroscopy:

Raman spectroscopy relies on the polarizability of molecules. When a sample is irradiated with a monochromatic beam, two types of scattering can occur, the elastic one and the inelastic one. High intensity laser is used with wavelengths in the range of visible or near-IR. An oscillating vibration in the molecules is produced from the photons that excite the molecules by the induction of an electric dipole. [59] At this moment, either there is interaction between the polarization and a vibrational state different than the one occupied by the molecule, or either there is no interaction. This latter corresponds to the elastic scattering (Rayleigh diffusion) and there is no change in the energy of the beam when it interacts with the matter. This is the phenomenon that is mainly observed. The first possibility corresponds to the inelastic scattering. It results in either a gain (Anti-Stokes) by the photon of vibrational energy

of the irradiated species. This corresponds to the difference E_v between the excited vibrational state and the fundamental one. Or a loss (Stokes) of energy occurs induced by the photon, which transfers a part of its energy to the irradiated species. It is thus an activation of the molecule vibration. Therefore, here the energy of the diffused light is inferior to the initial beam. Only chemical species that do not have a net dipole moment are affected by the Raman effect.

The resulting spectrum obtained is composed of bands representing the active vibrations in the sample. Different molecules have different vibrational spectra because these depend on the masses of the atoms involved, the strength of their chemical bonds and atomic arrangement. This allows to identify the chemical species contained in a sample. [60]

Raman spectroscopy was used for solid and liquid samples. Therefore, two machines were used. For the liquid samples the analyses were performed in a Kaiser RXN spectrometer (diode-pumped frequency doubled Nd-YAG laser 532 nm wavelength, power ca. 50 mW, Mk II filtered probe head with 5.5-inch noncontact objective, spot-size ca. 0.7 µm). The resolution was 5 cm^{-1} and the frequency was analysed in the 4400 – 100 cm^{-1} regions. For each reported spectrum, 5 scans were accumulated, with an exposure time of 30 sec. For solid samples, a FT-Raman Perkin Elmer (Spectrum 2000) equipped with a Nd-YAG laser with 1064 nm wavelength and its power set at 100 mW was used. All the spectra recorded are the sum of 50 scans accumulated at room temperature in the 3500 to 100 cm^{-1} regions with a resolution of 4 cm^{-1}.

2.5 Nuclear Magnetic Resonance:

The general principle of NMR rests on the fact that many nuclei have a spin and that all these nuclei are electrically charged. If an external magnetic field is implemented, an energy transfer is possible between the fundamental energy to a higher level. This energy transfer corresponds to wavelengths in radio range. When the spin returns to its base level, energy of that same frequency is emitted. By measuring this signal and processing it, NMR spectrum of the concerned nucleus are obtained. [61]

2.5.1 H-NMR

Proton nuclear magnetic resonance is a technique to identify accurately the structure of hydrogen-containing molecules. Every hydrogen atom behaves as a small magnet and then aligns with a bigger external magnetic field B_0 produced by the machine. Also, there is another less stable alignment which corresponds to as situation when the magnetic field of the hydrogen nucleus is opposed to the external one. It is therefore possible to flip from one to another alignment by supplying exactly the right amount of energy (another external magnetic field via a gradient). The resonance condition happens when the alignment gives the lowest energy state. Peaks on the spectra for different molecular structures are at distinct places because, they need slightly different external magnetic fields to bring them into resonance at a particular radio wave frequency, thanks to a shielding by the nearby valence electrons. [62] Next to this, the size (ratio of area under the peaks) of the peaks gives information about the number of hydrogens in each environment. Spin-Spin coupling is the phenomenon allowing structural assignments of the spectra. The protons signals are in fact split into two or more sub-peaks. The cause is the magnetic interaction between neighboring, non-equivalent NMR-active nuclei and their spin. [63]

A 300Mhz H-NMR was used to identify and confirm the purity of the synthesized terpyridines and those that were synthesized one year ago by Simon de Crane [64]. To do so, about 5 mg of ligands were dissolved in 500µl of deuterated chloroform ($CDCl_3$ Eurisotop, 99.80% D). Solvents that are either deuterated or aprotic are necessary in order to avoid having protons coming from the solvent that could interfere with those coming from the sample. Deuterated solvents are used to in NMR to stabilize the magnetic field strength. [65]

2.5.2 Liquid ^{31}P-NMR:

^{31}P-NMR was also achieved to identify the leached species of the catalysts. It is a much less sensitive technique than proton-NMR but remains more sensitive than ^{13}C-NMR because ^{31}P has an abundance of 100% [66], [67]. This method is massively applied for the characterization of organic and inorganic molecular structures. The obtained spectra are relatively easy to interpret since the coupling constant and chemical shift properties are similar to the one of 1 H-NMR [67]. The principle remains the same as in H-NMR.

^{31}P NMR spectra were recorded at room temperature (296 K) on a Bruker Avance 500 spectrometer operating at 202.46 MHz for the selected nucleus. Experiments were run under TopSpin program using a BBO{1H,X} probehead equipped with a *z*-gradient coil. NMR signals were referenced to the ^{31}P NMR frequency of an 85% H_3PO_3 solution in H_2O (δ = 0.00 ppm). A standard zgpg program was employed using a Waltz-16 decoupling scheme with a pulse of 80 µsec. The number of scans was 256, the spectral window was 100 ppm (with O1P at 0.00 ppm) and the acquisition time was set to 1.6 sec.

2.6 Nitrogen physisorption (BET)

Gas (N_2) adsorption is used to measure the porosity and the specific surface area of porous solid samples [68]. The method consists in calculating the pore size distribution by the adsorbed quantity of the gas at a specific pressure and temperature. But first, before putting the sample in contact with a known volume of nitrogen, the sample is degassed to drive off all the compounds adsorbed in normal conditions. The known amount of nitrogen inserted and measuring the remaining amount after adsorption, a pressure drop is obtained. So, one can determine the number of adsorbed molecules. [69] In this case, nitrogen condenses at the meniscus of liquid in the pore only if the equilibrium vapor pressure P on the meniscus is smaller than the saturated vapor pressure Po. Therefore, a relation between P/P_0 and the number of adsorbed molecules n_{ads} can be established. Graphically, this is represented by isotherms that can be interpreted by models like the one developed by Brunauer, Emmet and Teller (BET), allowing to have the specific surface area. For correct measurements, value of P/P_0 above 0.30 and lower than 0.1 cannot be taken. [69].

The pore size analysis is based on the application of the Kelvin equation on adsorption, with a multilayer thickness correction on the pore walls. The method of Barrett, Joyner and Halenda (BJH) in 1951 is the most popular way of deriving the pore size distribution from an appropriate nitrogen isotherm. [69] The pore size-range that can be assessed by nitrogen physisorption is 2-50 nm.

A known amount of sample (around 120 mg) was introduced in a tube with a filler rod to reduce to the maximum the volume of dead space and minimizing the errors concerning due to it. The tubes were degassed with a Vacprep 061 degasser from Micrometrics at 100°C until

a pressure in between 50 and 100 mTorr was reached (6 hours). Then, the sample weight was measured once again and the tubes, along with isothermal jackets, were here introduced in a Micrometrics Tristar 3000 analyser. Liquid N_2 was used to cool down the tubes.

2.7 TPD Temperature Programmed desorption with ammonia

TPD is a characterization technique used to characterize the number and strength of acid sites on oxide surfaces. It is based on the chemisorption of ammonia on the surface of the sample. Ammonia spontaneously adsorbs on surface to minimize its energy. This phenomenon being exothermic, the number of adsorbed molecules decrease with increasing temperature. The small molecular size of ammonia allows it to penetrate into all pores of the solid. [70] The desorption temperature of the ammonia can be correlated to the strength of the interaction between ammonia and the acid sites on the surface. This allows to determine the strength of the acidic sites. [71]

This technique was specifically developed in the field of catalysis, and it studies the interaction of gases with solid surfaces. It is therefore a useful tool to assess active sites on catalyst surfaces but also to understand the catalytic reaction mechanisms that lie under adsorption, surface reaction, and desorption [72], [73]. Concretely, a normal run is performed with a small amount of catalyst that is placed in a reactor and put in contact with the adsorbent (ammonia). Inert gas is then flowed into the catalyst at a programmed heating rate. The heating allows the adsorbed gas (ammonia) to return to the gas phase and is monitored by a Mass spectrometer. The obtained results are a record of concentration of the desorbed gas as a function of time. Usually, the spectra consist of one or more peaks. Finally, the shapes and positions of the peaks are related to the desorption process and furnish information on the way the gas is adsorbed.

NH_3 is used for TPD measurements to detect acidic sites since this species has basic properties. First, a weighed amount of sample is introduced in a quartz TPD tube between two layers of glass wool. The tube is then inserted in a Hidden Isoschema Catlab Microreactor module coupled to a Hidden Analytical QGA quantitative gas analysis system. A specific temperature and gas flow program were applied. The sample is subject to a temperature increase from 40°C to 150°C in 10 min followed by an isotherm stage at 150°C during 2h, in an air (Class 2,

UN 1002) flow (50mL/min). After that, the temperature is decreased to 50°C in 10 min under an Argon flow (UN 1006, purity 99.99%) (50mL/min). Next, an isothermal stage at 50°C during 1h10min under NH_3(5% volume)-Ar flow (20-30 mL/min). This flow is then replaced by Ar flow (50mL/min) during 1h50 and kept at 50°C, later a temperature rise from 50°C to 800°C in 1h10min is applied and a final isothermal stage at 800°C during 1h.

2.8 Inductive coupled plasma -Atomic emission spectroscopy (ICP-AES)

This technique allows to identify and measure chemical elements present in samples. It can be used for both liquid and solid samples. Solid samples must first be dissolved in a solvent (typically acid) to obtain a solution. Any traces of organic element in the sample must be removed. The concentrations or trace of major elements can be determined through this technique with a detection limit in the parts per billion range. [74] An ICP apparatus is constituted of an ICP torch as presented on the figure 9 below, that is made of three concentrically arranged tubes of quartz glass.

The sample solution is first introduced as a fine aerosol of droplets. This aerosol passes into a spray chamber where the larger droplets are removed. Then, the analyte passes in the torch body. There, it is mixed with argon. A coupling coil transmits radio frequency wave and heats the Argon (up to 10000 K) and produces an argon plasma. This latter dries any remaining solvent and leads to the sample atomization. Finally, the atomic emissions of the atoms present in the sample return to their fundamental state yielding light that is then detected.

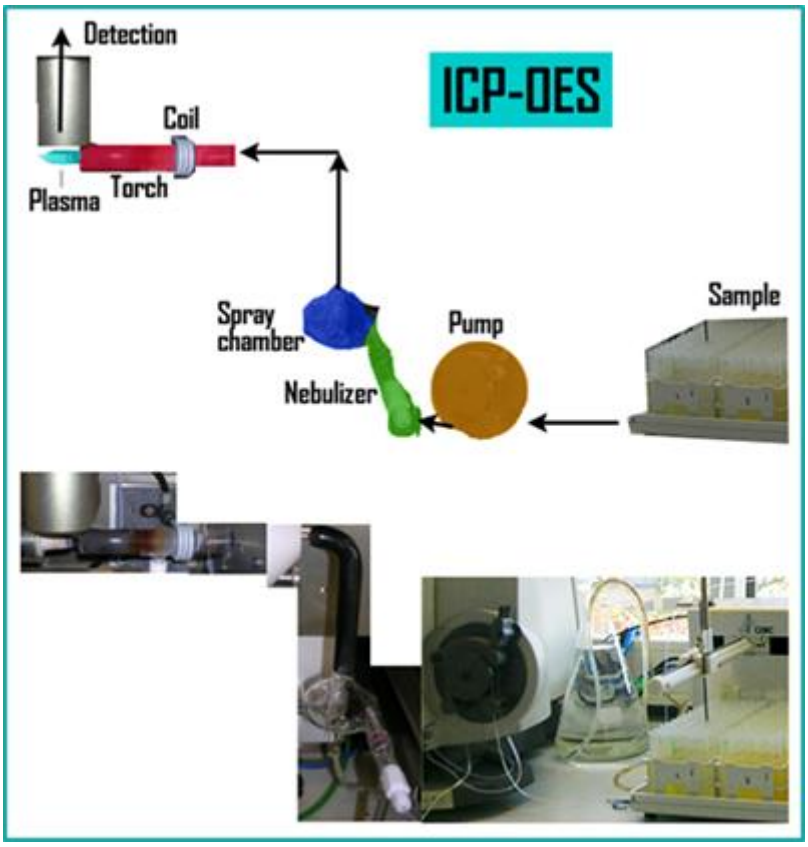

Figure 9: illustrating the schematic apparatus of an ICP [75]

The machine used was an ICAP 6500 Thermo Scientific equipment. The samples were calcined at 500°C to burn the organic matrix and were then decomposed via mineralization by sodium peroxide fusion in glassy carbon crucibles. The detection limit depends on the element analysed but is approximately equal to 1 to 10 ppb. These experiments were carried out at the Earth and Life Institute (ELI) of the UCLouvain, by Anne Iserentant.

2.9 Synthesis of the Hybrids:

In order to synthesize the PW4 hybridized with the functionalized terpyridines, the first aspect to take into account was to use as minimum as possible of hydrogen peroxide to solubilize the tungstic acid. Indeed, when a terpyridine is in presence of hydrogen peroxide, it is easily oxidized and yields a N-O species that is unwanted. Furthermore, according to the literature [76], N-O species could also be able to oxidise olefins. But, in the framework of this project, only PW4 is desired to oxidise the olefin. The role of the ligand is only to heterogenize the catalyst and alter its hydrophobic properties. In this case, a liquid Raman study of the minimum amount of hydrogen peroxide to use to solubilize tungstic acid was performed. 5

equivalents of H_2O_2 versus 1 equivalent of H_2WO_4 (Sigma-Aldrich, 99% purity, powder) is the correct ratio to apply.

Once the quantity of hydrogen peroxide is known, the rest of the synthesis can go on by working stoichiometrically. Theoretically the reaction to reach PW4 is the following.

$$4H_2WO_4 + H_3PO_4 + 8H_2O_2 \underset{\leftarrow}{\rightarrow} [PW_4O_{24}]^{3-} + 12H_2O + 3H^+ \qquad \text{Equation 5}$$

As mentioned earlier, the stoichiometric amount of hydrogen peroxide cannot be respected since a high excess of hydrogen peroxide is needed to solubilize tungstic acid. Yet, Ischii-Venturello use an excess of 10-times the amount of H_2O_2 versus W. While here, only 5-fold excess versus W is used. Therefore, the reaction can be rewritten as:

$$4H_2WO_4 + H_3PO_4 + 20H_2O_2 \underset{\leftarrow}{\rightarrow} [PW_4O_{24}]^{3-} + 12H_2O + 3H^+ + 12H_2O_2 \qquad \text{Equation 6}$$

It is of primary importance to be very accurate when performing this reaction knowing that there exists a lot of different peroxo species that can be obtained according to the ratio used.

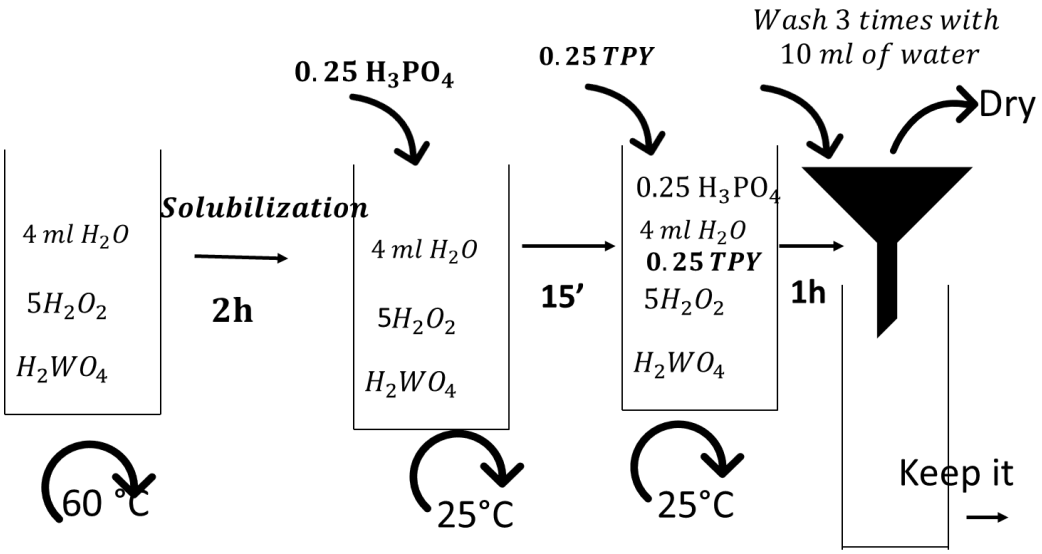

Figure 10: Schematic representation of the short-stirring time synthesis. All the quantities are represented in equivalent.

Once the phosphoric acid (Merck, 85% in weight) is added at room temperature, we stir for 15 min and then pour into the solution the functionalized ligand and stir for one more hour. After that, the suspension was filtered on Büchner and rinsed three times with 10 ml of water. The recovered solid was then dried under vacuum and the filtrate kept preciously in a flask. The hybrids obtained by this synthesis method are called "short-stirring time hybrids" since the stirring after the addition of the ligands is only 1h long.

The Ischii-Venturello method to synthesize PW4 hybridized with a quaternary ammonium salt (tetrahexylammonium chloride) was also performed. The protocol is described in Annex II part A.

Finally, the synthesis which was kept and used to synthesize all the hybrids that were characterised is as follows:

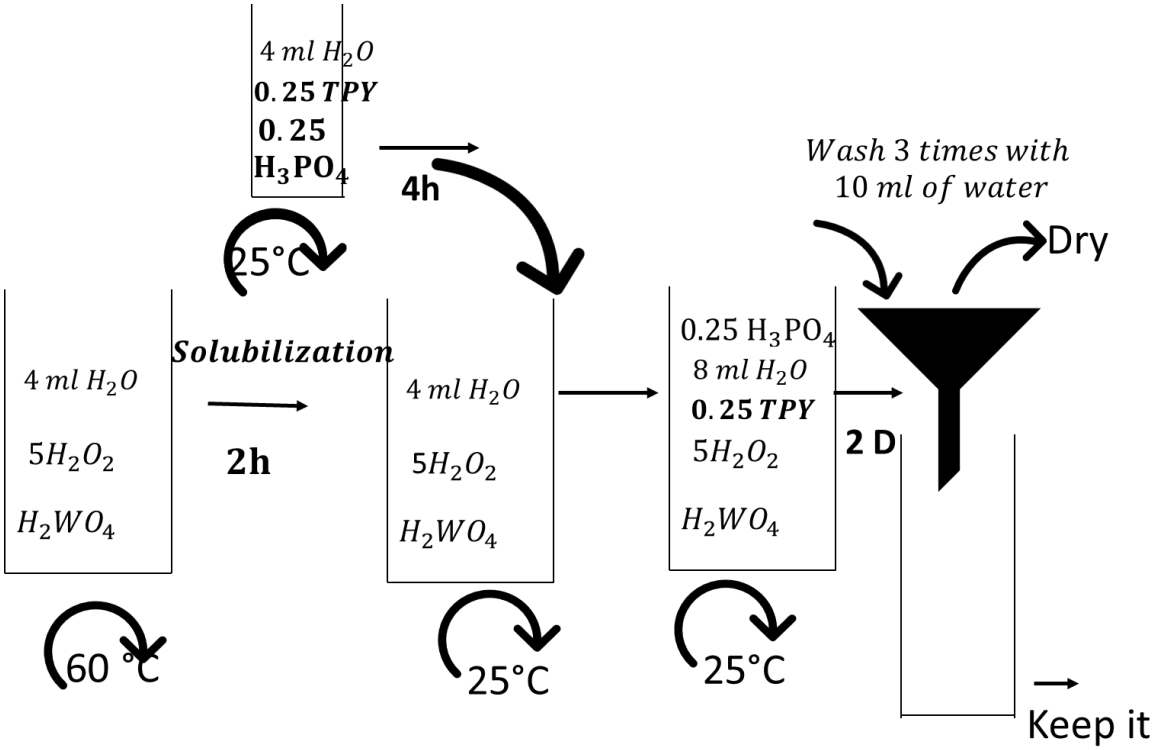

Figure 11: Schematic representation of the final synthesis protocol to synthesize PW4 long-stirring time hybrids with organic functionalized Terpyridine

First the solubilization of the tungstic acid precursor is still the same. Next to that the organic TPY is mixed in an aqueous solution with phosphoric acid for 4 hours. Then these two solutions are mixed thoroughly for two days. Eventually, the filtration was performed on Büchner to recover the solid. The hybrids synthesized by the method described on figure 11 are called "long-stirring time hybrids" since the stirring time after addition of the ligands is 2 days long.

2.10 Synthesis of the ligands

Some of the ligands were freshly synthesized and others were already synthesized by Simon de Crane, the previous Master student working on this project in 2017-2018, in the same laboratory [64]. His ligands were characterized by H-NMR to check if they were still pure (see Annexe II part B) while others that were lacking, were synthesized according to the protocols

found in Annexe II part B. Only the Naked-TPY was not synthesized, but bought at Sigma-Aldrich, > 98.5% purity.

2.11 Catalytic tests:

In order to assess the activity and the efficiency of the hybrid catalysts, the catalytic tests were performed. Cyclooctene (CO) was used as a reagent, H_2O_2 is the oxidative agent, dibutylether was also added as an internal standard and finally acetonitrile as the solvent. The choice of DBE as internal standard is not random. Indeed, it is very close in composition and in retention time to the CO, and furthermore, it remains unchanged throughout the whole reaction. This internal standard helps to account for all the possible losses of sample that can take place during the many steps from the catalytic test until the GC measurement itself. Indeed, sample loss is possible simply by systematic error, matrix effects or even by transfers.

The reaction takes place in a 10 mL double-ended flask where 9.18 ml of ACN (VWR chemicals, 99.9% purity), 170.8 µl of DBE (TCI, >99% purity), 136.5 µl of CO (TCI, >95% purity) and 510.6 µl of H_2O_2 (Roth, 30% purity) are introduced. The reactor is immerged in an oil bath at 70°C during the whole reaction, linked to a refrigerant that is hermetically sealed with a rubber plug. The catalyst is added before the CO whose addition launches the reaction at time 0. 0,01 mmol of the hybrid catalyst is used. An aliquot is taken every hour starting at time 0. 200 µl is extracted via a syringe and diluted with 350 µl of acetonitrile. The mixture is then filtered with a 0.2 µm pore size syringe filter in order to remove the solid catalyst. After that, the sample is ready to be run on the GC. 8 points are taken in one day.

0.01 mmol of catalyst is not a random quantity that has been chosen. Indeed, with this amount, the ratio of olefin over catalyst is of 100. Venturello either used a ratio of 50 or of 266. Another Chinese group [77] used a ratio of 100 as well.

2.12 Gas chromatography (GC)

Gas chromatography was used to quantify and identify the reaction products during the catalytic reaction. This technique is very efficient to analyse volatile compounds. It is an analytical instrument which principle is to inject the sample solution in a gas stream which carries the sample into a separation tube called the column. Nitrogen is used as the carrier gas. Then the various components are separated inside the column. The detector measures the quantity of the components that exit the column. Also, to measure the concentration of a given sample, a

calibration curve has been done with a standard sample of cyclooctene and cyclooctane oxide (Sigma-Aldrich, 99% purity, solid) with known concentration and then the area can be compared to calculate the respective concentration of those compounds in the unknown samples [78]. The detector is a FID which stands for Flame Ionization Detector. This latter is recognized as the standard method of measuring hydrocarbons and has a detection limit in the low picogram or femtogram range. Here, the sample gas in introduced into an air-hydrogen flame after exiting the column. The high temperature causes any hydrocarbons in the sample to produce ions when burning. These ions are detected by a metal collector that is biased with a high DC voltage. The collected current is thus proportional to the rate of ionisation which itself depends upon the concentration of hydrocarbons. [79]

The results are displayed on a graph where in the x- axis, is the retention time. This corresponds to the time that each species stayed in the column. The volatility, bulkiness and steric factors of each compound is responsible for this event. Also, the peak area is related to the amount of species that were detected. This means that the higher the peak area is, the more concentrated the sample was in the specific compound. In order to calculate the exact concentration, a calibration curve was performed.

To do so, solutions of known concentrations in cyclooctene, cyclooctane oxide and internal standard were measured in order to establish the calibration curve. The ratio of the areas $A_{sample}/A_{internal\ standard}$ are plotted versus the ratios of the concentrations $C_{sample}/C_{internal\ standard}$. This yields the calibration curve following a simple linear equation:

$$\left.A_{sample}\right/_{A_{IS}} = m \times \left.C_{sample}\right/_{C_{IS}}$$

Equation 7: Linear equation of the calibration curve. m corresponds to the response factor, A_{sample} is the area of the unknown sample and C stands for concentration. IS stands for internal standard.

The response factor is different for each species. It is determined by the slope of the calibration curve of the respective species. By isolating C_{sample} in Equation 7 one obtains the concentration of the unknown sample.

The gas chromatograph is a GC-2010 Plus with a FID-2010 Plus detector bought to Shimadzu. It is combined with an AOC-20s auto-sampler and an AOC-20i auto-injector. 1 µl is the injected volume in split mode. Thus, the injector is heated to 275 °C before injection of the liquid sample so that it volatilises, sample is there contained within a quartz glass line. Then the sample gas is swept by the carrier gas and enters either into the GC column or is evacuated by the split line. [80] This method offers the advantage to be easy to use and produce narrow

analyte band on the column. However, it is not sensitive to compounds present in traces and also for thermal sensitive compounds.

The column is a SH-Rtc-5 column from Shimadzu as well. It is a low-polarity stationary phase of 5% diphenyl polysiloxane and 95% dimethyl polysiloxane, with a length of 15 m, an inner diameter of 0.25 mm and a film thickness of 0.1µm, heated at a column temperature of 60°C. The temperature program is divided in two steps: a first segment from 60° to 100°C (7.5 °C/min) and a second fragment from 100 to 240°C (30°C/ min). Helium is used as carrier gas at a flow rate of 30 mL/min. 1 µL aliquot is injected into the GC column.

2.13 Leaching tests, recyclability tests and statistical tests:

Leaching tests are primordial in order to know if the catalyst is indeed heterogeneous. To start such an experiment, the complete conversion curve of the catalyst of interest is necessary. Then the test starts just as an ordinary catalytic test but is stopped after a time $t_{1/2}$, corresponding to the half of the maximum conversion. There, all the liquid in the vial is up taken, centrifuged 15 min at 15000 rpm. Next, the supernatant is filtered with a syringe (0.2µm of pores diameter) and the filtrate is poured in a new clean beaker with a new clean stirrer and heated to 70°C. After, aliquots are taken every hour to check whether there is still a catalytic activity or not.

Concerning the statistical analysis of the catalytic activity, several tests are needed. Indeed, it is of primary importance to know if the variance in between each catalyst is coming from either the organic part, the anionic part or just the random errors. Indeed, with only one catalytic test from one sample, it is impossible to know if the test is representative. However, if at least 3 tests are run with the same catalyst (coming from the same batch), then an error can be calculated. This evaluates only the difference coming from one same sample. After that, repeatability tests can be performed, assessing the variability coming from different samples, synthesized under the exact same conditions. At the end, one can compare if the variability between two different batches is only coming from the random errors or from the difference between the batches.

2.14 Expression of the catalytic performance:

In the aim of evaluating the catalyst performance, some parameters, have to be correctly defined to avoid any misunderstanding.

The conversion of a reactant *r* is defined as the quantity of this reactant *r* transformed at a given reaction time as a function of the initial quantity of reactant r_0.

$$Conversion\ [\%] = \frac{n_{r0} - n_r}{n_{r0}}$$

Where n_{r0}, is the initial mole number of reactant *r* and n_r the mole number of *r* at a given reaction time.

The selectivity of a product *p* is defined as the quantity of product *p* formed at a given reaction time as a function of the quantity of the reactant *r* transformed.

$$Selectiviy\ [\%] = \frac{n_p}{n_{r0} - n_r} \times 100$$

Where n_p is the mole number of product *p* formed at a given reaction time.

The yield of a reaction corresponds to the conversion times the selectivity.

The reaction rate [$mol_{reactant}$/L.h] can also be calculated. It corresponds to the number of moles of reactant transformed per liter and per hour.

Figure 12: Picture of the reaction set-up.

3 Part I: The synthesis of the hybrids:

In this section, the results are presented in a chronological and ordered way to reflect to the best the reflexion that has been made during the whole time spent at the laboratory. It starts with the results of the solubilization test of tungstic acid, then continues with the different hybridization trials until the final synthesis plus the characterizations of the first hybrids. A discussion follows these results to evaluate the success of the synthesis.

3.1 Results

3.1.1 H2WO4 solubilization

H_2WO_4 is acid [81]. However, in its solid state, it does not dissolve in water at any temperature. [82] Therefore, in order to bring it to a homogeneous aqueous state, an excess of hydrogen peroxide is needed. This oxidation process takes place at 60°C under vigorous stirring until all the suspended particles of H_2WO_4 disappear. [83]

As hydrogen peroxide is present in excess in the aqueous mixture, the terpyridine ligands that will eventually be added to the mixture, can also undergo an oxidation process. Indeed, the nitrogen atoms contained in the ligands, can easily become N-O species in an oxidative environment. Therefore, in order to check this hypothesis, a pure functionalized terpyridine precursor was mixed with an excess of hydrogen peroxide and was analysed by ATR-FTIR.

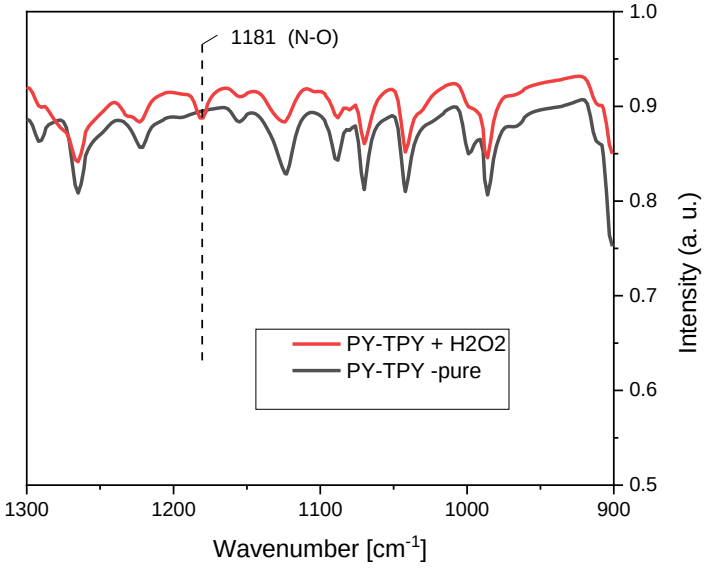

Figure 13

On figure 13, two spectral lines of pure ligand and the ligand that has been mixed with hydrogen peroxide are displayed. A peak at 1181 cm^{-1} for the oxidized ligand is present and

absent for the pure ligand. This vibration mode is characteristic for the vibration of a N-O group in a terpyridine. [84]

Therefore, in order to assess the stoichiometric amount of hydrogen peroxide needed to oxidize H_2WO_4, a stoichiometric and a kinetic study was performed by Raman. The solubilization of H_2WO_4 was evaluated with several amounts of H_2O_2 and characterized in vitro via liquid Raman spectroscopy.

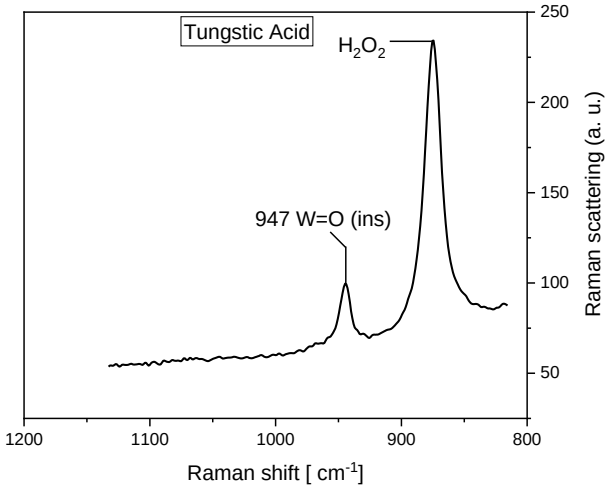

Figure 14: Liquid-Raman spectroscopy of H_2WO_4 precursor in water at time 0, when 6 equivalents of H_2O_2 have just been added. the peak of W=O vibration mode at 947 cm^{-1} illustrating when H_2WO_4 is insoluble (=ins)

Figure 14 illustrates the situation when H_2WO_4 powder is mixed with water and some hydrogen peroxide at time 0. The peak at 947 cm^{-1} corresponds to H_2WO_4 when it is insoluble. The peak that appears at 876 cm^{-1} belongs to the vibration mode of unreacted hydrogen peroxide

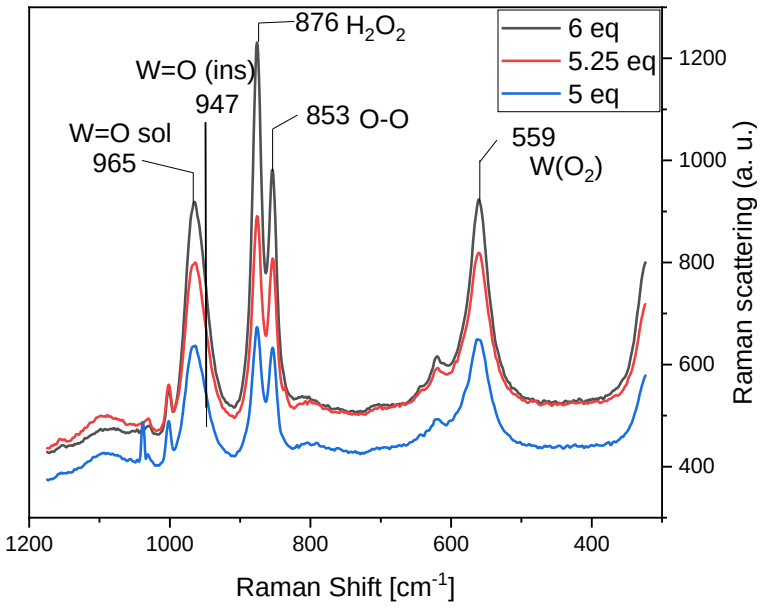

Figure 15: Stoichiometric test to assess the solubility of H_2WO_4 in water with hydrogen peroxide.

On figure 15, the analysis showed that the lowest[3] amount of hydrogen peroxide needed to completely oxidize one eq of H_2WO_4 is 5eq of H_2O_2. Indeed, the vibration band W=O of the insoluble H_2WO_4 precursor at 947 cm^{-1}, is shifted to 965 cm^{-1} when it becomes soluble [85], [41]. In fact, another indicator of solubilization of H_2WO_4 is the colour of the solution: once it is transparent, it means that the solubilization is complete. The peaks at 853 and 559 cm^{-1} correspond to the (O-O) and $W(O_2)$ vibration modes of pertungstic acid respectively.

Concerning the time needed for a complete solubilization, 5eq of H_2O_2 were added to 1eq of H_2WO_4 in presence of water at 60°C and the sample was analysed by Raman in vitro over time. Figure 16 shows the shift of the peak going from 947 cm^{-1} to 965 cm^{-1} as the time passes and finally after almost 2h, the shift is completed, and the solution had become clear.

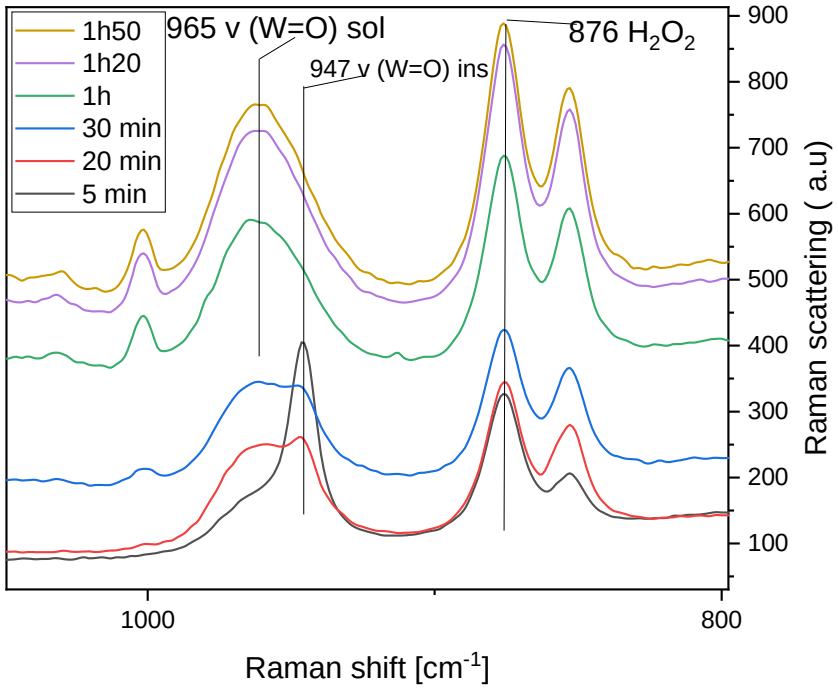

Figure 16: Liquid Raman spectra of the kinetic analysis for the solubilization of H_2WO_4 in water with hydrogen peroxide

3.1.2First hybridization trials

Before presenting the hybridizations tests, the 6 different ligands used were characterized to ascertain their purity. Indeed, some of them were synthesized in November 2017 by Simon de Crane [64] and some were freshly synthesized. These ligands were studied by IR and H-NMR.

[3] With 4 equivalents, there is no shift of the peak from 947 cm^{-1} to 965 cm^{1}, not shown here

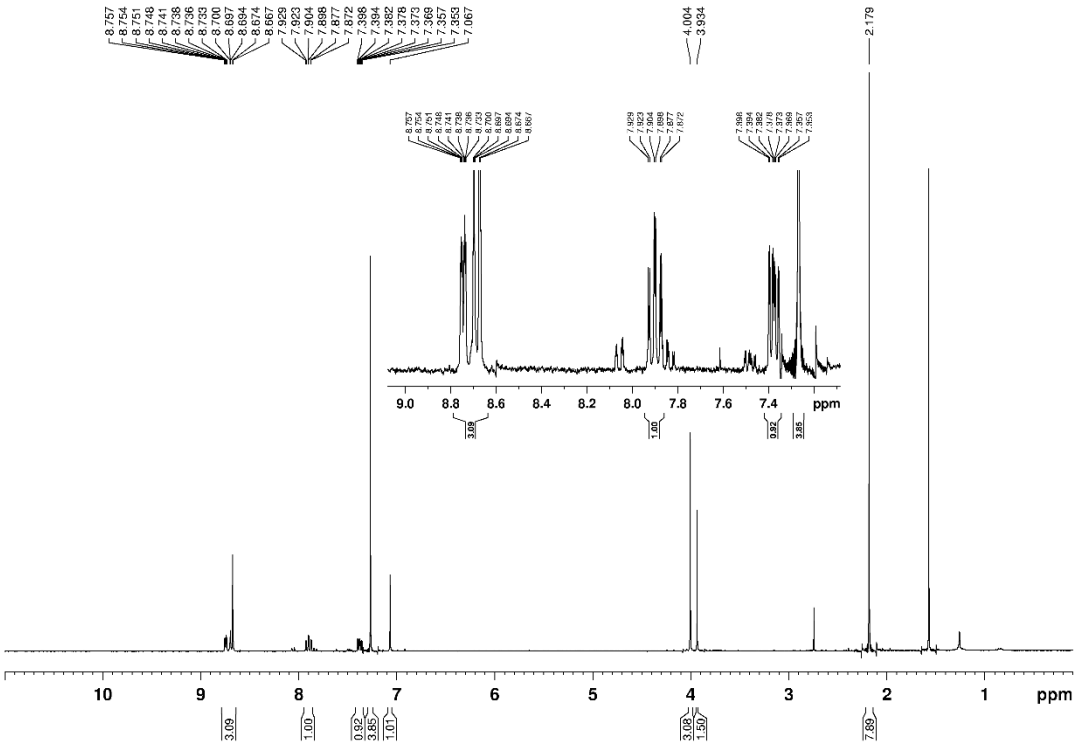

Figure 17: H-NMR spectrum of the Tri-TPY pure ligand in $CDCl_3$.

Figure 17 illustrates the Tri-TPY pure ligand analysed by H-NMR in $CDCl_3$. The NMR spectra of the other pure ligands are presented in the Annexe II part B. Thanks to both H-NMR and IR analysis their purity and chemical nature was confirmed.

The first hybridization test was performed using the pyridyl-Terpyridine ligand[4] , and the resulting hybrid was analysed by FTIR presented on figure 18. The figure 18 shows the pure organic ligand spectrum and the corresponding hybrid in order to compare the hybrid with its precursors. In order to see if the hybrid contains PW4 or not, the dotted vertical lines, corresponding to the expected peaks of PW4, are plotted. [86] By matching the bands of the hybrids with the PW4 bands, it seems that PW4 hybrid was not obtained. Indeed, almost all the peaks of the hybrid do not match with the peak positions of the expected Ischii-Venturello anion, except for the peak at 728 cm^{-1}. However, the peaks of pure ligand and of the hybrid are not that different from each other. Indeed, most of the peaks of the two species are similar or exactly the same. Therefore, the peak close to the expected PW4 band at 728 cm^{-1} in the hybrid spectrum, is probably not coming from the

[4] Since there was more of this ligand available from the ligands synthesized by S. de Crane than the others

vibration of the presumed PW4 but the 735 cm^{-1} bending of the aromatic ring-H bounds of the ligand as presented in Table 1. The full spectra of figure 18 can be seen in Annexe IV.

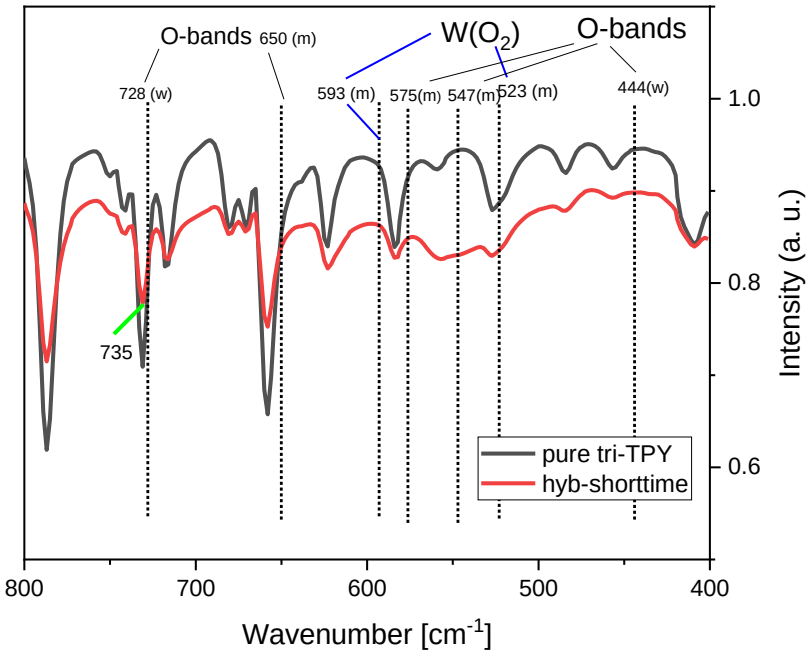

Figure 18: ATR-IR spectrum of the first hybridization test, where pure Tri-terpyridine ligand (black curve) is mixed with the aqueous mixture containing PW_4 species to form the hybrid (red curve). The vertical dotted lines correspond to the expected vibration peaks of PW4 species, as depicted by Ischii-Venturello [86]

It is known that the fingerprint of terpyridines on IR spectra is situated in the range 1600-400 cm^{-1} while, the one of the PW4 is situated from 400 cm^{-1} to 1100 cm^{-1}. An attempt has been done in order to assign the peaks of figure 18 and therefore recognize the composition of the sample. The vibration bands displaid on figure 18 can be correlated to the vibration bands of the ligands as listed in Table 1.

Table 1 ATR-IR vibrations bands corresponding for the Py-TPY ligand [87], [88]]

Observed	References	Description
-	1270	Overt. or inter-ring str. (not allowed)
-	1248	
-	1210	
-	1138	
1090	1090	Ring-H-in plane bend
-	1083	
1069	1063	Ring str. and bend and C-H Bend
1039	1039	Out-of-plane ring H-bend
-	991	Ring breathing
897	890	Ring-H-out-of-plane bend

751	753	Ring-H out-of-plane bend
735	738	Ring-H-out-of-plane bend
-	710	Ring torsion
653	651	Ring bend (in-plane)
618	618	Ring bend (in-plane)
400	398	Ring torsion

Note. Abbreviations: str.= stretching, overt.= overtone, bend.= bending, adj.= adjacent, s= strong, w= weak, m=medium, sh= shoulder

As presented in section 3.1.1, it is possible that the nitrogen in the terpyridines is oxidized by the excess of hydrogen peroxide. However, according to the IR spectra illustrated on figure 19, no oxidation is observed at 1181 cm^{-1}. Indeed, no peak is present on the hybrid spectrum at this wavenumber value.

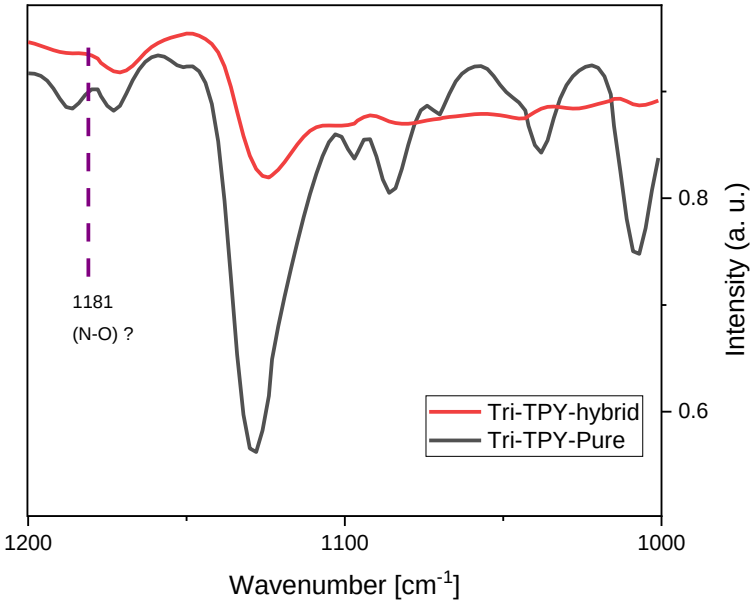

Figure 19

The thermogram on figure 20 shows a 20% inorganic content of the hybrid total mass at the end of the experiment. Moreover, there are 3 mass losses that occur at different temperatures: one at 100°C, the second at 350 °C and the third at 500°C. Thanks to the mass spectrometer placed after the TGA apparatus where the released compounds are analysed, it is known that the first mass loss corresponds to water, while the second and third ones correspond to the Tri-TPY ligand that is being burned because the masses that are detected are NO_2 and CO_2, which can only come from

the terpyridines. The inorganic part of the hybrid is not affected by the TGA measurement, which proves that it is a thermally stable species.

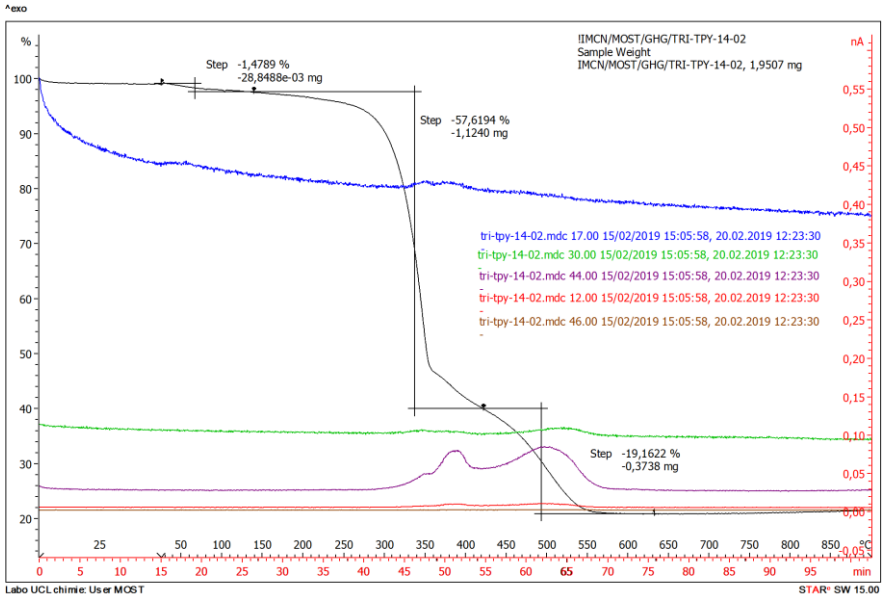

Figure 20: TGA-MS of the first synthesized hybrid (Tri-TPY hybrid) showing the decrease of mass as function of increasing temperature.

However, how can we explain the fact that the ligands are burning in two steps? The hypothesis is that the hybridization is not finished and that there is in the collected samples, a lot of unreacted terpyridines. While the ligands bound to the PW4 species are burning at around 500 °C, the linked ligands would need more energy to detach from the PW4 (whereas the not- interacting-ones need less energy to just burn). This would justify why two mass losses are detected. This hypothesis is verified by running a TGA of the ligand alone and comparing with the thermogram of the corresponding hybrid.

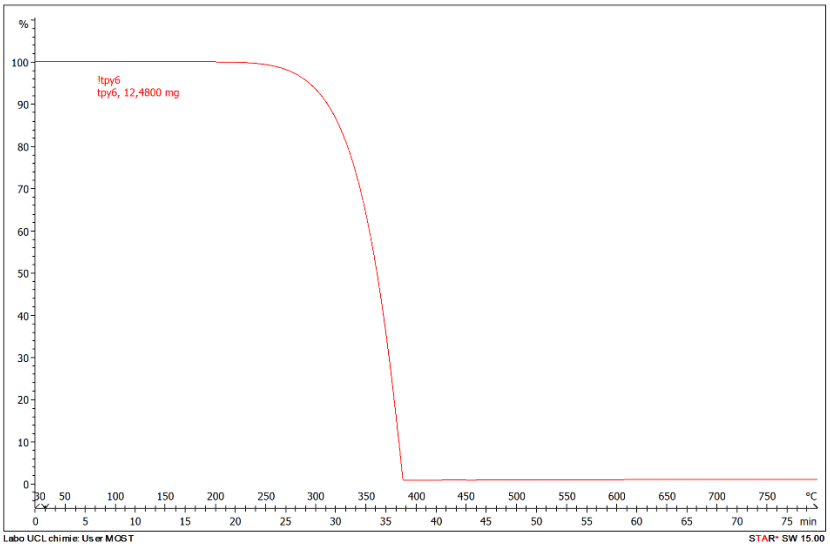

Figure 21: The TGA analysis of the pure Py-TPY ligand

Figures 21 reveals that the Py-TPY ligand is burning from 320 °C to 370 °C and that there is no remaining mass at the end of the analysis.

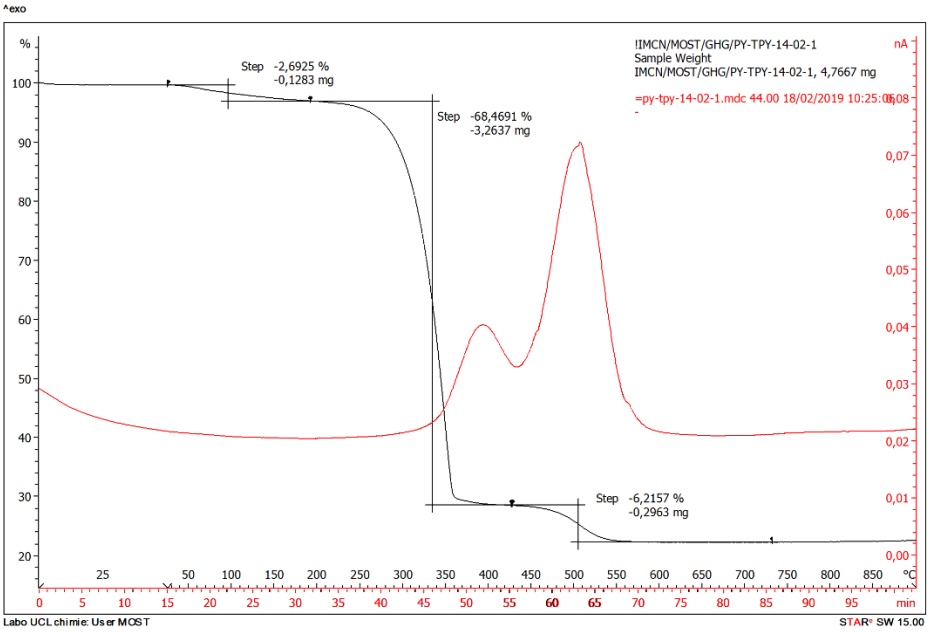

Figure 22: The TGA analysis of the short stirring time Py-TPY hyb.

Figure 22 shows that in the Py-TPY hyb, the ligand is burning in two steps, one between 300 °C to 360°C (= step 2) and then, between 460 °C and 520 °C[5] (= step 3). The idea that the collected hybrid is mainly composed of pure unreacted ligand, that burns during step 2 and only a few of PW4 correctly hybridized with the ligand, burning in step 3, is correct. By removing the mass of the unreacted ligand on figure 20, the exact amount of terpyridine ligands that has formed a hybrid

[5]Before that the ligand burns, there is also a loss of water, which is step 1.

with the PW4 species can be computed. Doing so, more information concerning the interaction between ligand and inorganic part of the hybrid can be obtained.

In the last step, around 6.21% of the initial mass (M_0) are lost, which are equal to 0.2963 mg of Py-TPY ligands that were probably linked to the PW4 species. At 800°C, about 23% of the initial mass remain, which are equal to 1.0791 mg of PW4 (1150 g/mol). Finally, when one calculates these results in moles, one obtains:

$$n_{ligand} = (0.0621 \times M_0) / MM_{ligand} = 9.6 \times 10^{-7} \text{ mol} \qquad \textit{Eq 8}$$

$$n_{PW4} = (0.23 \times M_0) / MM_{PW4} = 9.4 \times 10^{-7} \text{ mol} \qquad \textit{Eq 9}$$

Consequently, according to these results, one equivalent of PW4 binds one equivalent of Py-TPY ligand.

Still in the idea to identify the similarities and differences between the pure ligand and its corresponding short-stirring-time hybrid, XRD analysis were run. For instance, figure 23 illustrates the differences that were observed via XRD analysis. A first observation is that the hybrid has much lower crystallinity than the pure ligand. A second one, is that the highest diffraction peaks of the pure ligand are also present, as highest diffraction peaks in the hybrid situated at 14°, 12.6° and 11.2°. According to these results, we understand that the hybrid sample is mainly composed of pure ligands and probably something else, possibly PW4 hybridized with the ligands. Indeed, there must be a chemical species that is responsible for the amorphous behaviour that is observed on the diffractogram. Because if there were only pure ligands, the diffractogram of the hybrid would be exactly the same as the one of the pure ligand.

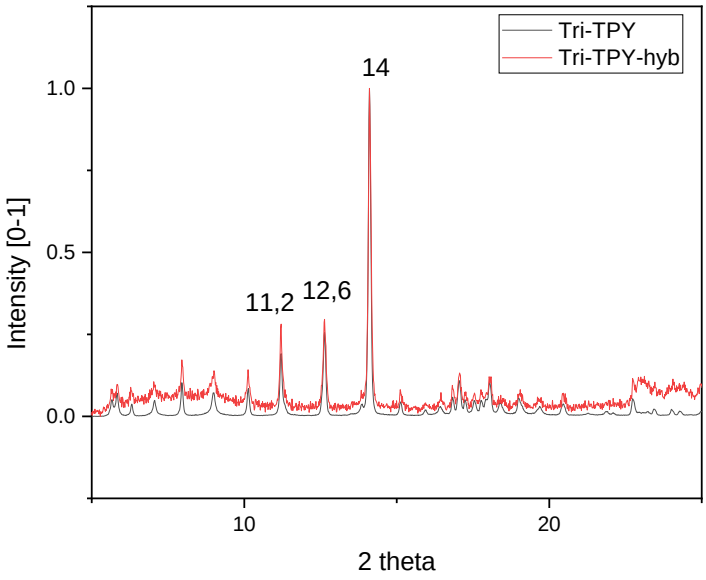

Figure 23

Another hybrid (Py-TPY hyb) has been synthesized according to the same procedure as Tri-TPY hybrid. However, for the sake of conciseness, its IR spectra, TGA and XRD results are displayed in the Annexes II part C and IV since the results and observations coming from these experiments are the same.

The Tri-TPY hybrid catalyst that was synthesized through this short-stirring-time synthesis method was then tested to see its activity towards the epoxidation reaction of cyclooctene.
The equation of the reaction is as follows:

$$\text{Cyclooctene} + H_2O_2 \xrightarrow[\substack{70°C \\ Hybrid\ Catalyst \\ Acetonitrile\ as\ solvent}]{} \text{Cyclooctane oxide} + H_2O \qquad \textit{Eq 11}$$

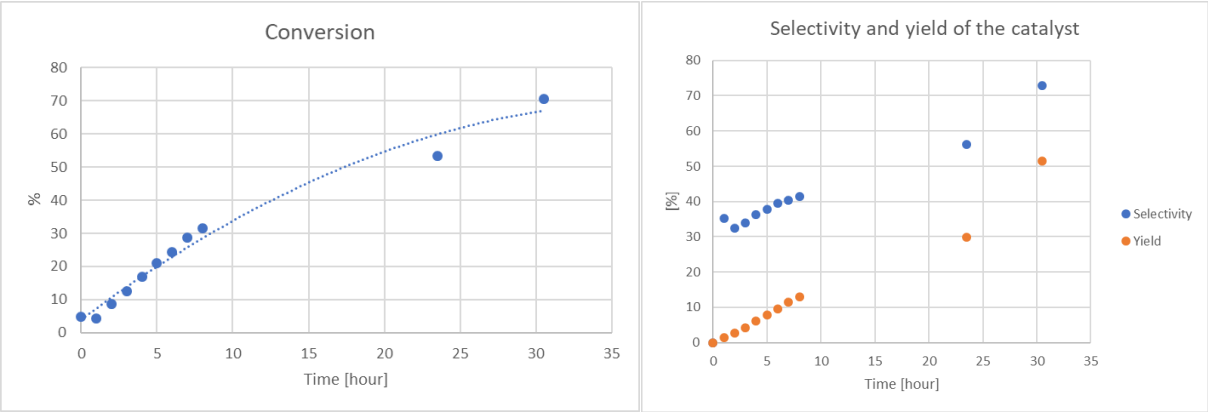

Figure 24: Conversion, Selectivity and yield profiles of the short-stirring time tri-TPY-hyb catalyst. (Conditions: 0.1 M cyclooctene, 0.1 M DBE, 9.18 µl acetonitrile, 0.01mmol catalyst, 0.5M H_2O_2, 70°C)

The graphs on figure 24 show the catalytic results of the Tri-TPY hybrid catalyst. The conversion of cyclooctene obtained with this catalyst accounts for 70% after 30 hours of reaction while the selectivity accounts for 75 %. In addition, the conversion does not seem to have reached a plateau. Probably, higher conversion values would have been reached after a longer time.

An extra experiment was performed to check whether the amount of catalyst inserted in the reaction mixture affected the catalytic activity. This was done by doubling the amount of Tri-TPY hybrid catalyst in the reaction mixture. As a result, no significative difference in the conversion and selectivity was observed, meaning that this is not the amount of catalyst in the system that limits the catalytic activity.

3.1.3 The long stirring time synthesis

The Ischii Venturello synthesis was performed in order to be able to compare the hybrids formed from the PW4 prepared as described by Ischii and Venturello. Indeed, according to the IR, TGA and XRD results shown until here, the different synthesized hybrids (Tri-TPY and Py-TPY short time) do not contain PW4, or at least it has not been confirmed. By comparing the collected hybrids with the true PW4 hybrid, the differences and similarities will appear between these latter. The exact protocol coming from Venturello [86] was thus reproduced. See Annexe II part A. The obtained catalyst was characterized by IR and the related spectrum is shown on figure 25.

The figure 25 illustrates clearly the vibration bands of the PW4 anion as it is referred in the literature. Only two peaks do not match exactly, these are the ones situated at 1087 and 1057 cm^{-1}. However, at 1057 cm^{-1}, the presence of a shoulder is noticed. While the peak supposed to be at 1087 cm^{-1} is shifted to higher value around 1090 cm^{-1}. One reason could be that the followed

protocol specified that after recovery of the white solid by filtration, the latter should be recrystallised in dichloromethane and diethyl ether to give a single crystal, which has not been done. The characteristic bands of the Ischii-Venturello anion appear at 1087 and 1057 (P-O), 984 and 971 (W=O), 855 and 845 (O-O), 593 &523 ($W(O_2)$), and other bands at 728, 650, 574, 547 and 444 cm^{-1}. [86]

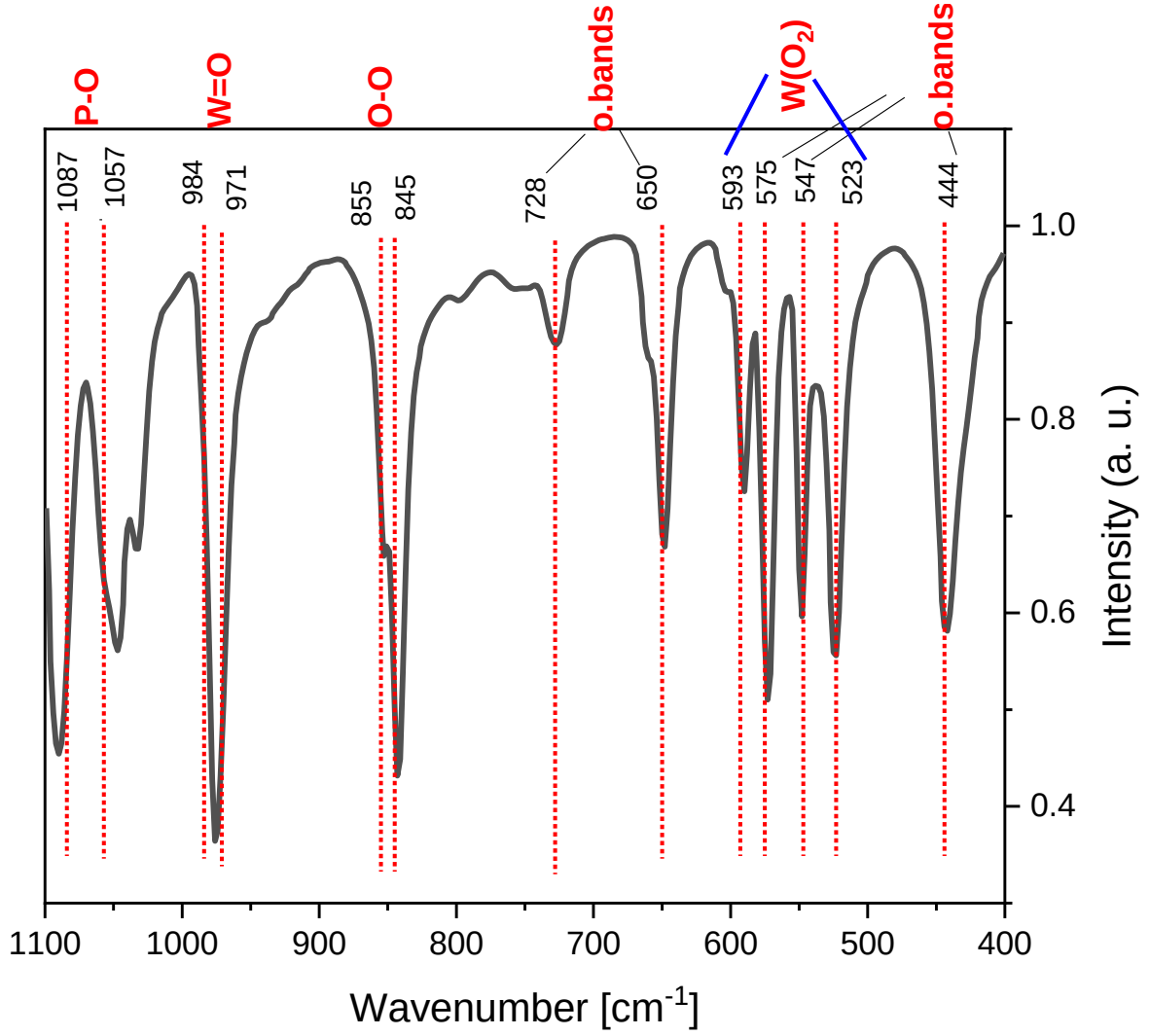

Figure 25: ATR-IR of the Ischii-Venturello PW4 anion hybridized with a quaternary ammonium salt (tetrahexylammonium chloride)

The Ischii-Venturello anion was easily formed by following the exact protocol described by Venturello. This questioned the impact of the biphasic conditions brought by this procedure and also the affinity of their ligand (tetrahexylammonium chloride) that is solubilized in an organic solvent (benzene). The idea of Ischii-Venturello is that the 2 phases conditions allow the ligand to easily fish the PW4 species at the interphase of the aqueous and organic phases. Maybe the tetrahexylammonium chloride has more affinity to PW4 than terpyridines have. Still, the Ischii-

Venturello protocol was applied with exception that the ligand was not their quaternary ammonium salt but instead, our functionalized terpyridine.

This experiment yielded two different solids (hybrid 1 and hybrid 2) that were collected simultaneously of which IR spectrum is displayed in figure 26.

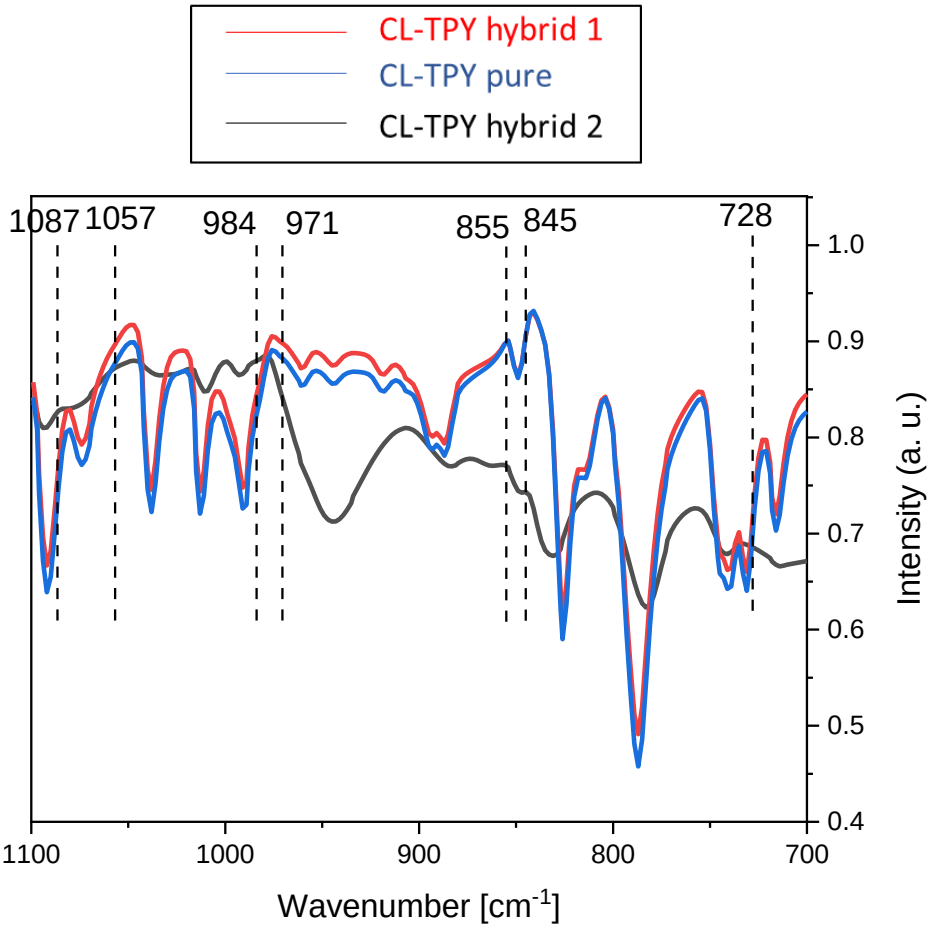

Figure 26: ATR-IR spectrum of CL-TPY pure (blue), CL-TPY-hyb1 (red) and Cl-TPY-hyb2 (black). The dashed vertical lines correspond to the PW4 fingerprint.

Figure 26 contains three IR spectra. In red (hybrid 1) and in blue are the short-stirring-time hybrid of Cl-TPY and the corresponding pure ligand respectively. These two have a very similar spectrum. While the last spectrum in black, hybrid 2 is different from the 2 others. This leads us to proposes that another species of hybrid is present[6]. The fact that 2 different hybrids were collected suggested that maybe not enough time was allowed for the hybridization to occur. And as illustrated by the TGA and XRD results, the short-stirring time hybrids are mainly

[6] To be more accurate, hybrid 2 is not a new chemical species. However, it contains less unreacted ligands and therefore the fingerprint of the pure ligand is less visible on the spectrum. On the contrary, the fingerprint of the hybrid is more visible. This explains the main difference spotted between hybrid 1 and hybrid 2 on their IR spectra.

composed of unreacted pure ligands. Therefore, the time of stirring before filtration is questioned.

Indeed, the terpyridines are not soluble in water even at acidic pH of 0.9 or at least not completely. This phenomenon causes that when the ligands and the inorganic species are mixed, no solubilization occurs either and that there is no external sign, warning that the hybridization is finished. The stirring must be strong in order to obtain a homogeneous suspension. And, without any further analysis, it is impossible to say when the hybridization is over. Therefore, the stirring time was arbitrarily increased to two days instead of 1h. Figure 27 is a strong example of the impact of the increase of stirring time on the collected species. For this long-stirring time synthesis, before hybridization, the ligand is first mixed in aqueous solution with phosphoric acid to be protonated. This is how a new species of hybrid was synthesized. The long-stirring synthesis (explained in 2.9) was thus tried for the other hybrids but without using the biphasic conditions of Ischii-Venturello.

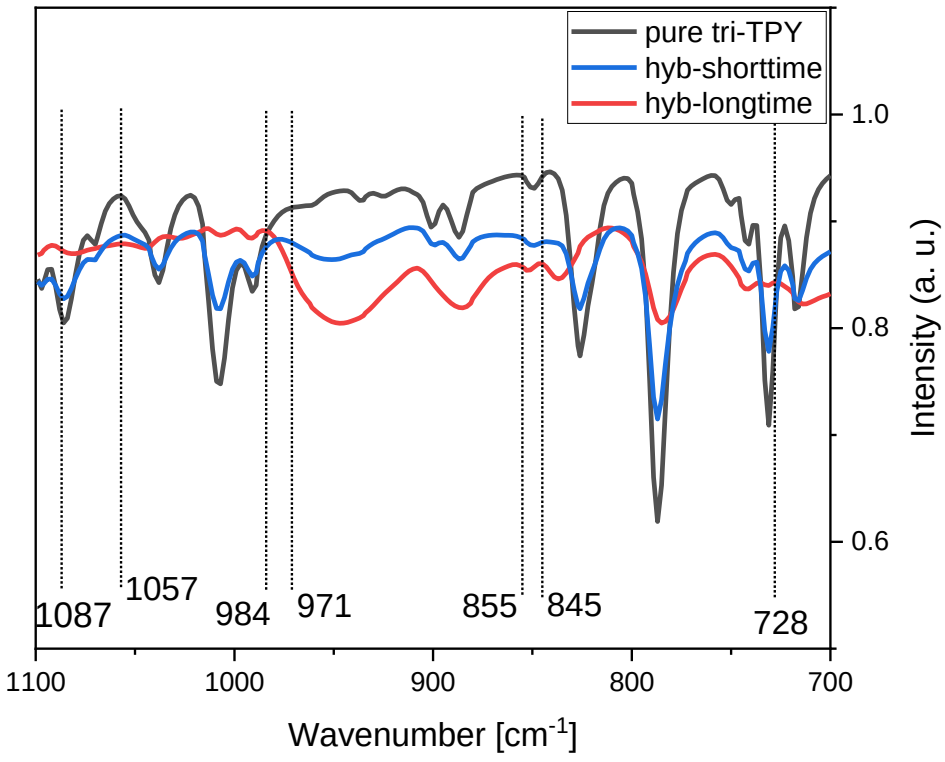

Figure 27: ATR-IR of Tri-TPY hybrids catalyst. In red long time for hybridization (2 days), in bleu short time (1h) and in black is the pure Tri-TPY.

Figure 27 shows the difference between a hybrid catalyst that had either a long or a short time of stirring before filtration. Here, as figure 18 displayed previously, the pure ligand and the short-stirring time hybrid present a similar spectrum while the spectrum of the long-stirring

time hybrid is clearly different. This confirmed that the stirring time has a real impact on the hybridization process. Once again, the vertical lines corresponding to the PW4 vibration bands are plotted in order to compare the fingerprint of the obtained hybrid with the one of PW4. No match of the PW4 bands of Ischii-Venturello with those of the new hybrid was found.
Another attempt was done to evaluate the difference between the short-stirring time hybrid and the pure ligand. The idea was that since these two species are so similar according to the IR spectra and the TGA results, it is sure that the short-stirring time hybrid samples contain some unreacted terpyridines ligands. Therefore, the experiment was to wash the collected hybrid sample with dichloromethane[7], to remove all the pure ligands possibly present, and analyse the obtained washed sample by IR. However, the obtained spectrum (illustrated in Annexe II part C) cannot be assigned to any known species among PW4 or the precursors and therefore the nature of the inorganic part was not identified.

The 5 other long-stirring time hybrids (naked-TPY, Cl-TPY, F-TPY, Ph-TPY, Py-TPY) were also synthesized and characterized by IR. For the sake of conciseness, their spectra are not presented here since the observations that were made for the long-stirring time Tri-TPY hybrid are the same for the others. Therefore, these spectra can be found in the Annexe V.

3.2 Discussion:

In this section, the results obtained and illustrated in the previous section are analysed and interpreted.

3.2.1 Short-stirring time hybrids

According to the IR spectra section 3.1.2 figure 18, it seems that the Tri-TPY ligand is purely recovered after the filtration on Büchner, and that only a fraction of the ligand was hybridized with the PW_4 species present in solution. Indeed, the IR spectra of the different hybrids and their corresponding ligands do not reveal noticeable differences.

The TGA results have proved that the short-stirring time hybrids are composed of mainly pure unreacted ligands. However, these results have also shown that these hybrids contain some

[7] This test has been done only once, maybe additional investigation should be done to confirm the results.

inorganic species hybridized with the terpyridines. It has also been proved that 1 equivalent of terpyridines is interacting with 1 equivalent of PW4. Therefore, since the charge of PW4 is supposed to be "-3", it suggests that the ligands are protonated three times. However, previous studies made by S. de Crane [64], stated that the terpyridines are only protonated twice, giving $[H_2tpy]^{2+}$ species. It is thus possible that the inorganic part of the hybrid is not only composed of PW4 but also of PW3 and PW2 species that are less negatively charged (-1 or -2). These latter would react with less the terpyridines in a ratio where less than 1 equivalent of ligand is needed to hybridize 1 equivalent of PW3 or PW2 (for instance, 1 TPY for two PW3 or PW2 species). Overall, it gives a ratio of 1 equivalent of ligand for 1 equivalent of inorganic species.

According to the TGA, IR and XRD characterization of the short-stirring time Tri-TPY hybrid. It was expected to have poor catalytic activity since the hybrid is merely composed of PW4. In addition, one still does not know if it is PW4 that composes the inorganic part. By comparison, the Ischii-Venturello catalyst reaches conversion of more than 99% and selectivity in epoxide of 95% after 4h [86]. A hypothesis to explain the poor catalytic activity was that maybe not enough catalyst was inserted in the reaction mixture. However, doubling the amount of catalyst has not shown any differences.

3.2.2 Venturello synthesis, Long-stirring synthesis

The IR spectra obtained in figure 25 with the biphasic conditions revealed two different hybrid species. This suggested the idea that the time of reaction is affecting the result of the synthesis.

However, even if no match between the long-stirring hybrid of figure 27 and PW4 can be done, the presence of PW4 as inorganic part in the hybrid cannot be confirmed or denied. Indeed, the bands are so large that maybe they are hiding minor bands coming from PW4. Also, as with the short-stirring time hybrids, it is possible that some ligands are left unreacted. And because some expected peaks for PW4 are close (1 to 5 cm^{-1}) to the vibration bands of terpyridines, it is thus hard to dissociate two peaks that are close to each other. Or also, two peaks (one coming from PW4 and one from the terpyridine) might form only one peak. This prevents us to do a correct identification of the chemical species present in the hybrid samples.

A hypothesis is that several peroxo species are hybridized with the TPY, yielding hybrids of PW4, PW3 and PW2 species. This is supported by the results reported by Gao et al [43] stating that PW4 often coexist with other PWx species. This could explain these large bands observed on the IR spectra.

The rest of the analysis and characterizations will be performed on these long-stirring time hybrids even though they are not 100% PW4 in organic part. It is even possible that they do not contain PW4 species at all but only PW3 or PW2 species. Therefore, since we do not know if the inorganic species present in the hybrid is actually PW4 or not, we will call these species PWx.

3.3 Conclusion of Part I:

Hybrids of polyoxometalates have been synthesized. The results of these hybrids characterized by IR have shown that the terpyridines are not oxidized by the excess of hydrogen peroxide used to perform the synthesis. However, no analysis can assure that they contain PW4 in their inorganic part. The chemical affinity between the organic terpyridines and the PW4 can be questioned. Indeed, when the cation of Ischii-Venturello is used (tetrahexylammonium chloride), pure PW4 is fished at the interface of the aqueous and organic solutions. However, when these same conditions are used with a functionalized terpyridine, PW4 is not fished or just partially, with plenty of other PWx species. In addition, many terpyridines remain unreacted. One difference to notice between the TPY ligand and the Ischii-Venturello ligand is that the latter is already positively charged when inserted in the mixture, while the TPY is not. Yet, considering the low pH of around 1 in the aqueous phase containing the W precursor, the terpyridines must be directly protonated when they reach the interlayer of the two phases. Therefore, this difference between the two ligands is not supposed to affect the result of the synthesis. Next to that, it is possible that in the exact Ischii-Venturello conditions, the equilibrium between PW4 and the other PWx species is pulled towards the formation of PW4 because the ligand only attaches the latter and nothing else. This means that the ionic affinity between PW4 and tetrahexylammonium chloride is strong. Whereas the organic TPY has maybe an equal affinity to PW4 and to the other peroxo species present in the aqueous solution.

By increasing the stirring time in the synthesis, less unreacted ligands are collected alongside the hybrid. The excess of ligands is therefore related to the stirring time. Indeed, the TGA and XRD results confirm that there is, in the short-stirring time hybrids, a big part of unreacted ligands. Whereas concerning the long-stirring time hybrids, this has not been confirmed yet (since those results are presented in Part II). However, the IR spectrum of the long stirring Tri-TPY hybrid is already different than the spectrum of the corresponding pure ligand. This suggests already that the stirring time has clearly an impact.

The collected solid after filtration can probably be washed with a solvent that solubilizes the ligands and not the hybrids. However, as explained in section 3.1.3, an additional experiment was done to assess this eventuality, and this did not yield anything concluding.

4. Part II: Characterization, catalytic tests and post-tests characterization of the hybrids

In this second part, the long-stirring time hybrids are deeply characterized to obtain more answers about the inorganic nature of these hybrids; their catalytic activity is also evaluated and finally their heterogeneity as well as their reusability is assessed.

All the long-stirring time synthesis were performed several times[8] giving 3 different batches of each hybrid. The average mass of powder collected at the end of the synthesis is illustrated in Table 2 below.

Table 2: Illustrating the mass and substituent properties for the synthesized hybrids when 1 mmol of tungstic acid was used. EDG/EWG meaning electron donating / withdrawing group, -I meaning inductive captor group.

Product	Mass [g]	Property of functional group
Naked TPY	0.1500	-
Py-TPY	0.2332	EWG
Ph-TPY	0.0928	EDG
Cl-TPY	0.1147	-I
F-TPY	0.1354	-I
Tri-TPY	0.1652	EDG

4.1 Characterization

4.1.1 Thermogravimetric analysis (TGA)

A new aspect of the long-stirring-time hybrids is their inorganic species content. As presented earlier in section 3.1.2, the short-stirring-time hybrids have an inorganic content of 20% of mass while here, some of the hybrids have an inorganic content of more than 50% as shown by figure 28 and in Table 3. Thanks to the MS coupled to the TGA, it is known that only the ligand is being burned between 200 ° and 550°C, and that under those temperatures, it is physisorbed water and crystalline water that is desorbed during step “1”. The thermal stability of the hybrids is also evaluated. The thermograms on figure 28 reveal that these hybrids are thermally stable until 200°C. Then, just as in section 3.1.2, the amount of organic and inorganic compounds contained in the hybrid samples can be calculated. A first observation is that there

[8] Except for Ph-TPY hybrid for which only 2 batches were synthesized because of lack of ligands.

are less unreacted ligands in the long-stirring time hybrids than in the short-stirring time ones. However, there is still a step "2" during which the pure unbound ligands are burned.

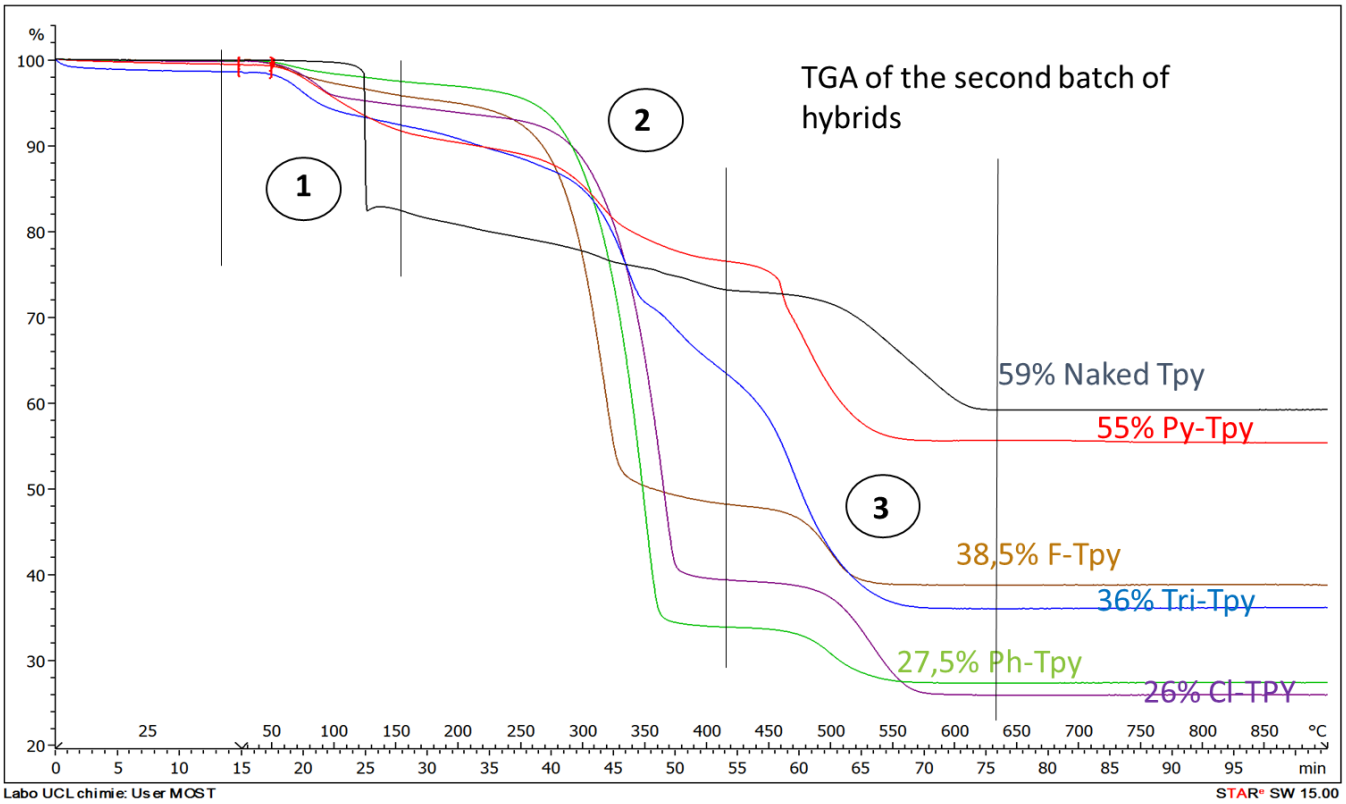

Figure 28: Thermogravimetric analysis of the 6 hybrids.

Similarly to the calculations made in Part I section 3.1.2, the correct amount of ligands forming a hybrid with the PW4 species can be computed. Those calculations were done according to the following reasoning with Cl-TPY as an example: M_0 being the initial mass of sample, here 10.10 mg.

$M_{ligand} = M_{end\ of\ stage\ 2} - M_{end\ of\ stage\ 3}$

$n_{ligands} = = M_{ligand} / \text{Molar Mass}_{ligand}$

$n_{PW4} = M_{PW4} / \text{Molar Mass}_{PW4}$

M_{ligand} being the actual mass of Cl-terpyridines bound to PW4 and M_{PW4} being the remaining mass at the end of step 3. $n_{ligands}$ being the number of moles of Cl-terpyridines bound to PW4 and n_{PW4} being the number of moles of PW4 contained in the hybrid.

Depending on the ligands, one obtains these several results summarized in the Table 3

Table 3: The different molar ratios of ligands versus the anionic part of the hybrids. 2 batches of each hybrid were analysed to acquire more accurate analysis

Ligand	Batch number	Mass PW4 [mg]	Mass Ligands [mg]	Ratio moles [moles ligands/mole PW4]
Py-TPY	1	55%	20%	**1.34**
	2	55.5%	17%	**1.14**
Tri-TPY	1	55%	15%	**0.79**
	2	36%	16.5%	**1.32**
Ph-TPY	1	27.5%	6.5%	**0.88**
F-TPY	1	38%	10%	**0.92**
	2	48.5%	12%	**0.87**
Cl-TPY	1	33%	13%	**1.32**
	2	26%	9%	**1.16**
Naked-TPY	1	59%	13%	**1.09**
	2	59%	14%	**1.17**

According to the results presented in table 3, all the hybrids are similar in their ratio ligands moles / PW4. Overall, the general trend is that 1 equivalent of ligands is bound to 1 equivalent of PW4 in the hybrids, as shown by the last column of table 3. The same hypothesis as in section 3.2.1 can be made concerning the positive charge of the terpyridines. This latter is probably of +2, while the charge of PW4 is -3. However, since probably there are also PW3 and PW2 species that are charged -2 or -1, as a whole, it gives that 1 equivalent of ligand binds 1 equivalent of inorganic species. This explains why for some hybrids the ratio is greater than 1 while for others the ratio inferior than 1.

Another observation is that some hybrids, like Cl-TPY, F-TPY and Ph-TPY still have a lot of unreacted terpyridines, almost 50 % in mass, that were collected after filtration on Büchner. This means that even if the long-stirring time synthesis decreases the amount of unreacted ligands, there are still some remaining.

4.1.2 XRD:

The pure ligands and their corresponding hybrids were analysed respectively by X-ray diffraction. In Part I section 3.1.2 figure 23, the diffractograms of the Tri-TPY ligand and its related hybrid were both showing the same highest diffraction peaks. This observation confirmed the hypothesis that in the short-stirring time hybrids, there were a lot of unreacted ligands. Here on figure 29 with the long stirring time Tri-TPY hybrid, it is no longer the same situation. On the right-hand graph of the figure, the main peak of the pure ligand at 2 theta value of 14° is not present in the hybrid or maybe just a small peak but nothing significative. On the left-hand graph of figure 29, it is clear that the new hybrid does not show any crystallinity. Merging these 2 observations, it is sure that the long-stirring time Tri-TPY hybrid does not contain any unreacted ligands or at least not enough to be identified via XRD analysis.[9]

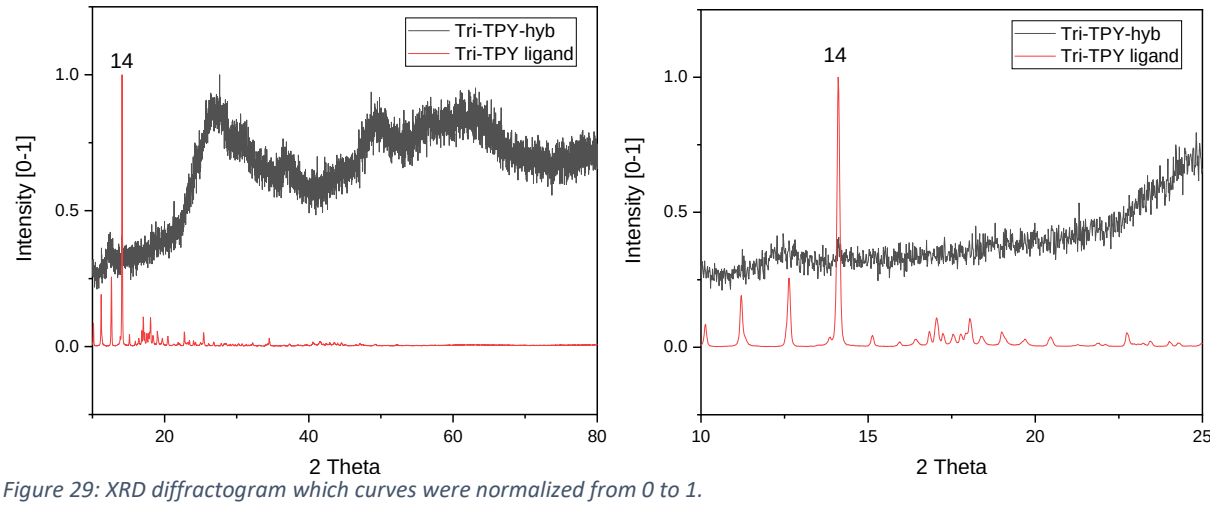

Figure 29: XRD diffractogram which curves were normalized from 0 to 1.

The diffractograms comparing the other hybrids with their corresponding pure ligands are not displayed here for sake of conciseness. The same observations as here are made for all of them except for one detail explained here. Indeed, Cl-TPY hybrid as well as Ph-TPY hybrid XRD diffractograms still show some crystallinity and in addition, the highest diffraction peaks of their corresponding terpyridines are also present. These observations are in agreement with their TGA results of figure 28 which reveal that they still contain large amount of unreacted ligands.

[9] However, the thermogram of Tri-TPY hyb on figure 28 show that around 12 % of the initial mass is being burned in step 2, suggesting that there are still a few unreacted ligands present.

Also figure 30 contains the diffractogram of every hybrid and illustrates that they are all different. Their unit cells seem to be very different from one to another, and in addition they show few crystallinity.

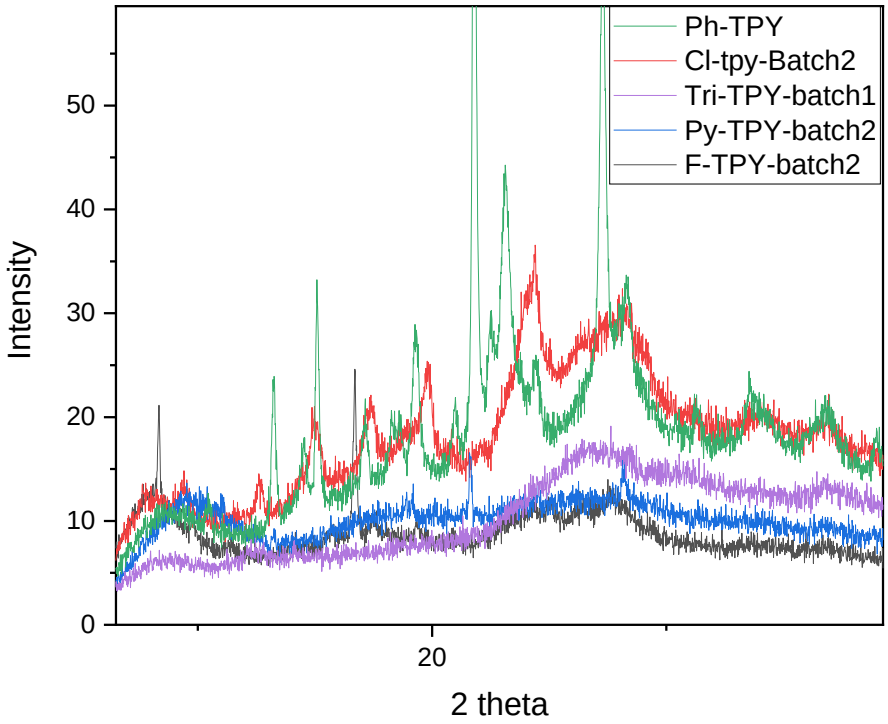

Figure 30: Diffractograms of 5 of the 6 hybrids[10]

4.1.3 Solid Raman:

On Figure 31 below, the Ischii-Venturello hybrid Raman spectrum is shown. A first observation is that the intensity of the signal is not high compared to the background noise. This will be discussed further in this section. The fingerprint vibration bands of the inorganic part (=PW4) of the hybrid is situated between 400 cm^{-1} and 1200 cm^{-1}. Strong vibration bands are observed at 981, 857 and 574 cm^{-1} corresponding to the vibrational modes of (W=O), (O-O), (WO_2) of PW4 anion respectively [43]. The peaks situated at 1440 and 1307 cm^{-1} belong to the Venturello counter cation (tetrahexylammonium chloride) [89]

[10] Not enough sample of Naked-TPY hybrid was available

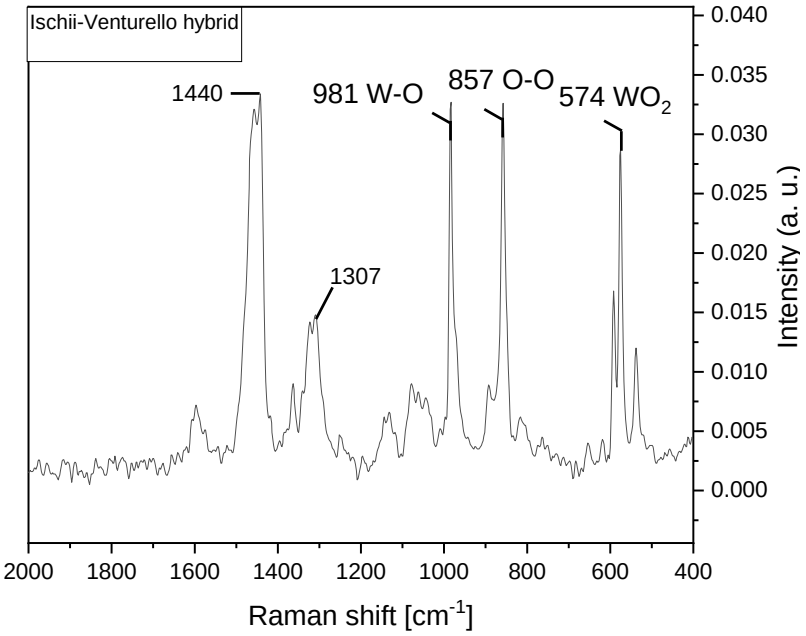

Figure 31: Solid Raman spectrum of the Ischii-Venturello hybrid

On figure 32, the Raman spectra of the solid Tri-TPY hybrid and the Tri-TPY pure ligand are plotted. In addition, the bands of PW4 observed in figure 31 with the Ischii-Venturello hybrid are represented by the three vertical lines, in order to compare the vibration bands obtained with the hybrid on figure 32. The spectrum of the Tri-TPY hybrid does not have the bands of PW4. All the peaks of the hybrid correspond to the peaks of the pure ligand. Indeed, there is one peak that is situated at 993 cm^{-1} and belongs to the tri-TPY ligand and not to PW4 as it could have been if it was situated at 981 cm^{-1}. Similarly to the IR analysis, the fingerprint of the inorganic PW4 part is situated from 400 cm^{-1} to 1200 cm^{-1} and the one of the functionalized terpyridine from 400 cm^{-1} to 2000 cm^{-1}.

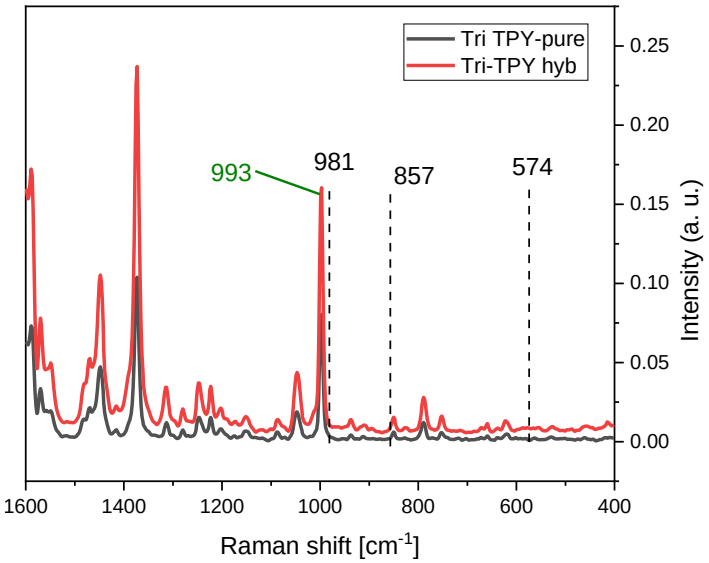

Figure 32

For a sake of conciseness, the Raman spectra of the other hybrids are displayed in the Annexe VI. All the results and observations made from the analysis of the Tri-TPY hybrid are also valid for the 5 other hybrids.

On figure 33, the main peaks correspond to the Py-TPY ligand fingerprint. As a comparison, the blue curve that belongs to the Ischii-Venturello sample and its major peak that is situated at 981 cm^{-1} on Figure 31 is almost flat on this graph. About that, it is because the scale of figure 33 is more extended than the one of figure 31 and therefore it makes sense that the spectra of the Ischii-Venturello hybrid is merely seen on the graph 33.

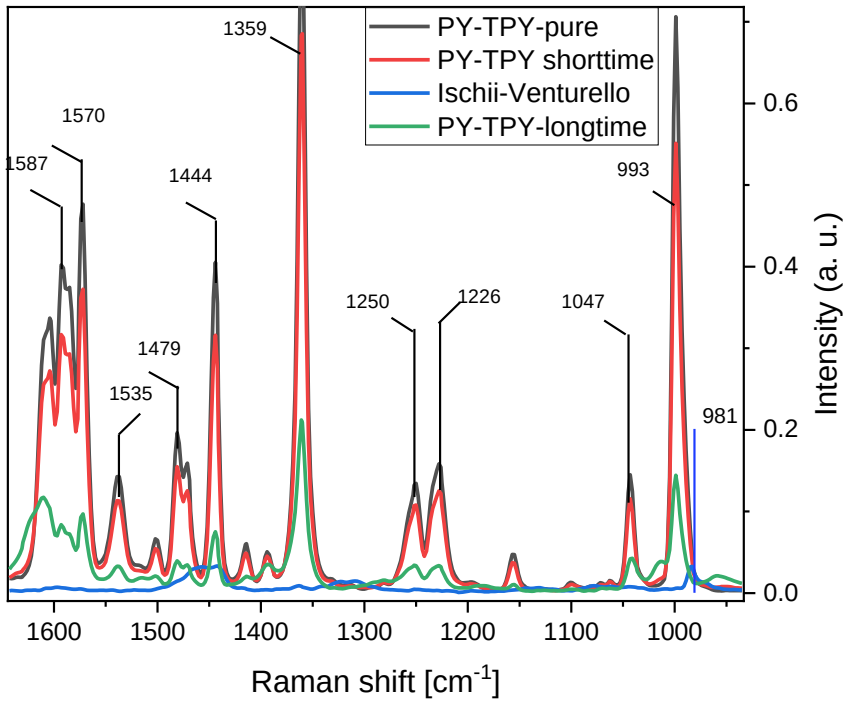

Figure 33: Solid Raman spectra the pure Pyridil terpyridine, the long and short time terpyridine hybrids and the Ischii-Venturello hybrid.

The peaks that are shown on figure 33 are described and listed in Table 4.

Table 4: Solid Raman vibration bands [90], [91].

Observed	References	Description
1587	1587	i.p ring stretch (C=N and C=C) + N-H+ i.p. def
1570	1569	i.p ring stretch (C=N and C=C)
1535	-	
1479	1481	ring str. (C=N, C=C) + C-H i.p. def
1472	-	
1444	1444	ring str. (C=N, C=C) + C-H i.p. def.

1359	1358	
1250	1250	C=C inter-ring str. + ring str.
1226	1226	(C=C, C=N) + C-H i.p def
1047	1042	C-H i.p def. + ring str. and def
993	993	Ring breathing

Note. Abbreviations: i.p = in plane, o.p = out of plane, str.= stretching, def. = deformation.

4.1.4 Nitrogen physisorption, surface area measurements and pores size:

Surface area measurements based on the BET model and the interparticular pores diameters based on total pores volumes are illustrated in Table 5. All the isotherm plots of the hybrids present a type II curve and are presented in the Annexe VI, which indicate a non-porous, or macroporous solid.

Table 5: Surface area and pores diameter of the hybrid catalysts, determined by the TriStar 3000 software.

Hybrids	BET Surface area [m^2/g] [11]	Average pore size diameter [Å]
TRI-TPY	34	276
F-TPY	16	210
PY-TPY	7	176
Cl-TPY	15	236
Naked-TPY	9	218
Ph-TPY	20	226

4.1.5 Ammonia Temperature desorption program (TPD):

The residual acidity of the hybrid catalysts was studied through ammonia TPD. As stated in the introduction, a too high acidity might favour the formation of alcohol by ring-opening of the epoxide. During the desorption stage, ammonia and water are detected. The presence of water is not surprising since the pre-treatment only goes to 150°C. Therefore, some crystalline water still remains at the surface and is desorbed when the temperatures go higher than 150°C

[11] Average of two measurements

during the desorption stage. Table 6 sums up the diverse acidity values of the hybrids, these are expressed in µmol/ g of catalyst and in µmol/ m^2 of catalyst.

Table 6: Acidity of the catalysts as probed by NH_3-TPD and expressed in total acidity in (µmol per g of catalyst) and in surface acidity (µmol per m^2 of catalyst)

Hybrids[12]	Acid sites [µmol/g]	Acid sites [µmol/m^2]
TRI-TPY	39	0.07
F-TPY	34	0.10
PY-TPY	142	1.67
Cl-TPY	70	0.19
Naked-TPY	149	0.75

Figure 34 illustrates the TPD profile of ammonia desorption. Some hybrids as Naked-TPY and Py-TPY show higher acidity among other hybrids. Consequently, their selectivity towards cyclooctane oxide might be lower than the other hybrids which display less acidity.

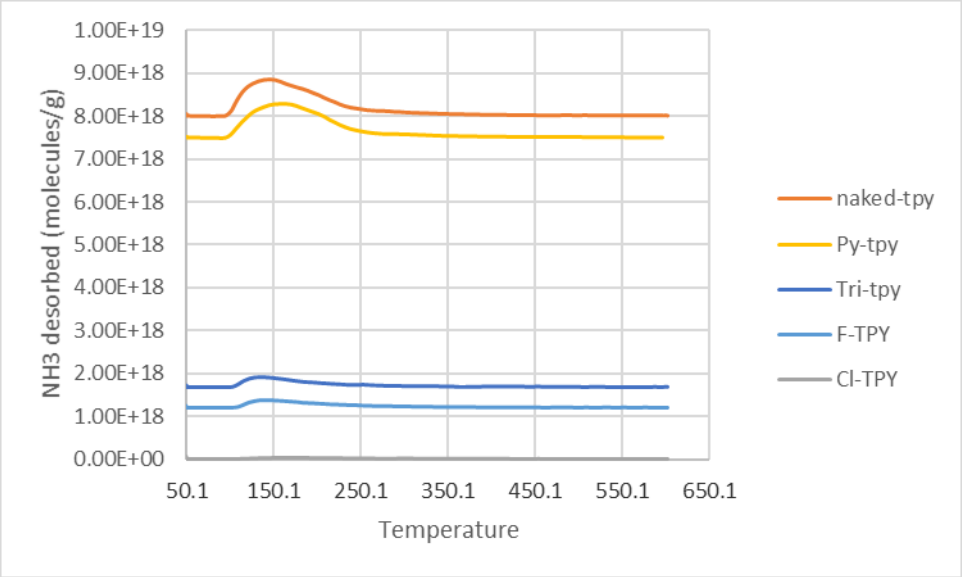

Figure 34: NH_3 desorption during the TPD analysis of the hybrid catalysts

4.1.6 Inductive coupled plasma analysis (ICP)- atomic emission spectroscopy (AES):

The ICP analysis was performed in order to quantify the amount of W and P in the inorganic part of the hybrids. Thanks to the TGA in Figure 28, it is known that after a long calcination period at 500°C of the hybrids, no organic molecule remains. Indeed, after the calcination the same mass percentage of the initial mass was remaining as after the TGA. As a result, the samples that are analysed by ICP are only constituted of their inorganic part (W, P and O). Therefore, if the amount of W and P is known, the amount of O can be easily calculated. All these results are included in Table 7.

[12] Ph-TPY hyb was not analysed because of lack of sample.

Table 7: ICP-AES results giving the amount of P, W and O contained in the inorganic part of the hybrids.

Hybrids	W %[13]	W %[14]	P % [13]	P % [14]	calculated O %[13]	W/P in Mass	O/P in Mass	O/W in Mass
Ph TPY	18	71	0.78	3.1	26	3.8	16.4	4.3
F TPY	23	64	1.22	3.5	33	3.1	17.9	5.8
CL TPY	20	67	1.01	3.4	30	3.4	17.5	5.2
Tri TPY	36	70	1.83	3.5	28	3.3	15.2	4.6
PY TPY	37	70	2	3.7	27	3.2	14.4	4.6
Naked-TPY	39	657	0.23	0.4	34	30	179	6.2

The diverse values obtained for the respective hybrids are similar for 5 of the 6 hybrids. Indeed, only for the naked-TPY hybrid the values are different and therefore will not be considered since only one measurement was performed.

4.2 Catalytic results:

The catalytic performance of all the 6 hybrids was evaluated in the epoxidation reaction of cyclooctene with hydrogen peroxide. The conversion, selectivity and yield are displayed on the next figures 35, 36, 37. The catalytic reaction is still the same as presented by eq 11 in section 3.1.2

Statistical tests were performed with the Tri-TPY hybrid to assess the influence of the manipulations and have more representative values. The confident interval obtained is thus assumed to be the same for the other catalysts. More information about this statistical test can be found in Annexe VII.

[13] Percentage of W or P atom in the hybrid after calcination but counting the mass of the fused sodium peroxide.

[14] Percentage of W or P or O in the hybrid after calcination but without counting the mass of sodium peroxide.

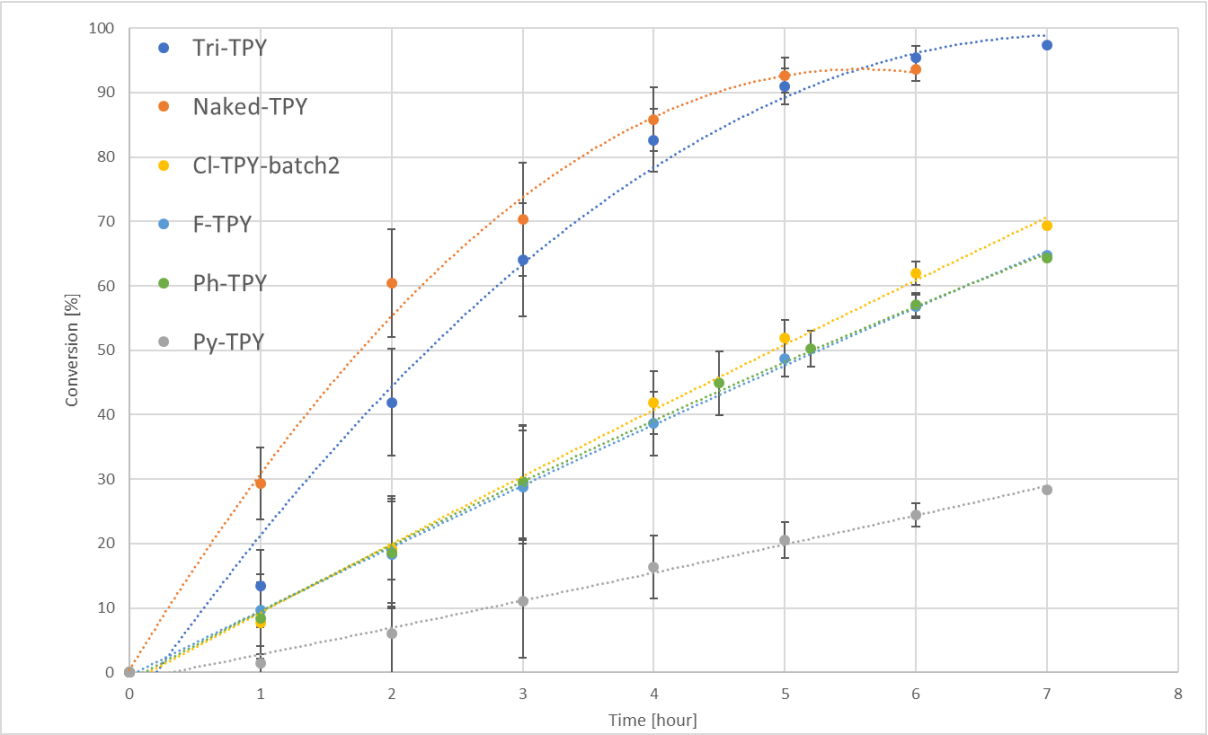

Figure 35: Conversion of cyclooctene (Conditions: 0.1 M cyclooctene, 0.1 M DBE, 9.18 µl acetonitrile, 0.01mmol catalyst, 0.5M H_2O_2, 70°C)

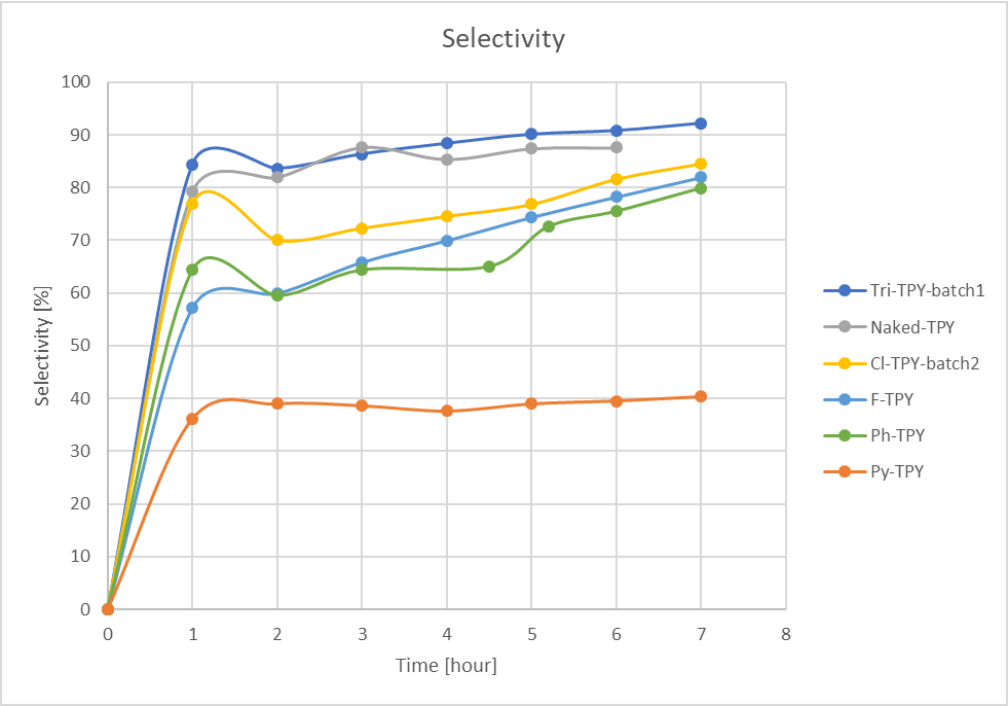

Figure 36

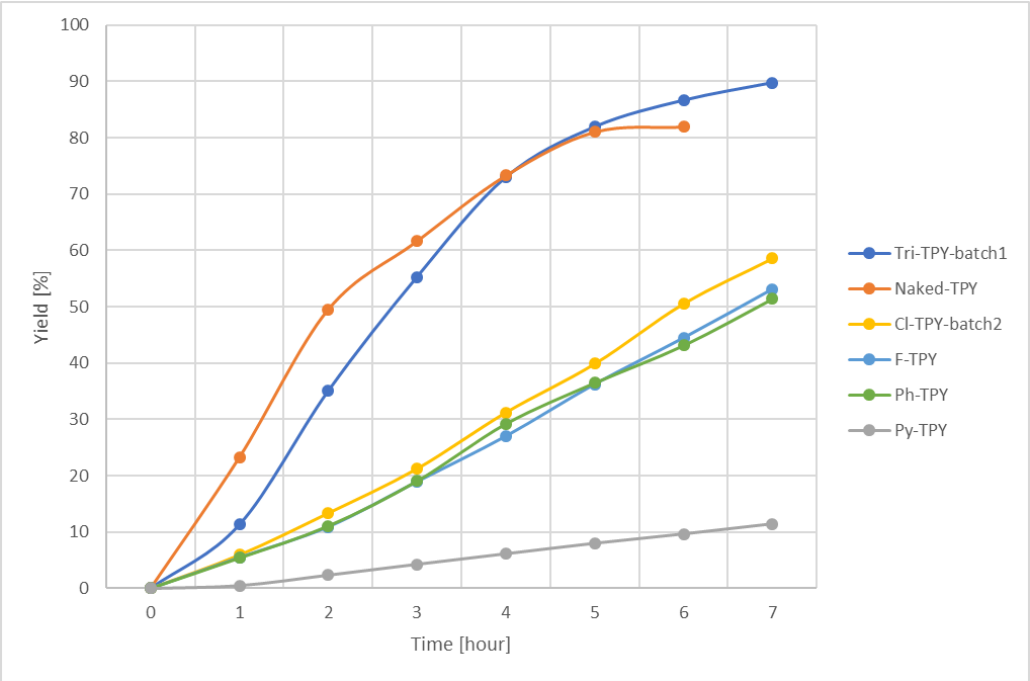

Figure 37: yield profile of the six hybrid catalysts

Table 8 below sums up the results obtained in the 3 previous graphs 35, 36, 37. The naked-TPY hyb and the tri-TPY hyb show the best results with a conversion superior to 95% after 6h and selectivity for epoxidation averaging 90%.

Table 8: Summing up the results of the 6 catalyst towards their conversion, selectivity and yield.

Hybrid	Conversion of cyclooctene [%]	Selectivity in cyclooctane epoxide [%]	Yield of cyclooctane epoxide [%]
Naked-TPY	96	87	81
PY-TPY	28	40	11
Ph-TPY	69	79	51
F-TPY	69	81	53
Cl-TPY	71	81	50
TRI-TPY	98	92	90

4.3 Post Cata charachterization tests

A significant aspect of the catalyst that must be analysed is its heterogeneity. Indeed, the role of the hybridization with the ligand was to alter the hydrophilic character of the catalyst but also to heterogenize it. Therefore, the heterogeneity of the catalysts in the conditions of the catalytic reactions is evaluated.

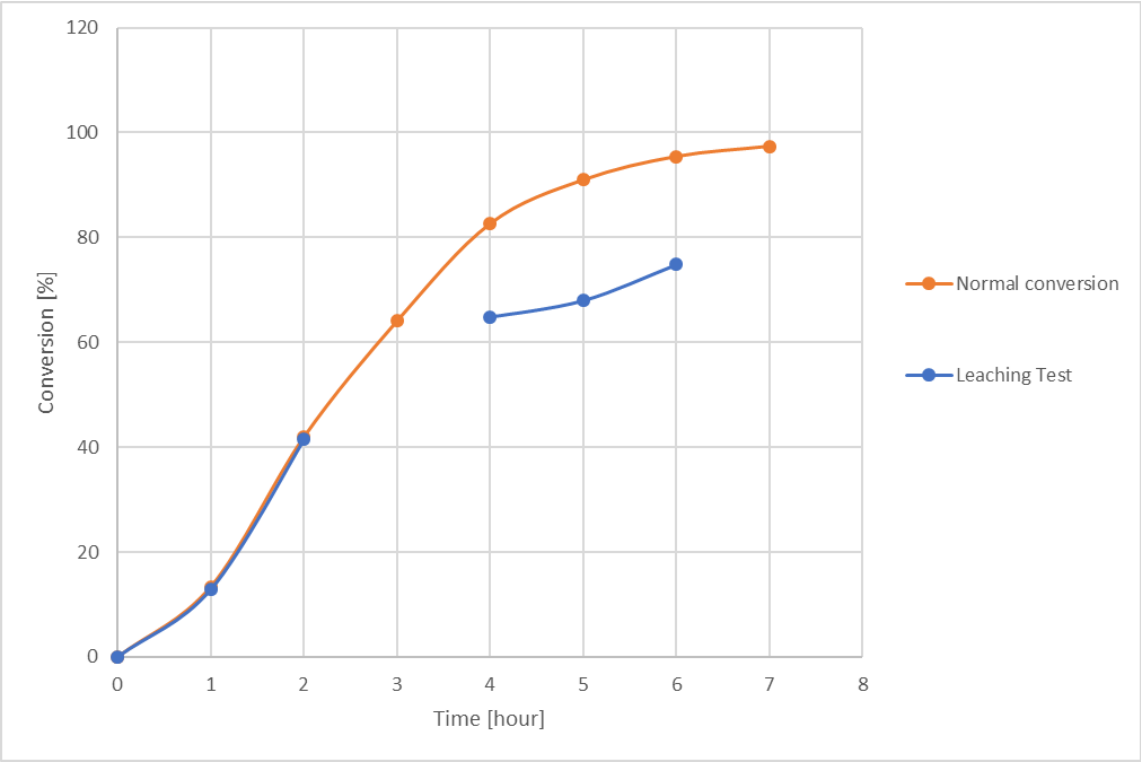

Figure 38: Leaching test with Tri-TPY hybrid.

The leaching test consisted in launching a standard catalytic reaction and then, the reaction was stopped after 3h, the whole suspension was uptaken and centrifuged for 20 min at 15000rpm, and then filtrated with a 0.2 µm syringe. The surnatant was placed in a clean beaker with a clean stirrer and reheated to 70°C. New aliquots were taken to assess the catalytic activity.

Undoubtedly, as figure 38 illustrates, there is leaching since after centrifugation and filtration there is still conversion and cyclooctane oxide production. It means that there is still catalyst present in the system, but this catalyst is not heterogeneous. A result of the leaching is that the nature of the active species is not known. Indeed, it is impossible to know if the catalytic activity that has been observed in figures 35, 36, 37 comes from the leached species alone or also from the heterogeneous part of the hybrids.

In order to accurately identify the active species, two extra catalytic tests were run. One where the catalyst (Naked-TPY hyb) was the solid collected after centrifugation of the reaction mixture (once the reaction is finished and no cyclooctene remains). This collected catalyst is placed in a clean vial with fresh reagents. A second run was then launched, and GC measurements taken every hour. (Test 1)

The other test was to, once the catalytic reaction was over, evaporate the solvent and all liquid products; fresh solvent was added to resolubilize the leached species and the solution centrifuged, then the surnatant was filtrated and poured in a clean vial, and finally the missing reactants and standards (DBE, cyclooctene and hydrogen peroxide) were added before starting the catalytic reaction. (Test 2)

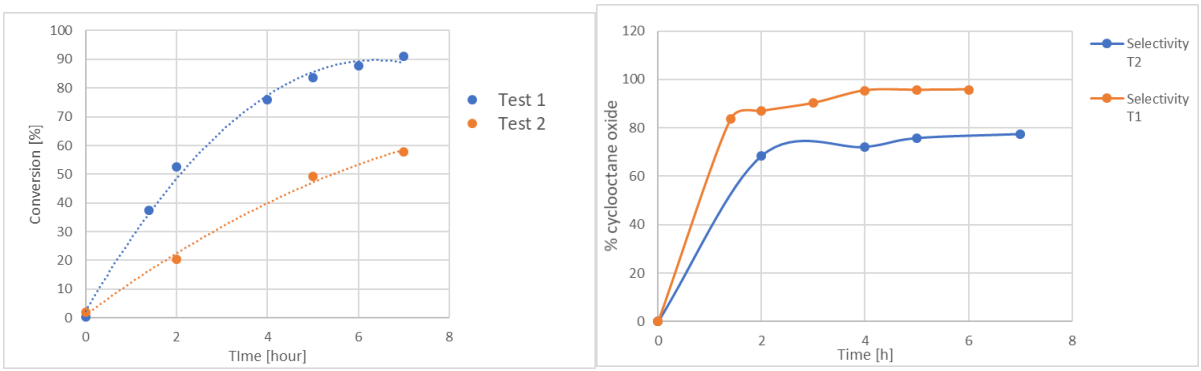

Figure 39: On the left conversion of cyclooctene versus the time. On the right, selectivity in cyclooctane oxide.

These tests confirm that the leached species are the catalytically active species in the epoxidation reaction as shown by the selectivity obtained for both tests. Indeed, the conversion and selectivity obtained with the Test 1 (homogeneous part) are the same than the ones obtained in an ordinary catalytic test. In addition, as shown on figure 39, there is also a high conversion with the heterogeneous part (test 2). This is explained by the fact that leaching is still occurring, the leached species are responsible for the main activity. Therefore, the activity of the heterogeneous part alone cannot be determined.

To identify the leached species, ^{31}P-NMR of the centrifuged and filtrated supernatant were realised. If phosphorous is present in the sample, then a peak should appear at a value of 0 ppm on figure 40. In addition, satellites peaks should also be on the spectra, witnessing the presence of W. However, those satellites peaks will not be detected if no P is present in the sample.

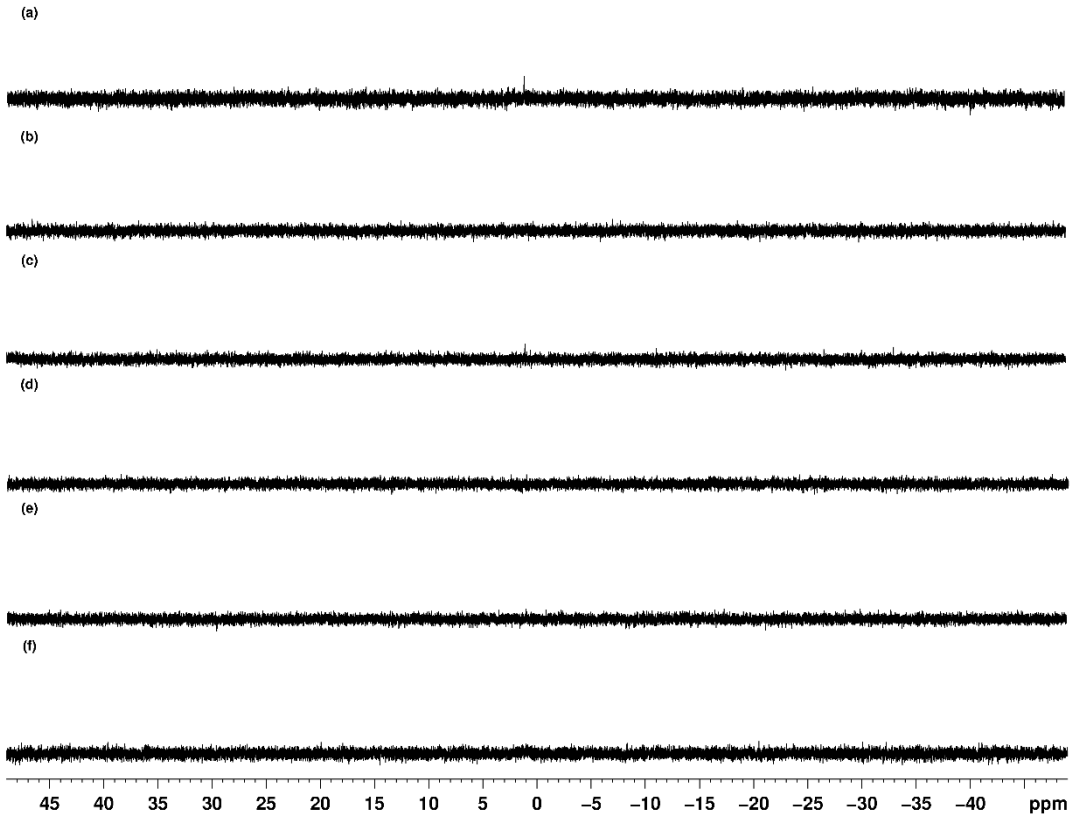

Figure 40: ^{31}P-NMR spectra of the catalytic mixture after centrifugation and filtration. This mixture contains the leached species that are active towards the epoxidation of cyclcooctene. a) Tri-TPY hyb b) Cl-TPY hyb c) Py-TPY hyb d) F-TPY hyb e) Naked-TPY hyb and f) Ph-TPY hyb. The presence of Phosphorous is giving a peak at 0 ppm.

These analyses did not reveal any P-containing compound. This probably means that the leached species are only composed of W and O.[15]

Finally, since there is leaching, it is not necessary to analyse the hybrids after one catalytic test. Indeed, the IR spectra of the fresh hybrid and after one catalytic run are different as illustrated on figure 41.

[15] Or if there is Phosphorous in the leached species, as we can consider for the spectrum in a) (Tri-TPY hyb) with the small peak at 0 ppm, this is only a low amount. Indeed, the detection limit of P-NMR is 50-70 ppm [92] and the concentration of the catalyst without leaching is 1700 ppm. Therefore, it more than 3% in mass of the catalyst leaches, it should be seen.

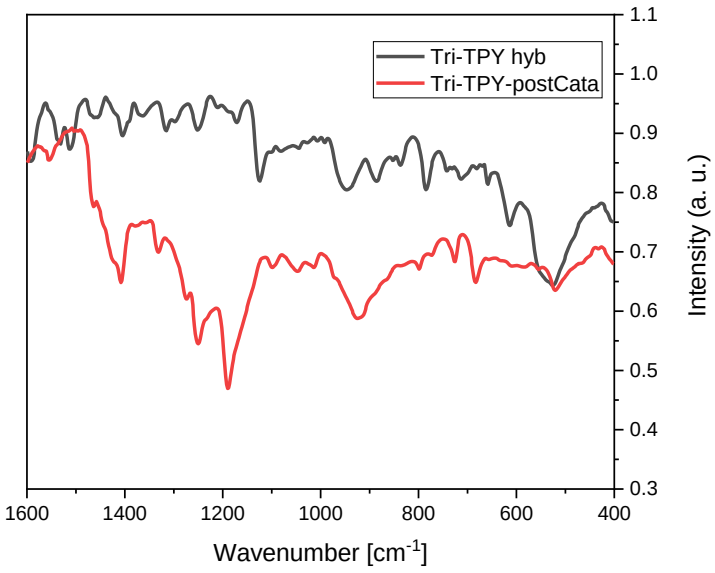

Figure 41

4.4 Discussion:

In this section, the results obtained and illustrated in the previous section are analysed and interpreted. Mainly the different characterization data of the hybrids but also, the catalytic reactions tests are explained as well as the post-tests characterization.

4.4.1 Concerning the physicochemical characterizations

The 6 different hybrids have been deeply characterized by diverse techniques, mainly in order to know what their inorganic content is, but also to know their acidity, surface area and thermal stability. As specified at the end of Part I, the IR analysis cannot certify if the hybrids contain PW4 species.

The TGA results clearly expose the presence of inorganic species. Some hybrids contain more unreacted ligands than others. However, as table 3 illustrates, the ligands that are correctly hybridized to the PWx species are, whatever which functionalized terpyridines it is, in a 1 ligand for 1 PWx species equivalency. So, as a result, when 0.01 mmol of catalyst[16] was inserted in the catalytic mixture to perform the epoxidation reaction, for some hybrids there

[16] This 0.01mmol of catalyst was weighed as if the chemical was “functionalized TPY- PW4”

were more than 50 % of pure ligands that were inserted. While for other hybrids (Naked-TPY hyb and Py-TPY hyb) there were only about 15 % of unreacted ligands. This means, that the inserted amount of catalyst was not the same between different catalysts. Therefore, from the respective amount of inorganic compound in each of the hybrid sample, the catalytic activity, for every hybrid, cannot be normalized to the amount of catalyst, inserted in the reaction.

Because of these results, one can imagine that the samples containing the highest amount of true hybrids (or the least amount of unreacted ligands) will be more active for the epoxidation reaction. While the ones with the least amount (or highest amount of unreacted ligands) will have a lower activity. Indeed, the organic ligands are not supposed to be catalytically active, but only the PWx part of the hybrids.

Next to that, XRD analyses were performed on the hybrids and these bring more information concerning the hybrids and unreacted ligands that are contained in the hybrid samples. Indeed, some diffractograms show no crystallinity at all, as for instance the one of Tri-TPY hyb or Py-TPY hyb, that are among the hybrids that contain the least amount of unreacted ligands. Whereas, the diffractograms of Cl-TPY hyb and Ph-TPY hyb show more crystallinity and contain the major peaks of their corresponding pure ligand (see graphe in Annexe VI). These observations are in agreement with the results obtained by TGA where there, the Py-TPY hyb contain almost no unreacted ligands and the Cl-TPY hyb and Ph-TPY hyb contain more than 50% of unreacted ligands in their sample mass.

Then, solid Raman analyses were run but no clear results were obtained. Indeed, the intensity of the peaks corresponding to the PW4 species are a lot smaller than the ones related to the ligands, as illustrated with Figure 31 and the Ischii-Venturello anion. However, with the hybrids, there is not even the sign of a peak at the expected wavenumber values of PW4. Also, the Raman spectra of the hybrids are similar to the one of the pure ligands. Just as it was the case with the short-stirring-time hybrids TGA and XRD results. At the end of Part I, it was not possible to say with 100% of certitude whether the long-stirring time hybrids were still containing pure unreacted ligands. The TGA results have suggested that it was the case and mostly for Ph-TPY and Cl-TPY hybrids. However, according to the XRD analysis of these long-

stirring time hybrids, some of them (Py-TPY and Naked-TPY hyb) do not contain unreacted ligands.
And now, according to the Raman analyses the hybrids still contain pure ligands.

In fact, in the Raman analyses, a shift is supposed to be observed between the bands corresponding to the ligands that interact with the PWx species and the ones that are not interacting. Indeed, the interaction of the H-bond between the PWx species and the terpyridines is supposed to affect the chemical vibrations in the molecule which would result in a shift on the Raman spectrum. But no shift is observed.

A key experiment that brings many answers concerning the nature of the inorganic part is the ICP-AES. This chemical analysis gives exactly the amount of P, W and O contained in the hybrids. The ratio of W versus P for every hybrid, provides a significant information about the potential nature of the inorganic part of the catalysts. For instance, the Ph-TPY hybrid has a W/P ratio of 3.82 which is close to 4. This probably means that it contains some PW4 species but also PW3 and other PWx species which overall, give the ratio of 3.82. Most of the hybrids have a W/P ratio superior to 3. Consequently, it attests of the presence of different PWx species such as PW4, PW3 or even PW2. In addition, the W/O ratio gives a hint concerning the number of oxygen atoms present in one PWx species. In PW4, this number is supposed to be 24 oxygens. While here, the number of oxygen atoms is around 16 and 18. Therefore, there are less oxygen atoms as expected.

The nitrogen physisorption experiment provides information about the surface area as well as the average pores size of the catalysts. Major differences in pores size diameters could also lead to major differences in catalyst activity. Indeed, the smaller the pores are, the higher is the resistance to diffusion and the reactants can be prevented from being adsorbed on the catalyst surface. Also, the higher the specific area is, the more active sites are exposed for the reagents to be adsorbed and then react. Usually, it is considered that to avoid any diffusion limitation, the size of the pores needs to be 7x bigger than the size of the diffusing molecules (cyclooctene), which is about 8 Å of diameter. Consequently, for every hybrid the diffusion step should not be limiting, since the average pores diameter exceed largely 56 Å (they range

between 180 and 280 Å). The highest surface area goes for the Tri-TPY hybrid while the lowest is for the Py-TPY hybrid. The isotherms being of type II, it confirms that the catalyst are macroporous materials.

The ammonia TPD analysis reveal differences in residual acidity among the hybrids. However, this acidity is mainly weak as illustrated by figure 34 by the desorption peak being at around 150°C. The most acid ones will probably have a poorer selectivity towards cyclooctane oxide formation since it favours the formation of alcohol by ring-opening of the epoxide.

4.4.2 Catalytic tests & Post-cata tests:

The hybrids differ by the nature of their ligands. Indeed, the goal is to evaluate the influence of the ligand on the hydrophobic properties of the hybrid and therefore see how it affects its catalytic activity.

Before analysing the results, one can remind some hypothesis towards the eventual outcome of the catalytic activities. For instance, the F-TPY and Cl-TPY are two ligands that are very similar, they differ only by one atom and it turns out that Cl and F are both halogens. This family of compounds have very similar properties such as being electron inductive captor compounds. Their catalytic behaviour is expected to be the same, or at least very close. It is the same hypothesis that is stated concerning the Tri-TPY and the Ph-TPY ligands. Indeed, in this case they are both electron-donating group. While oppositely, Py-TPY ligand is an electron-withdrawing group. It would be surprising that Py-TPY and Tri-TPY hybrids have a similar catalytic activity and that Ph-TPY has a different one than Tri-TPY.

Another assumption was also made; it is concerning the relative amount of inorganic part in the hybrid samples. As revealed by the TGA analysis, the different hybrids contain more or less unreacted ligands. The idea is that since only the organic part of the hybrids is responsible for the catalytic activity, it is expected that the hybrids containing the highest amount of inorganic part have a higher activity.

The graphs 35, 36, 37 represent the conversion, selectivity and yield of the different hybrids. 2 hybrids (Naked-TPY and Tri-TPY) are performing better than the others and show conversion that reaches about 99% after 6 hours of reaction. They show selectivity superior to 90% and

have a yield of around 90%. These two hybrids are among the ones with the highest amount of inorganic part (and least amount of unreacted hybrids). Next to that, 3 other hybrids have very alike conversion, selectivity and consequently yield as well. These are the Cl-TPY, F-TPY and Ph-TPY. The three of them have very similar ligands which could explain the close activity they have. Finally, the worst hybrid is the Py-TPY, which reaches a conversion of only 28% after 6h. As it was suggested, Py-TPY (EWG) has an opposite catalytic behaviour than Tri-TPY and Ph-TPY (EDG). It seems then, that the diverse ligands have a significant impact on the catalytic activity of their corresponding hybrid.

Also, in opposition to what was expected, Py-TPY which is one of the hybrids with the highest inorganic part content (and least unreacted ligands content), has the lowest activity. Therefore, the differences in amount of catalyst inserted in the catalytic reactions do not seem to affect significantly the catalytic activity.

Next to that, the selectivity of each hybrid does not seem to be affected by the differences in acidity observed via the ammonia TPD measurement. Eventually, all these observations are interesting and can be deeper explained, except that, the leaching test is questioning all these observations.

Indeed, as 38 illustrates, the hybrid catalysts are leaching and figure 39 clearly shows that these are the leached species that are the most active towards the epoxidation reaction. This brings two problems, first is that one can no longer state that this catalyst is heterogeneous and second, this prevents to make any conclusion about the potential impact of the ligand and the overall hydrophobicity of the hybrid on the catalytic effect. The leached species need to be identified. Yet, the P-NMR did not reveal anything. One does not know if theses leached species contain a ligand part. It is more than likely that all the catalysts leach the exact same species and that the differences in catalytic activities that are observed are only due to the stability of the hybrids in the reaction mixture. As consequence, it means that for instance Tri-TPY hyb and naked-TPY hyb are the least stable hybrids. On the contrary, Py-TPY would be the most stable hybrid, explaining its very low activity since it leaches less than the others.

Additional experiments must be done to identify the nature of the leached species and also the reason explaining the leaching. ^{13}C-NMR and ^{183}W-NMR are more than necessary to do so.

However, these techniques are less sensitive than ^{31}P- and ^{1}H-NMR because of their natural abundance.

4.5 Conclusion of the second Part

This second part has as objectives to characterize more the hybrids and to evaluate their catalytic activity. As a result, it is sure that the hybrids are not entirely composed of PW4 but some of them might contain a few PW4 compounds. Also, the TGA, XRD and Raman results converge to the same observation. Indeed, the long-stirring-time hybrids still contain some unreacted hybrids. But the difference is that some hybrids contain higher quantities of pure terpyridines than other that contain just around 10 % of the total mass of the hybrid sample. Next to that, the catalytic tests have shown that indeed the different hybrids are all active and reveal high selectivity. It means therefore that they mainly produce cyclooctane oxide, as wished. Also, distinct catalytic activities were reported but these do not represent the influence of the catalyst polarity on its catalytic performance. Indeed, because of the leaching that every catalyst undergoes, and furthermore the fact that the catalytically active species was not identified, it becomes impossible to pull any conclusion regarding the link between the catalyst hydrophobicity and its catalytic activity.

5. General Conclusion

This Master thesis aimed to study the influence of the catalyst polarity, on the catalytic reaction of epoxidation of cyclooctene by hydrogen peroxide. The catalyst chosen was $\{PO_4[W(O)(O_2)_2]_4\}^{3-}$ (=PW4), a polyoxometalate which is able to perform this reaction with high conversion and selectivity. The latter must be heterogenized for mainly two reasons. One is that the catalyst degrades rapidly in homogeneous conditions plus, a heterogeneous process would be more favourable for the industry. The second one is that by hybridizing this catalyst with different organic ligands, one can change its hydrophobic properties. PW4 being hydrophilic because of its anionic nature, cyclooctene being more hydrophobic, these 2 must interact for the reaction to occur. The hybridization with hydrophobic ligands would favour the apolar interaction between the surface of the catalyst and the reactants.

First, the hybrids needed to be synthesized. To do so, a bottom-up approach was chosen to synthesize the inorganic part of the hybrids with its precursors being H_3PO_4, H_2WO_4 and H_2O_2. Then the hybridization occurred in the same pot, the hybrid catalysts were recovered after filtration on a Büchner. Several characterizations of the hybrids were realised, mainly in the aim to know if the PW4 part of the catalyst was correctly synthesized. According to IR and solid Raman, this is not the case. However, ICP analysis reveals that it is likely that different peroxo species are part of the hybrids, some are PW4, some PW3, some maybe PW2 and even other species. The TGA analysis have exposed that some hybrids have linked more ligands than others and therefore that some hybrid samples contain more unreacted ligands than others. Also, the TGA results have revealed that 1 equivalent of ligand is interacting with 1 equivalent of PW4.

The catalytic tests exposed different activity among the hybrids as it was expected. However, deeper analyses along the leaching tests revealed that the hybrids actually leach in the reaction mixture. The catalysts can no longer be characterized as heterogeneous. The leached species were investigated, and it turns out that these are the main active species for the epoxidation reaction of cyclooctene with hydrogen peroxide. Nevertheless, the exact nature of these leached species was not elucidated. According to P-NMR, they do not contain any phosphorous trace. Even if these active species are not only composed of PW4, they show

very similar activity since they reach high conversion (up to 99%) and high selectivity in epoxide (95%). The differences in catalytic activity that were observed are probably related to the stability of the respective hybrids in the reaction mixture and their tendency (or not) to leach.

5. Bibliography :

[1] Ranade, V. V., & Joshi, S. S. (2016). Catalysis and Catalytic Processes. In Industrial Catalytic Processes for Fine and Specialty Chemicals (pp. 1–14). Elsevier. https://doi.org/10.1016/b978-0-12-801457-8.00001-x
[2] Davis, M. E., & Suib, S. L. (Eds.). (1993). Selectivity in Catalysis. ACS Symposium Series. American Chemical Society. https://doi.org/10.1021/bk-1993-0517
[3] NPTEL. "Lecture 31 Homogeneous Catalysis." Chemical Engineering – Catalyst Science and Technology, [Online]. Available : http://www.nptel.ac.in/courses/103103026/pdf/mod3.pdf. [Accessed April 2019]
[4] Helfferich, F. G. (2001). Homogeneous Catalysis. In Comprehensive Chemical Kinetics (pp. 195–260). Elsevier. https://doi.org/10.1016/s0069-8040(01)80029-7
[5] Ethz.ch. (2019). [Online] Available at: https://www.ethz.ch/content/dam/ethz/special-interest/chab/icb/van-bokhoven-group-dam/coursework/Catalysis/2018/Homogeneous_Heterogeoenous_catalysis_MesoporousMaterials.pdf [Accessed 20 Jan. 2019].
[6] Bligaard, T., & Nørskov, J. K. (2008). Heterogeneous Catalysis. In Chemical Bonding at Surfaces and Interfaces (pp. 255–321). Elsevier. https://doi.org/10.1016/b978-044452837-7.50005-8
[7] Mechanisms in Homogeneous and Heterogeneous Epoxidation Catalysis. (2008). Elsevier. https://doi.org/10.1016/b978-0-444-53188-9.x0001-6
[8] Scotti, N., Ravasio, N., Evangelisti, C., Psaro, R., Penso, M., Niphadkar, P., … Guidotti, M. (2019). Epoxidation of Karanja (Millettia pinnata) Oil Methyl Esters in the Presence of Hydrogen Peroxide over a Simple Niobium-Containing Catalyst. Catalysts, 9(4), 344. https://doi.org/10.3390/catal9040344
[9] Fettes, E. M. 1964. *Chemical reaction of Polymers,* New York: Interscience Publishers.
[10] Horváth, I. (Ed.). (2002). Encyclopedia of Catalysis. John Wiley & Sons, Inc. https://doi.org/10.1002/0471227617
[11] "2.3 Ethylene Oxide Production." 2.3 Ethylene Oxide Production | Global CCS Institute, [Online]. Available : http://hub.globalccsinstitute.com/publications/ccs-roadmap-industry-high-purity-co2-sources-sectoral-assessment-%E2%80%93-final-draft-report-2. [Accessed April 2019]
[12] Markets, Research and. "Global Ethylene Oxide Market Report 2018 - Forecast to 2023: The Growing Demand for PET Bottles from the Packaging Industry." PR Newswire: News Distribution, Targeting and Monitoring, 26 Nov. 2018, [Online]. Available : http://www.prnewswire.com/news-releases/global-ethylene-oxide-market-report-2018---forecast-to-2023-the-growing-demand-for-pet-bottles-from-the-packaging-industry-300755179.html.- Accessed January 2019

[13] “US8080677B2 - Process for Selective Oxidation of Olefins to Epoxides.” Google Patents, Google, [Online]. Available : http://www.patents.google.com/patent/US8080677. -Accessed January 2019
[14] Eliyas, A., Petrov, L., & Shopov, D. (1988). Ethylene oxide oxidation over a supported silver catalyst. Applied Catalysis, 41, 39–52. https://doi.org/10.1016/s0166-9834(00)80380-2
[15] Sienel, G., Rieth, R., & Rowbottom, K. T. (2000). Epoxides. Ullmann’s Encyclopedia of Industrial Chemistry. Wiley-VCH Verlag GmbH & Co. KGaA. https://doi.org/10.1002/14356007.a09_531
[16] Wade, Leroy G. “Epoxide.” Encyclopædia Britannica, Encyclopædia Britannica, Inc., 20 Dec. 2011, [Online]. Available : http:/www.britannica.com/science/epoxide. [Accessed May 2019]
[17] CECC. Propylene Oxide Production Technology Roadmap Progress. 20 Feb. 2014, [Online]. Available : http://www.cecc-tech.com/Item/445.aspx. [Accessed May 2019]
[18] ACS Network Chemistry Community Online.” Nontraditional Career Paths in Chemistry | ACS Network, [Online]. Available : http://www.communities.acs.org/community/science/sustainability/green-chemistry-nexus-blog/blog/2016/08/18/is-hydrogen-peroxide-actually-a-green-reagent. [Accessed April 2019]
[19] Strukul, G. (Ed.). (1992). Catalytic Oxidations with Hydrogen Peroxide as Oxidant. Catalysis by Metal Complexes. Springer Netherlands. https://doi.org/10.1007/978-94-017-0984-2
[20] Kozhevnikov, I. *Catalysis by Polyoxometalates*; 2002.
[21] “Electronic Properties of Polymers Orientation and Dimensionality of Conjugated Systems Proceedings of the International Winter School, Kirchberg, (Tyrol) Austria, March 9-16, 1991. by Hans Kuzmany et al., Springer Berlin, 2013, pp. 475–479.
[22] Gumerova, N. I., & Rompel, A. (2018). Synthesis, structures and applications of electron-rich polyoxometalates. Nature Reviews Chemistry, 2(2), 112. https://doi.org/10.1038/s41570-018-0112
[23] Ammam, M. (2013). Polyoxometalates: formation, structures, principal properties, main deposition methods and application in sensing. Journal of Materials Chemistry A, 1(21), 6291. https://doi.org/10.1039/c3ta01663c
[24] J. T. Rhule, C. L. Hill, D. A. Judd, R. F. Schinazi, Chem. Rev. 1998, 98, 327.
[25] Berzelius, J. “*Poggendorff’s*”. *Ann. Phys*. 1826, 6, 369-383
[26] R. Contant, G. Herve, The heteropolyoxoungstates: relationships between routes of formation and structures, Rev. Inorg. Chem. 2002, 22, 63.
[27] J. F. Keggin, Structure of the molecule of 12-phosphotungstic acid, Nature 1933, 131, 908.
[28] S. M. Kulikov, I. V. Khozhevnikov, Izv. Akad. Nauk SSSR. Ser. Khim. 1981, 492.
[29] I. V. Khozhevnikov, S. T. Khankhasaeva and S. M. Kulikov, Acidity of concentrated heteropoly acid solutions, Kinet. Catal., 1988, 29, 76–80
[30] Qi, W., & Wu, L. (2009). Polyoxometalate/polymer hybrid materials: fabrication and properties. Polymer International, 58(11), 1217–1225. https://doi.org/10.1002/pi.2654

[31] Song, Y.-F., & Tsunashima, R. (2012). Recent advances on polyoxometalate-based molecular and composite materials. Chemical Society Reviews, 41(22), 7384. https://doi.org/10.1039/c2cs35143a
[32] Katsoulis, Dimitris E. "A Survey of Applications of Polyoxometalates." Chemical Reviews, vol. 98, no. 1, 1998, pp. 359–388., doi:10.1021/cr960398a.
[33] Lomakina, S. V., Shatova, T. S., & Kazansky, L. P. (1994). Heteropoly anions as corrosion inhibitors for aluminium in high temperature water. Corrosion Science, 36(9), 1645–1651. https://doi.org/10.1016/0010-938x(94)90059-0
[34] Yeang, H. Y.; Sunderasan, E.; Bahri, A. R. S. J. Nat. Rubber Res. 1994, 9, 70; Chem. Abstr. 1994, 122, 298992
[35] Rohm, H.; Benedikt, J.; Jaros, D. Food Sci. Technol. 1994, 27, 392.
[36] Wu, N.; Wang, S.; Wang, Z.; Xu, H.; Fang, J. Yingyong Huaxue
1993, 10, 5; Chem. Abstr. 1993, 119, 186166n.
[37] Venturello, C.; Alneri, E.; Ricci, M. *J. Org. Chem.* 1983, vol. *48* (4), 3831–3833.
[38] Yasutaka, I.; Yamawaki, K.; Toshikazu, U.; Yamada, H.; Yoshida, T.; Masaya, O. *J. Org. Chem.* 1988, vol. *53* (15), 3587–3593.
[39] Duncan, D. C., Chambers, R. C., Hecht, E., & Hill, C. L. (1995). Mechanism and Dynamics in the H3[PW12O40]-Catalyzed Selective Epoxidation of Terminal Olefins by H2O2. Formation, Reactivity, and Stability of {PO4[WO(O2)2]4}3-. Journal of the American Chemical Society, 117(2), 681–691. https://doi.org/10.1021/ja00107a012
[40] Salles, L.; Aubry, C.; Robert, F.; Chottard, G.; Thouvenot, R.; Ledon, Trans. 1993, 2683-2688. H.: BrBgeault. J.-M. New J. Chem. 1993. 17. 367-375.
[41] Swalus, Colas. Polyoxometalate hybrid catalysts in epoxidation reactions: study of the hydrophobic effect. Prom.: Gaigneaux, Eric ; Devillers, Michel
[42] Venturello, C., D'Aloisio, R., Bart, J. C. J., & Ricci, M. (1985). A New peroxotungsten heteropoly anion with special oxidizing properties: synthesis and structure of tetrahexylammonium tetra(diperoxotungsto)phosphate(3-). Journal of Molecular Catalysis, 32(1), 107–110. https://doi.org/10.1016/0304-5102(85)85037-9
[43] Gao, J., Chen, Y., Han, B., Feng, Z., Li, C., Zhou, N., … Xi, Z. (2004). A spectroscopic study on the reaction-controlled phase transfer catalyst in the epoxidation of cyclohexene. Journal of Molecular Catalysis A: Chemical, 210(1–2), 197–204. https://doi.org/10.1016/j.molcata.2003.09.018
[44] K. B. Sharpless, J. M. Townsend, D. R. Williams, J. Am. Chem. Soc. 1972, 94, 295-296.
[45] C. Jahier, Polyoxométallates dendritiques énantiopurs recyclables pour la catalyse asymétrique. Prom Sylvain Nlate, Université Bordeaux 1,
[46] N. Mizuno, K. Kamata, K. Yamaguchi, in Bifunctional Molecular Catalysis, Vol. 37 (Eds.: T. Ikariya, M. Shibasaki), Springer Berlin Heidelberg, 2011, pp. 127-160.
[47] R. A. van Santen, M. Neurock, in Molecular Heterogeneous Catalysis, Wiley-VCH Verlag GmbH & Co. KGaA, 2007, pp. 1-17.
[48] aS. Ajaikumar, A. Pandurangan, Journal of Molecular Catalysis A: Chemical 2007, 266, 1-10; bJ. Chi-Sheng Wu, T.-Y. Chang, Catalysis Today 1998, 44, 111-118; cG. Guo, Y. Hu, S.

Jiang, C. Wei, Journal of Hazardous Materials 2012, 223–224, 39-45; dJ. Stelzer, M. Paulus, M. Hunger, J. Weitkamp, Microporous and Mesoporous Materials 1998, 22, 1-8; eC.-H. Xu, T. Jin, S. H. Jhung, J.-S. Chang, J.-S. Hwang, S.-E. Park, Catalysis Today 2006, 111, 366-372
[49] Wang, J.-P., Guo, G.-L., & Niu, J.-Y. (2008). Hydrothermal syntheses, crystal structures of three new organic–inorganic hybrids constructed from Keggin-type [BW12O40]5− clusters and transition metal complexes. Journal of Molecular Structure, 885(1–3), 161–167. https://doi.org/10.1016/j.molstruc.2007.10.025
[50] E. Rafiee and S. Eavani, RSC Adv., 2016, DOI: 10.1039/C6RA04891A.
[51] Clemente-León, M., Agricole, B., Mingotaud, C., Gómez-García, C. J., Coronado, E., & Delhaes, P. (1997). Toward New Organic/Inorganic Superlattices: Keggin Polyoxometalates in Langmuir and Langmuir−Blodgett Films. Langmuir, 13(8), 2340–2347. https://doi.org/10.1021/la960576v
[52] Haddadi, H., Hafshejani, S. M., Farsani, M. R., & Babahydari, A. K. (2015). Heterogeneous epoxidation of alkenes with H2O2 catalyzed by a recyclable organic–inorganic polyoxometalate-based framework catalyst. New Journal of Chemistry, 39(12), 9879–9885. https://doi.org/10.1039/c5nj01661d
[53] Thermo Scientific. Introduction to FTIR. [Online]. Available : tools.thermofisher.com/content/sfs/brochures/BR50555_E_0513M_H_1.pdf.01, 2019. [Accessed 01, 2019.]
[54] Wypych, G. (2013). PHOTOPHYSICS. In Handbook of Material Weathering (pp. 1–25). Elsevier. https://doi.org/10.1016/b978-1-895198-62-1.50004-4
[55] Ausili, Alessio & Sánchez, Marina & Gómez-Fernández, Juan. (2015). Attenuated total reflectance infrared spectroscopy: A powerful method for the simultaneous study of structure and spatial orientation of lipids and membrane proteins. Biomedical Spectroscopy and Imaging. 4. 159-70. 10.3233/BSI-150104.
[56] Materazzi, S. (1998). Mass Spectrometry Coupled to Thermogravimetry (TG-MS) for Evolved Gas Characterization: A Review. Applied Spectroscopy Reviews, 33(3), 189–218. https://doi.org/10.1080/05704929808006777
[57] “X-Ray Diffraction (XRD) : Anton Paar Wiki.” Anton Paar, [Online]. Available : http://www.wiki.anton-paar.com/en/x-ray-diffraction-xrd/. [Accessed April 2019]
[58] Guske, Joshua T. “X-Ray Diffraction Shared Experimental Facility.” MIT CMSE X-Ray Diffraction Facility, [Online]. Available : http://prism.mit.edu/xray/. [Accessed April 2019]
[59] Princeton Instruments. “Raman Spectroscopy Basics - Application Note.” [Accessed April 2019]
[60] Kneipp, K., Kneipp, H., Itzkan, I., Dasari, R. R., & Feld, M. S. (1999). Ultrasensitive Chemical Analysis by Raman Spectroscopy. Chemical Reviews, 99(10), 2957–2976. https://doi.org/10.1021/cr980133r
[61] Hoffman, Roy. “What is NMR?”, 26 Dec. 2018, [Online]. Available : http://www.chem.ch.huji.ac.il/nmr/whatisnmr [Accessed May 2019]
[62] Clark, Jim. “Introduction to Proton NMR.” Chemistry LibreTexts, Libretexts, 5 June 2019,

[63] Alkorta, I., Elguero, J., & Denisov, G. S. (2008). A review with comprehensive data on experimental indirect scalar NMR spin–spin coupling constants across hydrogen bonds. Magnetic Resonance in Chemistry, 46(7), 599–624. https://doi.org/10.1002/mrc.2209
[64] de Crane, Simon. Hybrid heteropolyacid-terpyridine heterogeneous catalysts for the epoxidation of olefins with H_2O_2. Prom.: Gaigneaux, Eric; Elias, Benjamin
[65] Washington States University. "Center for NMR Spectroscopy." Center for NMR Spectroscopy: The Lock, nmr.chem.wsu.edu/tutorials/basics/lock/. [Accessed April 2019]
[66] FU, T., WANG, J., NI, J., CUI, Z., ZHONG, S., ZHAO, C., … XING, W. (2008). Sulfonated poly(ether ether ketone)/aminopropyltriethoxysilane/phosphotungstic acid hybrid membranes with non-covalent bond: Characterization, thermal stability, and proton conductivity. Solid State Ionics, 179(39), 2265–2273.
[67] Boulangé, C. L. (2017). Nuclear Magnetic Resonance Spectroscopy-Applicable Elements| Phosphorus-31 ☆. In Reference Module in Chemistry, Molecular Sciences and Chemical Engineering. Elsevier. https://doi.org/10.1016/b978-0-12-409547-2.14079-x
[68] "Characterization Methods : Basic Factors." Porous Materials: Processing and Applications, by Peisheng Liu and Guo-Feng Chen, first ed., vol. 1, Elsevier, 2014, pp. 464–472.
[69] Sing, K. (2001). The use of nitrogen adsorption for the characterisation of porous materials. Colloids and Surfaces A: Physicochemical and Engineering Aspects, 187–188, 3–9. https://doi.org/10.1016/s0927-7757(01)00612-4
[70] Thermal Desorption Spectroscopy, Toshiba Nanoanalysis Corporation, 22 Aug. 2017, [Online]. Available : http://www.nanoanalysis.co.jp/en/business/device_08.html.
[71] Kouva, Sonja. "Temperature-Programmed Methods for Probing Surface Interactions on Catalytic Oxidematerials." Department of Biotechnology and Chemical Technology, [Online]. Available : http://www.aaltodoc.aalto.fi [Accessed May 2019]
[72] Ishii, T., & Kyotani, T. (2016). Temperature Programmed Desorption. In Materials Science and Engineering of Carbon (pp. 287–305). Elsevier. https://doi.org/10.1016/b978-0-12-805256-3.00014-3
[73] Cvetanović, R. J., & Amenomiya, Y. (1972). A Temperature Programmed Desorption Technique for Investigation of Practical Catalysts. Catalysis Reviews, 6(1), 21–48. https://doi.org/10.1080/01614947208078690
[74] "Home." ICP Analysis, ICP-MS, ICP-AES | Laboratory Testing Inc., [Online]. Available : http://www.labtesting.com/services/materials-testing/chemical-analysis/icp-analysis/. [Accessed April 2019]
[75] "ICP-OES." General Instrumentation, [Online]. Available : http://www.ru.nl/science/gi/facilities-activities/elemental-analysis/icp-oes/. [Accessed April 2019]
[76] Gross, Z., & Ini, S. (1999). Dual Role of PyridineN-Oxides in Ruthenium Porphyrin-Catalyzed Asymmetric Epoxidation of Olefins. Inorganic Chemistry, 38(7), 1446–1449. https://doi.org/10.1021/ic981021l

[77] Hua, L., Qiao, Y., Li, H., Feng, B., Pan, Z., Yu, Y., … Hou, Z. (2011). Epoxidation of olefins with hydrogen peroxide catalyzed by a reusable lacunary-type phosphotungstate catalyst. Science China Chemistry, 54(5), 769–773. https://doi.org/10.1007/s11426-011-4251-9
[78] "Gas Chromatography." Gas Chromatography: SHIMADZU (Shimadzu Corporation), [Online]. Available: http://www.shimadzu.com/an/gc/index.html. [Accessed April 2019]
[79] "Flame Ionization Detector (FID) Principle." Cambustion, [Online]. Available : http://www.cambustion.com/products/hfr500/fast-fid-principles. [Accessed May 2019]
[80] Houston, Sam, and Thomas Dr. Thomas G. Chasteen. "Split/Splitless and On-Column Gas Chromatographic Injectors." Split/Splitless and On-Column Gas Chromatographic, [Online]. Available: http://www.Injectors, www.shsu.edu/~chm_tgc/GC/GCinject.html. [Accessed May 2019]
[81] Freedman, M. L. (1959). The Tungstic Acids. Journal of the American Chemical Society, 81(15), 3834–3839. https://doi.org/10.1021/ja01524a009
[82] "Tungstic Acid, H2WO4." Element Tungsten, W, Transition Metal, Available: https://tungsten.atomistry.com/tungstic_acid.html. Accessed may 2019
[83] "Fine-Tuning and Recycling Oh Homogeneous Tungstate and Polytungstate Epoxidation Catalysts." Mechanisms in Homogeneous and Heterogeneous Epoxidation Catalysis, by S. Ted Oyama, Elsevier, 2008, pp. 416–421.
[84] Amoroso, A. J., Burrows, M. W., Coles, S. J., Haigh, R., Farley, R. D., Hursthouse, M. B., … Murphy, D. M. (2008). The synthesis and structure of terpyridine-N-oxide complexes of copper(ii) perchlorate. Dalton Trans., (4), 506–513. https://doi.org/10.1039/b713444d
[85] Campbell, N. J., Dengel, A. C., Edwards, C. J., & Griffith, W. P. (1989). Studies on transition metal peroxo complexes. Part 8. The nature of peroxomolybdates and peroxotungstates in aqueous solution. Journal of the Chemical Society, Dalton Transactions, (6), 1203. https://doi.org/10.1039/dt9890001203
[86] Venturello, C., & D'Aloisio, R. (1988). Quaternary ammonium tetrakis(diperoxotungsto)phosphates(3-) as a new class of catalysts for efficient alkene epoxidation with hydrogen peroxide. The Journal of Organic Chemistry, 53(7), 1553–1557. https://doi.org/10.1021/jo00242a041
[87] Strukl, J. S.; Walter, J. L. *Spectrochim. Acta Part A Mol. Spectrosc.* 1971, vol. *27* (2), 209–221.
[88] Strukl, J. S.; Walter, J. L. *Spectrochim. Acta Part A Mol. Spectrosc.* 1971, vol. *27* (2), 223–238.
[89] Ding, Y., Zhao, W., Hua, H., & Ma, B. (2008). [π-C5H5N(CH2)15CH3]3[PW4O32]/H2O2/ethyl acetate/alkenes: a recyclable and environmentally benign alkenes epoxidation catalytic system. Green Chemistry, 10(9), 910. https://doi.org/10.1039/b808404a
[90] Castellucci, E.; Angeloni, L.; Neto, N.; Sbrana, G. *Chem. Phys.* 1979, vol. *43* (3), 365–373.
[91] Kamyshny, A. L.; Zakharov, V. N.; Fedorov, Y. V.; Galashin, A. E.; Aslanov, L. A. *journal colloid interface Sci.* 1993, vol. *158*, 171–182.

[92] R Creasy, William & Mcgarvey, David & S Rice, Jeffrey & O Connor, Richard & Dupont Durst, H. (2019). STUDY OF DETECTION LIMITS AND QUANTITATION ACCURACY USING 300 MHZ NMR.
[93] C. Venturello, R. D'Aloiso, J. C. J Bart, M Ricci, A new peroxotungsten heteropoly anion with special oxidizing properties: synthesis and structure of tetrahexylammonium tetra(diperoxotungsto)phosphate(3-), *J. Mol. Catal.* 32, 107-110 (1985)

Heteropolyacid ($H_3PW_4O_{24}$) hybridized with terpyridine ($C_{15}H_{11}N_3$) as heterogeneous catalyst for epoxydation of olefins

Résumé Présenté par Pierrick Van Roey

In the field of catalysis, epoxides production has seen many diverse types of catalysts being developed over the years. The uses of oxiranes compounds are broad, they are either employed to produce paints, resins, adhesives or even as intermediates in organic synthesis. Several processes have been exploited yet nowadays, the direct oxidation by air of alkenes on silver-based catalyst is the most widespread one. However, the latter is a major carbon emitter of the industry. Consequently, industries are looking for new eco-friendly catalytic processes to obtain a sustainable production of epoxides. Among the potential candidates to accomplish this reaction, polyoxometalates (POMs) have demonstrated their property of being a good oxidation catalyst for a wide variety of reactions. These large anionic molecules have many properties such as a strong acidity when protonated, thermal stability and eventually their ability to accept and release electrons without decomposing or changing their structures. One of them, $\{PO_4[W(O)(O_2)_2]_4\}^{3-}$ (=PW4) was reported to be very active and selective towards epoxidation of olefins in homogeneous conditions. Nevertheless, industries prefer having heterogeneous catalytic processes, especially when large quantities are produced. Changing the nature of this homogeneous catalyst to a heterogeneous one remains though a challenge. The hybridization of this POM species with organic ligands have already been reported being successful using bipyridine.

PW4 was chosen to be hybridized with organic terpyridines ligands containing different functionalization. The main objective is to assess the influence of the catalyst polarity, by hybridizing a hydrophilic peroxo-tungstate acid ($H_3PW_4O_{24}$) with hydrophobic terpyridine ligands, for the heterogeneous catalytic epoxidation of cyclooctene by hydrogen peroxide. To do so, trials to synthesize PW4 and then hybridize it with the organic ligands were performed. The idea is to use 6 distinct ligands, giving 6 hybrids to obtain the catalyst with the highest affinity with the reactants. The situation is that PW4 itself is very hydrophilic compared to an alkene, but the hydrophobicity brought by the terpyridine ligand is supposed to increase the affinity between reactants and catalyst.

These hybrids were synthesized even if, there is no certainty about the exact content in their inorganic part. Then, the catalytic activity of these hybrids was tested in the epoxidation of cyclooctene using hydrogen peroxide as oxidant and acetonitrile as solvent. Large differences between the hybrids was observed. Nonetheless for the best one of them, results similar to the Venturello anion in homogeneous phase were obtained.

Eventually, leaching tests to judge the catalyst heterogeneity were operated. These have exposed that the hybrids catalysts are prone to leaching. These tests were followed by other ones demonstrating that the active species of the hybrids are the leached compounds.

To conclude, this study has revealed that the hybridization of peroxotungstates with functionalized terpyridines yields an active catalyst that leaches. The nature of the leached species was not established, further works still has to be carried out. Additional investigation is needed concerning the exact identification of the inorganic part of the hybrids which seems to be composed of a mix of PW4, PW3 and PW2 species.